

**Identification of CLK2 and CLK4 as novel regulators of
DNA damage-induced NF- κ B activity by chemical
dissection**

Inaugural-Dissertation
to obtain the academic degree
Doctor rerum naturalium (Dr. rer. nat.)

submitted to the Department of Biology, Chemistry, Pharmacy
of Freie Universität Berlin

by
Patrick Mucka, M.Sc.
from Silver Spring, MD, USA

2023

The present work was carried out under the supervision of Prof. Dr. Claus Scheidereit from August 2017 to April 2023 at the Max Delbrück Centre for Molecular Medicine in the Helmholtz Association.

1st reviewer: Prof. Dr. Claus Scheidereit

Laboratory of Signal Transduction in Tumor Cells
Max-Delbrück Centre for Molecular Medicine Berlin

2nd reviewer: Prof. Dr. Oliver Daumke

Department of Biology, Chemistry, Pharmacy
Freie Universität Berlin

Date of the defense: November 30, 2023

Declaration of Independence

Herewith I certify that I have prepared and written my thesis independently and that I have not used any sources and aids other than those indicated by me.

Table of Contents

1. Indexes	7
1.1. List of Figures	7
1.2. List of Tables.....	9
1.3. List of Abbreviations.....	10
2. Summary	13
2.1. Zusammenfassung	14
3. Introduction.....	16
3.1. NF- κ B is a major regulator of cellular stress response.....	16
3.1.1. NF- κ B is a family of transcription factors	16
3.1.2. I κ B molecules are molecular switches for NF- κ B	18
3.1.3. Activation of the IKK complex is the core mechanism of NF- κ B signaling	19
3.2. Canonical NF- κ B activation	20
3.2.1. Activation by genotoxic stress.....	22
3.3. NF- κ B as a therapeutic target in cancer.....	25
3.3.1. Pathway specific inhibition of NF- κ B.....	26
3.3.2. Identification of specific inhibitors of genotoxic stress-induced NF- κ B	27
3.4. Cancer therapeutics targeting DNA damage repair.....	29
3.4.1. PARP inhibitors	29
3.5. Kinase inhibitors in the treatment of cancer	30
4. Aims.....	31
5. Materials	32
5.1. Instruments and devices.....	32
5.2. Chemicals and Disposables	32
5.3. Antibodies	34
5.4. Buffers.....	35
5.5. Eukaryotic cell lines.....	37
5.6. Oligonucleotides	37

5.7.	Kits and enzymes.....	38
5.8.	Software	38
6.	Methods	39
6.1.	Molecular biology methods	39
6.1.1.	RNA isolation	39
6.1.2.	Determination of nucleic acid concentration.....	39
6.1.3.	Reverse Transcriptase-PCR	39
6.1.4.	Quantitative real-time PCR (qRT-PCR)	39
6.1.5.	Mutagenic PCR	39
6.2.	Protein biochemical methods	40
6.2.1.	Whole cell lysis	40
6.2.2.	Subcellular fractionation	40
6.2.3.	Determination of protein concentration.....	40
6.2.4.	SDS-PAGE	41
6.2.5.	Western Blot.....	41
6.2.6.	Electrophoretic Mobility Shift Assay	42
6.2.7.	PIP Strip	42
6.3.	Cell biology methods.....	43
6.3.1.	Cell culture	43
6.3.2.	Stimulation of cells with cytokines.....	44
6.3.3.	Induction of DNA damage	44
6.3.4.	siRNA transfection	44
6.3.5.	Generation of CRISPR knockout cell lines.....	44
6.3.6.	Immunofluorescence staining and confocal microscopy	45
6.3.7.	Cell Harvesting.....	45
7.	Results	46
7.1.	Validation of DNA damage-specific NF- κ B inhibitors MW01 and MW05	46
7.2.	Investigation of treatment contexts for MW01 and MW05	50

7.2.1. MW01 and MW05 potentiate apoptosis by unbalancing the NF- κ B/p53 axis.....	50
7.2.2. MW01 and MW05 block NF- κ B activation from on-going DNA damage and potentiate the effects of PARP inhibitor Olaparib	54
7.2.3. MW01 and MW05 reduce cell viability in glioblastoma cell lines.....	55
7.3. Target Identification of MW01 and MW05	56
7.3.1. PIP4K does not mediate the effect of MW01 or MW05	57
7.3.2. MW01 and MW05 are kinase inhibitors	60
7.3.3. TRAF6 does not undergo PIP-mediated translocations which could be affected by MW01 and MW05's PI3K inhibition	63
7.3.4. NEDD4L is a potential new regulator of NF- κ B but does not mediate the effects of MW01 or MW05	68
7.3.5. Identification of CLK2 as a regulator of genotoxic stress induced NF- κ B by chemical pathway dissection	72
7.3.6. CLK2 and CLK4 are regulators of genotoxic stress induced NF- κ B	74
7.3.7. Structural derivatives of MW01 and MW05 confirm CLK2 and CLK4 target identification	76
8. Discussion.....	83
8.1. MW01 and MW05 are the first identified inhibitors of genotoxic stress-induced NF- κ B.....	83
8.2. MW01 and MW05 target the DNA damage response to potentiate apoptosis	83
8.3. CLK2 and CLK4 are the functional targets of MW01 and MW05	85
8.4. CLK2 and CLK4 are novel regulators of genotoxic stress induced NF- κ B	89
8.5. CLK2 and CLK4 are promising, druggable therapeutic targets in cancer	91
8.6. Future directions for the development of MW01 and MW05.....	92
9. Supplemental Information	97
10. Acknowledgments.....	111
11. References.....	113

1. Indexes

1.1. List of Figures

Figure 3-1: Members of the NF- κ B Family	17
Figure 3-2: Activation and regulation of the canonical NF- κ B signalling pathway.....	21
Figure 3-3: Activation of NF- κ B by genotoxic stress.....	23
Figure 3-4: Summary of screen for small molecule inhibitors of DNA damage-induced NF- κ B.	28
Figure 7-1: Validation of MW01 and MW05 inhibitory effect in primary NF- κ B activity assays.....	47
Figure 7-2: MW01 and MW05 inhibit NF- κ B reporter expression in a dose-dependent manner.....	48
Figure 7-3: MW01 and MW05 inhibit critical genotoxic stress pathway steps.....	49
Figure 7-4: MW01 and MW05 increase apoptotic markers following irradiation.	51
Figure 7-5: MW01 and MW05 reduce cell viability and induce markers of DNA damage and cell death in co-treatment with etoposide.	53
Figure 7-6: MW01 or MW05 pre-treatment leads to an accumulation of DNA damage in <i>BRCA1</i> -deficient cells.	55
Figure 7-7: MW01 and MW05 reduce cell viability in glioblastoma cell lines.	56
Figure 7-8: PIP4K2C and PIP4K2A knockdown reduces NF- κ B-DNA binding following irradiation.....	58
Figure 7-9: PIP4K2C, PIP4K2A, and PIP4K2C/2A knockout cells.....	59
Figure 7-10: MW01 does not inhibit PIP4K2C or PIP4K2A <i>in vitro</i>	60
Figure 7-11 : MW01 and MW05 are kinase inhibitors with differing inhibition profiles.	61
Figure 7-12: MW01 and MW05 share kinase targets and are active in cell-based assays.	62
Figure 7-13: TRAF6 does not accumulate in cytoplasmic, nuclear, or membrane fractions following irradiation.....	65
Figure 7-14: TRAF6 localization does not change following irradiation.....	66
Figure 7-15: TRAF6 and TRAF4 share homologous critical PIP-binding lysine.	66
Figure 7-16: TRAF6-K388E mutant expression is poor and the protein likely unstable.....	67
Figure 7-17: NEDD4L knockdown reduces p-p65 level and p-ATM nuclear export after irradiation....	69
Figure 7-18: TRAF6 binds PI3P, PI5P, and PI3,P <i>in vitro</i>	71
Figure 7-19: Chemical pathway dissection by inhibitors of shared kinase targets of MW01 and MW05.	72
Figure 7-20: p-p65 phosphorylation is reduced by MU-1210 but not negative control MU-140 following irradiation.....	73
Figure 7-21: MW01 and MW05 are CLK inhibitors with differing isoform specificity.....	74
Figure 7-22: Knockdown of CLK2 or CLK4 reduces p-p65 only after irradiation.	75

Figure 7-23: CLK2 and CLK4 knockdown reduces <i>NFKBIA</i> expression following DNA damage.....	76
Figure 7-24: Screening of MW01 derivative library for active inhibitors.	77
Figure 7-25: Screening of MW05 derivative library for active inhibitors.	78
Figure 7-26: Active derivatives of MW01 and MW05 DNA damage-induce NF-κB activation.	79
Figure 7-27: Inactive derivatives of MW01 and MW05 do not affect NF-κB activation.	80
Figure 7-28: Active derivatives of MW01 and MW05 target CLK2 and 4.....	81
Figure 8-1: Kinome tree map of targets of MW01 and MW05.....	86
Figure 8-2: Sequence alignment of CLK isoforms 1-4.	88
Figure 8-3: CLK2 and 4 are targeted by MW01 and MW05 and act between ATM and IKK in the genotoxic stress-induced NF-κB pathway.	90

1.2. List of Tables

Table 3-1: Permeability and percent absorption of MW01 and MW05 in CaCo2 cells.	28
Table 8-1: Structure and CLK isoform specificities of CLK inhibitors.....	92
Table 8-2: Percent inhibition of selected kinase targets of MW01 and derivatives.....	94
Table 8-3: Percent inhibition of selected kinase targets of MW05 and derivatives.....	95
Table 9-1: Broad kinase inhibition panel of MW01 and MW05.....	97
Table 9-2: MW01 and MW05 derivative library.	103
Table 9-3: Kinase panel of active and inactive derivatives of MW01 and MW05.....	109

1.3. List of Abbreviations

2A KO	U2-OS-PIP4K2A knockout
2C KO	U2-OS-PIP4K2C knockout
2D-TPP	two-dimensional thermal proteome profiling
ABC DLBCL	activated B cell-like diffuse large B cell lymphoma
ADP	adenosine diphosphate
AML	acute myeloid leukaemia
ARD	Ankyrin repeat domain
ATM	ataxia telangiectasia mutated
ATP	adenosine triphosphate
BAFF	B-cell-activating factor belonging to TNF family
BCR	B cell receptor
bp	Base pairs
BRCA	Breast Cancer gene
BTK	Bruton's tyrosine kinase
CC	coiled-coil domain
cDNA	complementary DNA
ciAP	cellular inhibitor of apoptosis
CLL	chronic lymphocytic leukemia
CML	chronic myelogenous leukemia
CO-IP	co-immunoprecipitation
DAPI	4',6-diamidino-2-phenylindole
DiD	dimerisation domain
DDR	DNA damage response
DD	death domain
DKO	U2-OS-PIP4K2A/2C double knockout
DSB	Double strand breaks
DUB	Deubiquitinase
ECL	enhance chemiluminescence
ELKS	protein rich in the amino acids E, L, K and S
EMSA	electrophoretic mobility shift assay
Eto	Etoposide
FDA	Food and Drug Administration
FMP	Leibniz-Institut für Molekulare Pharmakologie
GADD45 β	Growth arrest and DNA-damage-inducible protein beta
GFP	green fluorescent protein
GGR	Glycine-rich region
h	hour
HCS	high content screens
HR	Homologous repair
HRP	Horseradish peroxidase
IF	immunofluorescence

Ig	immunoglobulin
IKK	I κ B kinase
IL-1	interleukin-1
IP	immunoprecipitation
IPO3	importin 3
I κ B	nuclear factor- κ B inhibitor
K	Lysine
KD	kinase domain
KO	knockout
LUBAC	linear ubiquitin assembly complex
LZ	leucine zipper
M1-linked ubiquitin	linear Ubiquitin
MAPK	Mitogen-activated protein kinase
MCL	mantle cell lymphoma
MCPIP1	monocyte chemotactic protein-induced protein 1
min	minutes
MM	multiple myeloma
MMK7	MAP (Mitogen-activated protein) kinase kinase 7
mRNA	messenger RNA
mTOR	mammalian target of rapamycin
n.s.	non-specific
NBD	NEMO binding domain
NEDD4L	neural precursor cell expressed developmentally downregulated gene 4-like
NEMO	NF- κ B essential modifier
NF- κ B	nuclear factor- κ B
NLS	nuclear localisation signal
NTD	N-terminal domain
p-ATM	ATM phosphorylated at S1981
p-p65	p65 phosphorylated at S536
PAGE	polyacrylamide gel electrophoresis
PAMPS	pathogen associated molecular patterns
PAR	poly(ADP-ribose)
PARP1	poly(ADP-ribose)-polymerase-1
PCR	Polymerase chain reaction
PEST	region rich in Proline, Glutamic acid, Serine and Threonine
PI3K/PIK3	phosphatidylinositol-phosphate-3-kinase
PI4,5P	phosphatidylinositol-4,5-phosphate
PI5P	phosphatidylinositol-5-phosphate
PI	phosphatidylinositol
PIASy	protein inhibitor of activated STAT gamma
PIP	phosphatidylinositol-phosphate
PIP ₃	phosphatidylinositol-3,4,5-phosphate
PIP4K	Phosphatidylinositol 5-Phosphate 4-Kinase
PMCA	Plasma membrane calcium ATP-ase

PTM	posttranslational modification
qRT-PCR	quantitative real-time PCR
RANK	receptor activator for nuclear factor κ B
RHD	Rel homology domain
RIP1	Receptor-interacting protein 1
RNA	Ribonucleic acid
RT	Room temperature
S, Ser	Serine
SAR	structure-activity-relationship
SASP	senescence-associated secretory phenotype
SCF ^{BTrCP}	Skp, Cullin, F-box complex containing Beta-transducin repeat-containing proteins
SD	standard deviations
SDD	α -helical scaffold/dimerization domain
SEM	standard error of the mean
SEN2	Sentrin/SUMO-specific protease 2
SILAC	stable isotope labelling with amino acids in cell culture
siRNA	Small interfering RNA
SR	Serine-arginine rich
SSB	single stranded break
SUMO	small ubiquitin-related modifier
TAD	transactivation domain
TAK1	TGF β (transforming growth factor β)-activated kinase-1
TANK	TRAF family member-associated NF- κ B activator
TLR	Toll-like receptor
TNF	Tumour necrosis factor
TRADD	Tumor necrosis factor receptor type 1-associated death domain protein
TRAF	Tumour necrosis factor (TNF) receptor-associated factor
Ub	ubiquitin
ULD	Ubiquiting-like domain
UBAN	Ubiquitin-binding in ABIN and NEMO domain
USP10	Ubiquitin specific protease 10
UT	untreated
UV	ultraviolet
WB	Western Blot
WT	wildtype
XIAP	X-linked inhibitor of apoptosis protein
γ -irradiation	IR
γ H2AX	H2A histone family member X phosphorylated at S139

2. Summary

Chemotherapy and radiation are standard-of-care cancer treatments, but their effectiveness is often hampered by therapy resistance within the tumor. Numerous studies have demonstrated that tumor cells can evade cell death triggered by genotoxic therapies by activating IKK/NF- κ B pathway, thereby preventing apoptosis. The direct targeting of IKKs using pharmacological interventions is not a viable option due to the significant adverse effects caused by the essential role of IKK/NF- κ B signaling in various physiological processes. To circumvent this, previous work by our group identified structurally unrelated small molecule inhibitors, MW01 and MW05, that selectively inhibit IKK/NF- κ B solely in response to DNA double strand breaks induced by chemotherapy and radiation. Importantly, these compounds do not interfere with IKK/NF- κ B activation triggered by other physiological stimuli.

Initial work began by confirming the genotoxic stress-specific inhibition by the compounds before moving onto target identification studies. Considering the similar cellular effects of both compounds within the DNA damage-induced NF- κ B pathway, comparative target identification studies including kinase assay panels, structural derivatization, and molecular signaling characterization were performed, seeking targets shared between both lead compounds. Common regulators shared by other NF- κ B stimuli were first excluded as potential targets of the compounds before investigation of the several identified shared targets revealed a previously unknown regulators of genotoxic stress-induced NF- κ B activity, Cdc-like kinases (CLK) 2 and 4, as the functional target of MW01 and MW05. Silencing of the CLK2 and 4 revealed that they are essential for DNA damage-induced NF- κ B activity and promote the phosphorylation of IKK at Ser-85, a genotoxic stress specific ATM-dependent phosphosite, critically localizing the CLKs within the cascade between ATM and IKK. CLK2 and 4 were also confirmed as the target of active structural derivatives of MW01 and MW05 and were spared by inactive derivatives, confirming CLK2 and 4's role in genotoxic stress-induced NF- κ B. In addition, CLK inhibitor MU-1210 also inhibited NF- κ B following DNA damage, suggesting that CLK inhibitors could be used to potentiate the tumor killing effect of standard cancer treatments.

MW01 and MW05 were tested in co-treatment with DNA damaging agents, in the context of on-going DNA damage, and in patient derived glioblastoma cells to assess their potential clinical applications. Critically, neither MW01 nor MW05 exhibit general toxicity; instead, they notably enhance apoptosis specifically in tumor cells following genotoxic stress. In *BRCA1*-deficient cells and in co-treatment with PARP inhibitor Olaparib, both characterized by on-going DNA damage, MW01 and MW05 potentiated DNA damage and p53 levels, suggesting that the compounds unbalance the NF- κ B/p53 axis in favor of apoptosis. This approach introduces a novel therapeutic strategy to curb NF- κ B activity induced by DNA damage in cancer cells without impacting its essential functions in healthy cells.

2.1. Zusammenfassung

Chemotherapie und Bestrahlung gehören zu den Standard-Krebstherapien, ihre Wirksamkeit wird jedoch häufig durch das Auftreten von Therapieresistenzen im Tumor beeinträchtigt. Zahlreiche Studien haben gezeigt, dass Tumorzellen dem durch genotoxische Therapien ausgelösten Zelltod entgehen können, indem sie den IKK/NF- κ B-Signalweg aktivieren und so die Apoptose verhindern. Das direkte Angreifen von IKKs durch pharmakologische Interventionen ist keine praktikable Option, da die wesentliche Rolle der IKK/NF- κ B-Signalübertragung bei verschiedenen physiologischen Prozessen erhebliche negative Auswirkungen erwarten lässt. Um dies zu umgehen, hat unsere Gruppe strukturell nicht verwandte niedermolekulare Inhibitoren, MW01 und MW05, identifiziert, die die einzigartige Fähigkeit besitzen, die Aktivierung von IKK/NF- κ B ausschließlich als Reaktion auf durch Chemotherapie und Bestrahlung verursachte DNA-Doppelstrangbrüche selektiv zu hemmen. Wichtig ist, dass diese Verbindungen die durch andere normale physiologische Reize ausgelöste IKK/NF- κ B-Aktivierung nicht beeinträchtigen.

Die ersten Arbeiten begannen mit der Bestätigung der genotoxischen Stress-spezifischen Hemmung durch die Verbindungen, bevor die Studien zur Identifizierung der Targets fortgesetzt wurden. In Anbetracht der ähnlichen zellulären Wirkungen beider Verbindungen innerhalb des durch DNA-Schäden induzierten NF- κ B-Stoffwechsels wurden vergleichende Studien zur Identifizierung von Zielmolekülen durchgeführt, einschließlich Kinase-Assay-Panels, struktureller Derivatisierung und molekularer Signalcharakterisierung, um gemeinsame Zielmoleküle der beiden Leitverbindungen zu finden. Gemeinsame Regulatoren anderer NF- κ B-Stimuli wurden zunächst als potenzielle Ziel-Proteine der Verbindungen ausgeschlossen, bevor die Untersuchung der verschiedenen identifizierten gemeinsamen Ziel-Enzyme einen bisher unbekanntem Regulator der durch genotoxischen Stress induzierten NF- κ B-Aktivität, die Cdc-ähnlichen Kinasen 2 und 4 (CLK2 und 4), als funktionelles Ziel von MW01 und MW05 ergab. CLK2 und 4 wurden auch als Ziel-Kinasen aktiver Strukturderivate von MW01 und MW05 bestätigt und blieben von inaktiven Derivaten verschont, was die Rolle von CLK2 und 4 bei der durch genotoxischen Stress induzierten NF- κ B bestätigt. Darüber hinaus hemmte ein externer, strukturell unähnlicher CLK-Inhibitor, MU-1210, ebenfalls NF- κ B nach DNA-Schäden, was darauf hindeutet, dass CLK-Inhibitoren zur Verstärkung der tumortötenden Wirkung von Standard-Krebstherapien eingesetzt werden könnten.

Parallel zu den Studien zur Identifizierung der Zielmoleküle wurden MW01 und MW05 auch bei der gleichzeitigen Behandlung mit DNA-schädigenden Substanzen, im Zusammenhang mit laufenden DNA-Schäden und in Glioblastomzellen von Patienten getestet, um ihre potenziellen klinischen Anwendungen zu bewerten. Kritisch anzumerken ist, dass weder MW01 noch MW05 eine allgemeine

Toxizität aufweisen; stattdessen verstärken sie insbesondere die Apoptose in Tumorzellen nach genotoxischem Stress. In *BRCA1*-defizienten Zellen und bei gleichzeitiger Behandlung mit dem PARP-Inhibitor Olaparib, die beide durch anhaltende DNA-Schäden gekennzeichnet sind, verstärkten MW01 und MW05 den γ H2AX-Wert, einen Marker für DNA-Schäden, und den p53-Wert, was darauf hindeutet, dass die Verbindungen die NF- κ B/p53-Achse zugunsten der Apoptose aus dem Gleichgewicht bringen. Dieser Ansatz stellt eine neuartige therapeutische Strategie dar, um die durch DNA-Schäden in Krebszellen induzierte NF- κ B-Aktivität zu bremsen, ohne ihre wesentlichen Funktionen in gesunden Zellen zu beeinträchtigen.

3. Introduction

The ability to adapt to environmental changes is critical for the survival of organisms. Various environmental, chemical, physical, or microbiological challenges pose a threat to cellular homeostasis and the normal functioning of tissues, resulting in stress during development and physiological processes. An essential response to such stress is the activation of cellular signaling, which influences cellular functions by modulating gene expression programs. One key player in the cellular response to stress is the NF- κ B (nuclear factor kappa-light-chain-enhancer of activated B-cells) system. NF- κ B is a widely distributed and rapidly inducible transcription factor that was first discovered in 1986 as a regulator of the expression of the immunoglobulin κ light chain gene in B cells ¹. Since then, several hundred target genes regulated by NF- κ B have been identified ². These target genes primarily participate in the regulation of the immune system and inflammation, embryonic development, cell cycle control, proliferation, and cell death. In addition to its crucial functions in development and stress response, dysregulated NF- κ B activity is implicated in numerous diseases, notably chronic inflammation, autoimmune disorders, and, critically for this study, cancer.

3.1. NF- κ B is a major regulator of cellular stress response

The NF- κ B system is a widely expressed gene regulatory network in mammals. Its evolutionary origins can be traced back to more rudimentary and basic inducible signaling systems that existed in organisms preceding flies ³. NF- κ B signaling is activated by a diverse array of external and internal stimuli and governs the regulation of numerous target genes, thereby influencing various aspects of cellular physiology ^{2,4}. Examples of stimuli that trigger NF- κ B activation include pro-inflammatory cytokines, PAMPS (pathogen-associated molecular patterns), ligands of immune receptors, and various cellular stresses, such as γ -irradiation (IR). Upon activation, NF- κ B pathways orchestrate distinct cellular responses through the transcriptional regulation of target genes encoding non-coding RNA (ribonucleic acid) or proteins involved in the control of cell survival, proliferation, adhesion, matrix remodeling, lymphocyte activation, host defense, immunity, and inflammation.

3.1.1. NF- κ B is a family of transcription factors

NF- κ B constitutes a family of transcription factors playing significant role in inflammatory, immune, and anti-apoptotic gene expression. In mammals, this family is comprised of five members: p65/RelA, RelB, c-Rel, and p105/p50, as well as p100/p52, which form homo- and heterodimers in various

combinations⁴. Structurally, all NF- κ B subunits possess a Rel homology domain (RHD) that includes a N-terminal domain (NTD), a dimerization domain (DiD), and a nuclear localization signal (NLS) (Figure 3.2). The RHD is responsible for crucial functions such as dimerization with other subunits, nuclear localization, DNA binding, and interaction with I κ B proteins⁵.

The Rel proteins RelA, RelB and c-Rel are distinguished by the presence of a transactivation domain (TAD) located at their C-terminus, which is essential for activating transcription⁶. The precursor proteins, p105 and p100, are encoded by the *NFKB1* and *NFKB2* genes, respectively. Both precursors contain ankyrin repeats and a death domain (DD). Through ubiquitination and proteasomal processing, p105 and p100 undergo conversion into the mature NF- κ B subunits p50 and p52, respectively^{7,8}.

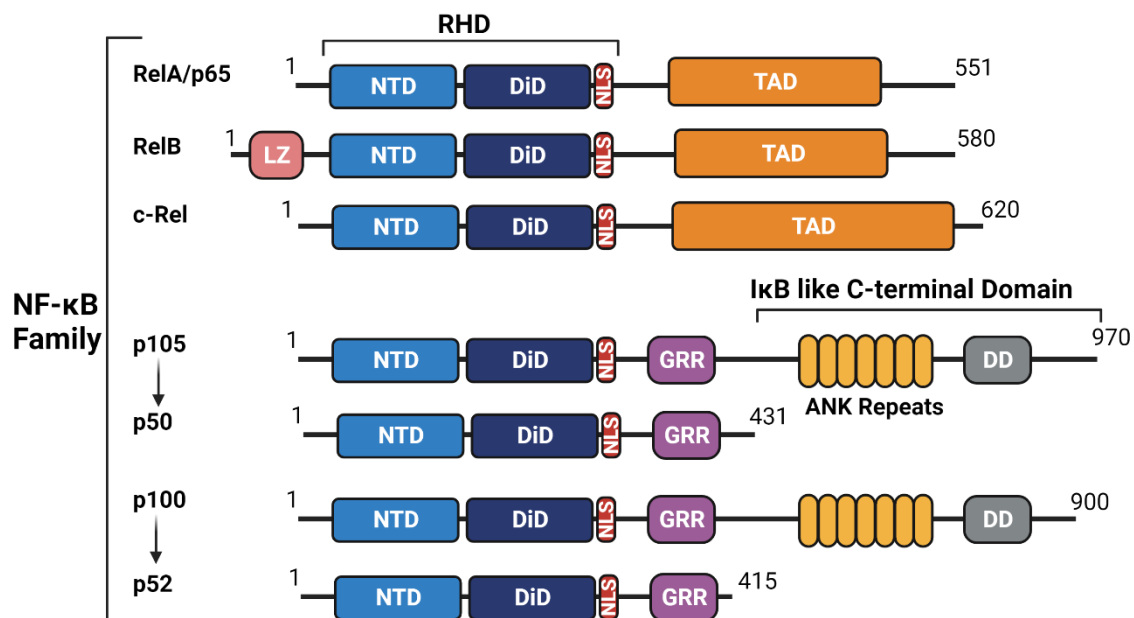


Figure 3-1: Members of the NF- κ B Family

All five proteins of the NF- κ B family share a conserved RHD. The subunits p65, RelB and c-Rel have a TAD. p105 and p100 proteins are inactive precursors of p50 and p52. Similar to I κ B α , β and ϵ , the C-terminus of p100 and p105 contains ankyrin (ANK) repeats, which mediate their inhibitory functions. In addition, the inactive precursors present a death domain (DD) that exerts its effects via self-association and/or interaction with death domain of other proteins. Their glycine-rich region (GRR) is essential for terminating proteasomal proteolysis to produce p50 and p52.

Due to the absence of the TAD, p50 and p52 are unable to activate transcription. Furthermore, it has been demonstrated that homodimers of p50 and p52 function as transcriptional repressors of NF- κ B target genes^{6,9}. Active NF- κ B heterodimers selectively bind to consensus DNA sequences that span 9-

11 base pairs (bp): 5'-GGGRNWYYCC-3' (where R represents a purine base, N represents any base, W represents either A or T, and Y represents a pyrimidine base)¹⁰. These sequences are characterized by a series of G nucleotides at the 5' end, and they are referred to as κ B sites. The crystallographic structures of NF- κ B:DNA complexes have revealed that the NF- κ B dimer interacts with the major groove of DNA through the RHD.

Various post-translational modifications (PTMs) of NF- κ B subunits, including phosphorylation and acetylation, induce conformational changes that affect ubiquitination, stability, protein-protein interactions, and the regulation of target gene expression¹¹. Inactive NF- κ B dimers are sequestered in the cytoplasm through their association with I κ B (inhibitor of nuclear factor- κ B) proteins (Section 3.1.2). Upon upstream activation by various NF- κ B activators, I κ B α is phosphorylated, marking it for lysine-48-linked (K48) ubiquitination and subsequent proteasomal degradation^{10,12}. Subsequently, the released NF- κ B dimers translocate into the nucleus where they regulate the transcription of target genes.

3.1.2. I κ B molecules are molecular switches for NF- κ B

To adapt to cellular disturbances, molecular switches are necessary to integrate and convert signals into appropriate responses. The I κ B proteins serve as such molecular switches by preventing the nuclear translocation of NF- κ B.

A distinctive structural feature of the I κ B proteins is the presence of an ankyrin repeat domain (ARD) (Figure 3.2), which facilitates their binding to NF- κ B dimers. The PEST domain (region rich in proline, glutamic acid, serine, and threonine residues), found in I κ B α and I κ B β , is thought to contribute to the rapid turnover of these proteins¹³.

The prototypic I κ B α , I κ B β , and I κ B ϵ proteins sequester NF- κ B dimers in the cytoplasm by masking the nuclear localization signal (NLS), and the activation of NF- κ B requires their release from the I κ Bs. In addition, further members of the I κ B family have been identified, such as Bcl-3, which associate with p50 or p52 homodimers in the nucleus and serve as transcriptional co-activators¹⁴. To release NF- κ B from I κ B α , phosphorylation by IKK (inhibitor of nuclear factor- κ B kinase) of two serine residues (S32 and S36) within the N-terminus is essential¹⁵⁻¹⁸. However, phosphorylation alone is not sufficient, and proteolytic degradation of I κ B α is also required¹⁹⁻²². It has been demonstrated that the destruction of I κ B α involves ubiquitination and is mediated by the 26S proteasome^{23,24}. In this context, SCF β TrCP (Skp, Cullin, F-box complex containing Beta-transducin repeat-containing proteins) was identified as

the essential ubiquitin E3-ligase responsible for the degradative ubiquitination of phosphorylated I κ B α ^{25,26}.

The inducible proteasomal degradation of I κ B α results in a rapid but transient reduction of the protein. I κ B α is a direct target gene of NF- κ B, and its activation leads to the rapid replenishment of I κ B α as part of an auto-regulatory feedback loop ^{19,27,28}. Binding of I κ B α to p65 masks the NLS, thereby affecting the subcellular localization of the p65/p50 heterodimer. This mechanism is supported by the crystal structure of the I κ B α /NF- κ B complex obtained through X-ray analysis ²⁹. The authors proposed that I κ B α binding to NF- κ B prevents the activation of transcription by NF- κ B. Recent studies utilizing mathematical simulations have further suggested that the binding of I κ B to the NF- κ B/DNA complex facilitates kinetically controlled molecular stripping of the NF- κ B/I κ B α complex from DNA through an allosteric mechanism ³⁰. Additionally, the presence of nuclear export sequences in I κ B proteins contributes to a dynamic equilibrium between nuclear and cytoplasmic shuttling of I κ B/NF- κ B complexes, with cytoplasmic distribution prevailing in resting cells. Following activation, this balance shifts toward NF- κ B nuclear localization due to induced degradation of I κ Bs.

3.1.3. Activation of the IKK complex is the core mechanism of NF- κ B signaling

The fundamental process governing NF- κ B signaling involves the activation of the IKK complex, comprised of the catalytic subunits IKK α and IKK β , along with the regulatory subunit IKK γ /NEMO (NF- κ B essential modifier) ³¹. The activation of the IKK complex relies on distinct structural attributes of its subunits. IKK α and IKK β exhibit a significant sequence homology (approximately 50% identity) and comprise a kinase domain (KD), a central ubiquitin-like domain (ULD), an α -helical scaffold/dimerization domain (SDD), and a C-terminal NEMO-binding domain (NBD) ³¹. Crucially, the kinase activity of IKK α and IKK β is contingent upon the phosphorylation state of serines 176/180 and 177/181, respectively, located in their respective t-loops ³²⁻³⁴.

Moreover, IKK complex activation is regulated by IKK γ , wherein different domains facilitate binding to IKK α / β and play crucial roles in I κ B α binding and ubiquitin binding ³⁵. Contradicting studies suggest that IKK γ binding to either K63-linked or linear (M1-linked) ubiquitin chains is essential to induce conformational changes, leading to IKK activation ³⁶⁻⁴⁰. Recent findings propose the involvement of mixed ubiquitin chains (linear and K63-linked ubiquitin) in this process ^{41,42}. Notably, IKK γ itself can be subjected to ubiquitin-ligase-mediated modification, with lysine residue 285 (K277 in murine IKK γ)

identified as an acceptor site for both mono- and linear ubiquitination, both of which are critical for IKK complex activation^{39,43,44}.

IKK complex activation requires various signaling events. Typically, upstream signaling leads to the ubiquitin-mediated auto-phosphorylation of the kinase TAK1 (TGF β -activated kinase-1), accomplished by recruiting TAK1/TAB2/3 complexes to K63-linked ubiquitin chains⁴⁵⁻⁴⁸. Activated TAK1 subsequently phosphorylates IKK α and IKK β in their activation loops at S176 and S177, respectively⁴². Phosphorylation of IKK β at S177 primes it for subsequent auto-phosphorylation at Ser181, most likely occurring in trans⁴⁹. The phosphorylation of both activation loop serines (S176/180 for IKK α and S177/181 for IKK β) is crucial for their full kinase activity. Additionally, the IKK complex phosphorylates not only I κ B proteins but also the NF- κ B subunit p65 within its TAD, with the IKK β -mediated phosphorylation of p65 on S536 believed to enhance its transactivation potential^{31,50}.

Beyond its role as the I κ B kinase complex, IKK is implicated in NF- κ B-independent functions, such as the regulation of apoptosis, cell cycle arrest, immune functions, insulin resistance, and the modulation of the MAPK (Mitogen-activated protein kinase) pathway^{51,52}. Moreover, IKK can influence mRNA stability, as evidenced by its impact on IL6 expression following IL-1-receptor (IL-1R) stimulation via controlling the stability of Regnase⁵³. In addition, recent work by our group has shown that IKK controls the stability of thousands of mRNAs by phosphorylation of enhancer of decapping 4 (EDC4)⁵⁴.

3.2. Canonical NF- κ B activation

Canonical IKK/NF- κ B activation exhibits its most potent response to inflammatory stimuli, such as cytokines like IL-1 (interleukin-1) and TNF α (Tumor necrosis factor alpha), as well as Toll-like receptor agonists⁴². Upon ligand binding to their cell membrane receptors, the signaling cascade is transduced into the cytoplasm. Adapter proteins play a crucial role in recruiting signaling components, including kinases and ubiquitin ligases, to the receptor complex. The activation of canonical NF- κ B involves a complex interplay of ubiquitin chain attachments and protein recruitments, culminating in the poly-ubiquitin binding of IKK γ and phosphorylation of IKK α/β by TAK1 (Figure 3-2).

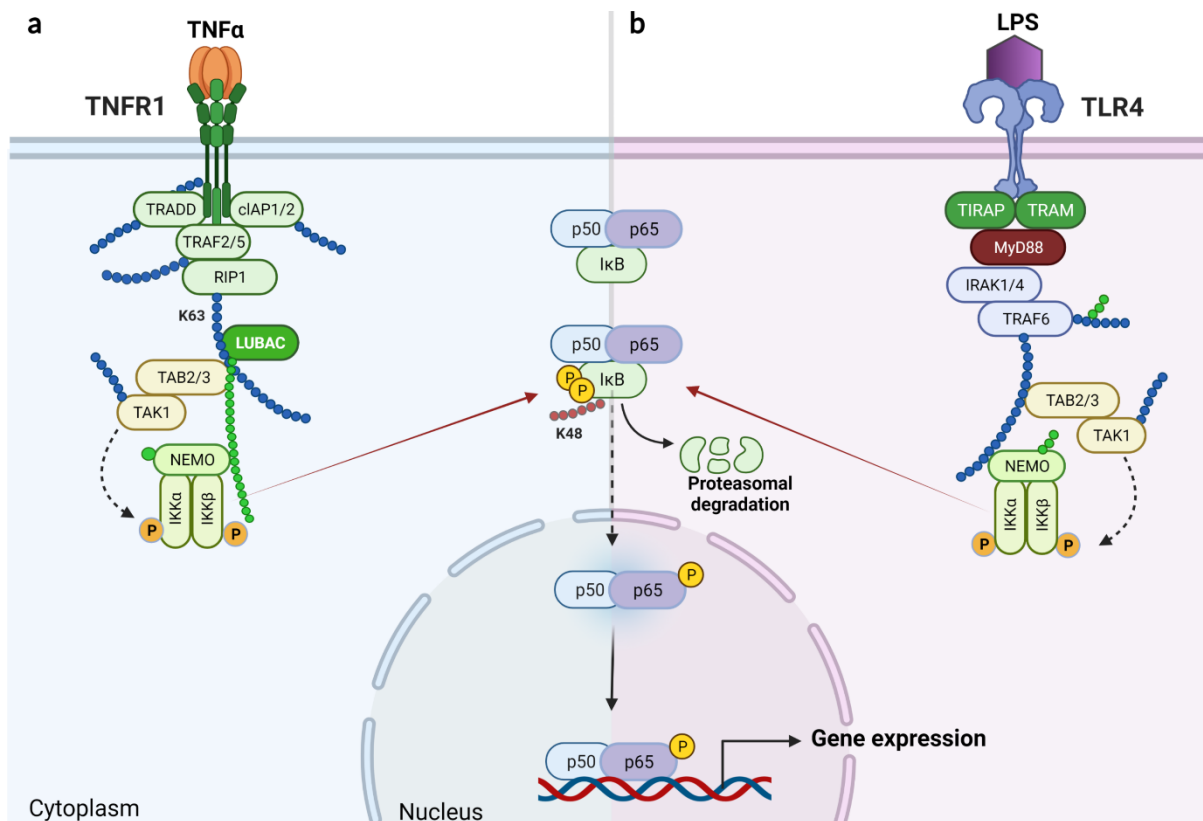


Figure 3-2: Activation and regulation of the canonical NF-κB signalling pathway.

(a) TNF α ligand binding to the TNFR receptor leads to the recruitment of Tumor necrosis factor receptor type 1-associated DEATH domain protein (TRADD) and interaction with the E3 ubiquitin ligases cellular inhibitor of apoptosis (cIAP)1/2 and tumor necrosis factor receptor associated protein (TRAF)2 with the protein kinase receptor interacting protein (RIP)1. This enables recruitment of the LUBAC complex, which subsequently mediates ubiquitination of several signaling proteins. Subsequently, RIP1 is K63-ubiquitinated and recruits NEMO, which results in the formation of the TAK1-IKK complex. TAK1 phosphorylates and activates the IKK complex. The IKK complex then phosphorylates I κ B α , which leads to its ubiquitination (K48-ubiquitination; red) and proteasomal degradation. This allows p65:p50 to translocate to the nucleus, where induce target gene expression. (b) TLR4 mediates signal transduction through MyD88 that is recruited by TIRAP and TRAM. MyD88 then induces the recruitment of IRAK1 and IRAK4, which further recruit TRAF6 to activate the TAK complex and subsequently the IKK complex as described in main text. Ubiquitin chains are represented in green and blue.

Following the previously discussed IKK-dependent phosphorylation events (3.1.2, 3.1.3), the active p65/p50 heterodimer translocates into the nucleus and governs the transcription of target genes. As a negative feedback mechanism I κ B α is then resynthesized, dampening NF- κ B activation. Another regulatory feedback loop involves the expression of the deubiquitinating enzyme A20. Deubiquitinases (DUBs) control the ubiquitination status of signaling components, thereby influencing the activation of the IKK complex. A20, crucially, deubiquitinates RIP1 by cleaving attached K63-ubiquitin chains. Moreover, it exhibits E3 ligase activity, attaching K48-ubiquitin chains to RIP1, marking it for degradation^{55,56}.

An additional important regulator is the linear ubiquitin-specific DUB Otulin, which releases IKK γ and other LUBAC (linear ubiquitin chain assembly complex) substrates from linear ubiquitin chains, resulting in a reduction of IKK complex and NF- κ B activation^{57,58}. Furthermore, CYLD is involved in cleaving linear ubiquitin chains and K63-ubiquitin chains⁵⁹. As a result, CYLD serves as another significant regulator of NF- κ B activation by deubiquitinating various activators, including TRAF2, TRAF6, TAK1, and IKK γ ⁶⁰.

3.2.1. Activation by genotoxic stress

Cancer is characterized by uncontrolled cellular proliferation, and cancer therapies aim to halt undesired cell division and growth by inducing DNA damage through treatments such as irradiation or chemotherapeutics. Consequently, DNA damaging cancer therapies activate the extensively studied transcription factors, p53 and NF- κ B, as part of the DNA damage response (DDR)⁶¹. The DDR regulates cell fate decisions, including cell cycle arrest, DNA repair, senescence, and apoptosis, depending on the extent of genotoxic stress. This process, activated by either physiologically occurring DNA damage or therapy-induced DNA damage, significantly influences development, genetic diseases, aging, and cancer outcomes.

DNA double strand breaks (DSBs) initiate a nuclear-to-cytoplasmic signaling cascade, leading to IKK activation in a manner analogous to cytokine-induced NF- κ B activation⁶². However, genotoxic stress-induced NF- κ B activation follows bifurcated pathway of a nuclear origin rather than from cell surface receptor (Figure 3-3). Two independent molecular sensors, ATM (ataxia telangiectasia mutated) and PARP1 (poly(ADP-ribose)-polymerase-1), are recruited to DNA lesions and initiate the DDR. Both PARP1 and ATM play various roles in the DDR, from initiating stress responses to facilitating DNA damage repair. The primary substrate of the kinase ATM is the tumor suppressor protein p53, which exerts anti-proliferative and pro-apoptotic functions by regulating its target genes. Minor DNA damage leads to a reversible cell cycle arrest until the lesions are repaired, while irreparable DNA lesions trigger more extensive cellular responses. To safeguard against malignant transformation, affected cells either irreversibly enter a non-proliferative state called cellular senescence or undergo apoptosis⁶¹.

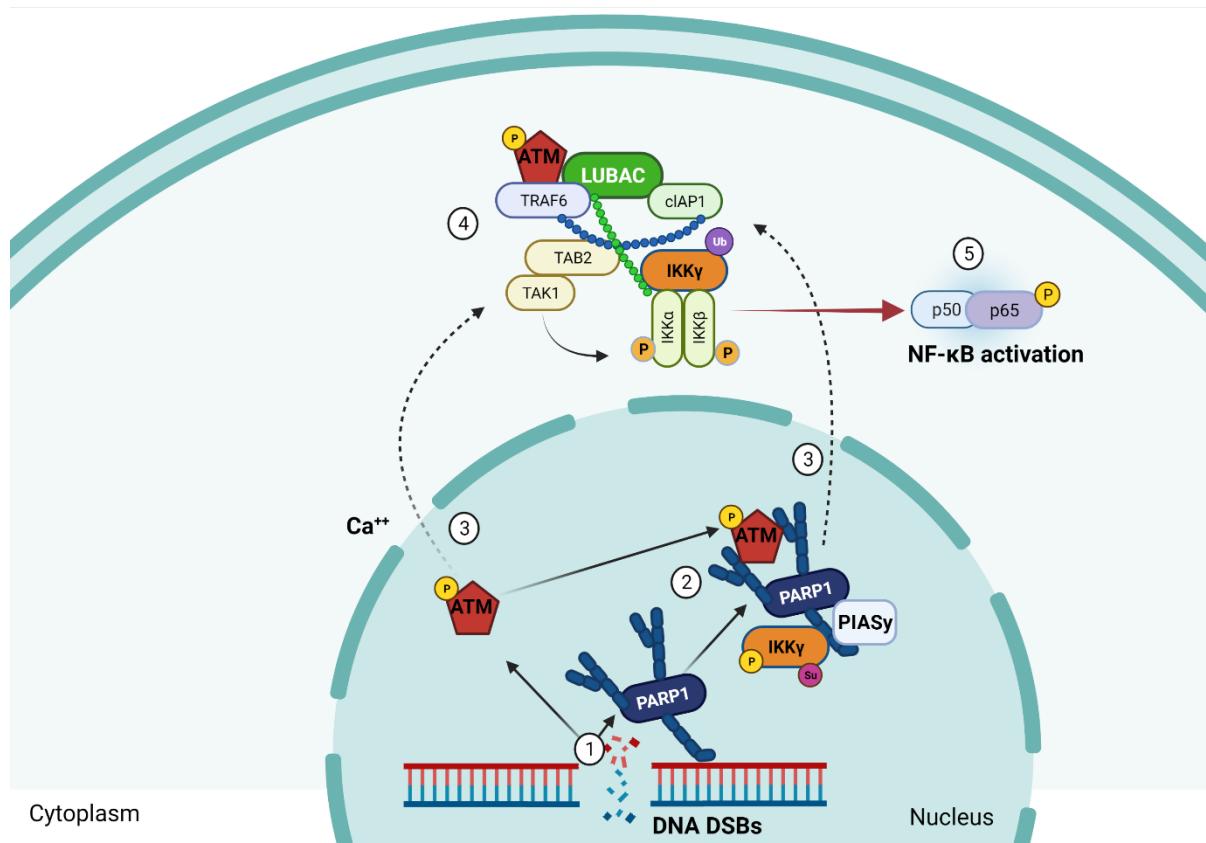


Figure 3-3: Activation of NF-κB by genotoxic stress

(1) PARP1 and ATM are activated by DSBs. **(2)** PARP1 nuclear signalosome forms **(3)** IKKγ and ATM are exported from the nucleus. **(4)** Cytoplasmic signaling complex forms. **(5)** Activation of the IKK complex and NF-κB, target gene expression.

Induction of DSBs activates the DNA damage sensor MRN complex, recruiting ATM to the lesion which is then activated through auto-phosphorylation and stimulates the synthesis of poly(ADP-ribose) (PAR) by PARP1, which is believed to serve as a scaffolding function⁶³. Subsequently, the activation of PARP1 leads to the formation of a nuclear signalosome containing ATM, PARP1, the SUMO E3-ligase PIASy (protein inhibitor of activated STAT gamma), ELKS (protein rich in amino acids E, L, K, S), and the IKK complex subunit IKKγ^{40,62,64}.

Upon genotoxic stress induction, IKKγ is transported into the nucleus by interacting with the nuclear importer IPO3 (importin 3)⁶⁵ and is recruited to the signalosome by binding to auto-PARylated PARP1. IKKγ then undergoes phosphorylation by ATM on serine 85, SUMOylation by PIASy, and is thereafter mono-ubiquitinated⁴³. Following this, IKKγ is transported into the cytoplasm and likely incorporated into newly formed IKK holocomplexes. Simultaneously, phosphorylated ATM translocates into the cytoplasm in a Ca²⁺-dependent manner and initiates the formation of a cytoplasmic signalosome⁴⁴. ATM triggers the activation of TRAF6, leading to Ubc-13-mediated K63-linked poly-ubiquitination. This

ubiquitin chain acts as a scaffold for recruiting cIAP1 and TAB2-TAK1, subsequently activating TAK1. Additionally, IKK γ undergoes linear ubiquitination through the involvement of LUBAC⁶⁶. Depending on the cellular context, cell type and type of stimulus, other regulatory components such as ELKS, XIAP (X-linked inhibitor of apoptosis protein), or RIP1 have been proposed to participate in this pathway's activation^{40,67-70}. Eventually, cIAP1-dependent mono-ubiquitination of IKK γ is essential for forming both the nuclear and cytosolic signalosomes, ultimately leading to the activation of the IKK complex, I κ B α degradation, and subsequent NF- κ B activation⁴⁴.

The activation of DNA damage-induced NF- κ B signaling is regulated by several auto-inhibitory negative feedback loops. Increased expression of I κ B α and A20 serves as negative regulators, and their mRNA stability is regulated by RCH3H1⁷¹. CYLD also contributes to the reduction of NF- κ B activation by cleaving IKK γ -attached linear ubiquitin chains under genotoxic stress conditions⁶⁶.

Sentrin-specific protease 2 (SEN2) expression is upregulated by NF- κ B activation following DNA damage, and it attenuates NF- κ B activity by deSUMOylating IKK γ ⁷². SENP1 has also been reported to cleave IKK γ -attached SUMO moieties, suggesting a potential redundancy between SENP1 and SENP2⁷³.

An additional feedback loop involves monocyte chemotactic protein-induced protein 1 (MCPIP1) and ubiquitin-specific peptidase 10 (USP10). MCPIP1 expression is regulated by NF- κ B upon DNA damage, and it facilitates the binding of USP10 to IKK γ , leading to the cleavage of IKK γ -attached linear ubiquitin chains, ultimately inhibiting the genotoxic stress-induced NF- κ B pathway⁷⁴.

Furthermore, TANK (TRAF family member-associated NF- κ B activator) plays a role in regulating NF- κ B activation upon genotoxic stress. Following DNA damage, TANK forms a complex with MCPIP1/USP10, promoting the deubiquitination of TRAF6 and subsequently attenuating IKK/NF- κ B activation⁶⁹.

The outcome of genotoxic stress-induced NF- κ B activation is similar to canonical NF- κ B signaling, involving the transcriptional regulation of anti-apoptotic genes. However, in addition to its role in apoptosis regulation, the genotoxic stress-induced IKK/NF- κ B pathway also has other functions. NF- κ B plays a significant role in genotoxic stress-induced senescence by driving the expression of SASP (senescence-associated secretory phenotype) with context-dependent effects in experimental tumor models. In lymphoma models, NF- κ B promotes senescence and enhances chemosensitivity^{72,75}. In contrast, in a melanoma model, the senescence-associated PARP1-IKK-NF- κ B cascade induces the release of a secretome with tumor-promoting and pro-metastatic properties⁷⁶.

3.3. NF- κ B as a therapeutic target in cancer

Constitutive activation of NF- κ B has been observed in various human cancers ⁷⁷, including hematopoietic and lymphoid malignancies such as multiple myeloma (MM), acute myeloid leukemia (AML), T cell lymphoma, and Hodgkin lymphoma ⁷⁸⁻⁸². Similarly, elevated NF- κ B activation has been found in melanoma cells, lung carcinoma cells, bladder cancer cells, breast cancer cells, and pancreatic adenocarcinoma cells ⁸³⁻⁸⁸. Over the past decades, significant insights have been made into the role NF- κ B plays in these malignancies.

The consequences of dysregulated NF- κ B in cancer are two-fold. A sustained inflammatory environment results from the continued expression of pro-inflammatory target genes and subsequent continuous secretion of pro-inflammatory cytokines, which is especially conducive to tumor growth ⁸⁹. In addition, and critically for this study, the upregulation of anti-apoptotic gene programs also leads to tumor cell survival ⁹⁰. Studies have shown that NF- κ B activation induced by TNF α and genotoxic stress regulates the expression of anti-apoptotic genes, leading to apoptosis inhibition ^{87,91-93}. This anti-apoptotic activity of NF- κ B is thought to contribute strongly to cancer therapy resistance, and targeting NF- κ B signaling may sensitize cancer cells to chemotherapy ⁹⁴⁻⁹⁶.

Proteasome inhibitors were among the first used inhibitors of the NF- κ B pathway. Treatment with proteasome inhibitors has been shown to sensitize cancer cells to apoptosis induction by chemotherapeutic agents ⁹⁷. Bortezomib, a proteasome inhibitor, has been approved for the treatment of multiple myeloma and mantle cell lymphoma (MCL) patients who have received prior therapy ⁹⁸. However, proteasomal inhibitors broadly target multiple NF- κ B pathways and may cause proteotoxicity due to accumulated misfolded proteins, leading to dose-limiting toxic effects.

To develop more specific inhibitors targeting the canonical NF- κ B pathway, efforts have been made to create IKK complex inhibitors. These inhibitors have shown promising results in blocking NF- κ B activation and inducing cell death in myeloma cells ^{99,100}. Nevertheless, they have not been approved for clinical use, likely due to the pleiotropic functions of IKK, both dependent and independent of NF- κ B ^{51,101,102} and because they may be toxic due to unknown off-target kinases that are co-inhibited.

In conclusion, NF- κ B pathway activation is considered a driving force in tumorigenesis and cancer therapy resistance. Pharmacological inhibition of NF- κ B may serve as a useful adjuvant for chemotherapeutic treatment. However, developing stimulus-specific NF- κ B inhibitors is desirable to avoid the adverse effects of prolonged general NF- κ B inhibition ^{51,94,101}.

3.3.1. Pathway specific inhibition of NF-κB

Considering the crucial role of NF-κB in cancer treatment resistance mechanisms, it is evident that targeted therapy approaches against this pro-survival pathway are necessary. Despite intense research on the NF-κB/IKK pathways, their pharmacological application in human disease remains limited. Clinical trials with general NF-κB inhibitors, like IKK inhibitors, were conducted but ultimately not approved by regulatory authorities. For example, the IKK inhibitor SAR113945 was tested for intra-articular application in knee osteoarthritis patients but did not meet the phase II study's primary endpoints and was subsequently discontinued^{103,104}.

The general inhibition of IKK/NF-κB pathways is likely to cause systemic toxicity and severe adverse effects due to their pleiotropic functions⁹⁰. Studies have shown that intra-articular inhibition of IKK led to systemic effects on immune system regulation in a mice model of collagen-induced arthritis¹⁰⁵. Therefore, there is a pressing need to develop new classes of pathway-specific inhibitors that only interfere with stimulus-specific NF-κB activation while leaving other modes of NF-κB activation intact.

Recent successful examples of stimulus-specific or pathway-selective NF-κB inhibitors have been reported. For instance, Guido Franzoso's lab developed a D-tripeptide inhibitor that targets the interaction between (Growth arrest and DNA-damage-inducible protein beta) GADD45β and (Mitogen-activated protein kinase kinase 7) MMK7, effectively killing patient-derived MM cells. Importantly, this inhibition is specific to MM cells, sparing normal cells from toxicity and side-effects in mice¹⁰⁶.

Another successful example is the Bruton's tyrosine kinase (BTK)-targeting drug ibrutinib, which specifically inhibits the B-cell receptor (BCR pathway, where BTK is often constitutively activated in lymphoid malignancies, leading to NF-κB activation. Ibrutinib demonstrated antitumor activity in clinical trials and was approved for treating mantle cell lymphoma and chronic lymphocytic leukemia¹⁰⁷⁻¹¹⁰. Additionally, ibrutinib showed high response rates in clinical trials for ABC DLBCL (diffuse large B cell lymphoma) patients¹¹¹, making it a successful BCR pathway-specific NF-κB inhibitor. Further investigation is required to explore its efficacy against other lymphoid malignancies and potential approvals for additional indications in the future.

In conclusion, the successful identification of pathway-specific NF-κB inhibitors proves their feasibility. The specific requirements of genotoxic stress-induced NF-κB activation such as unique protein-protein interactions (nuclear PARP1 signalosome), posttranslational modifications (SUMOylation and phosphorylation of IKKγ), and translocation processes (ATM nuclear export) offer a framework for identifying DNA damage-specific NF-κB pathway inhibitors. Moreover, the mechanisms of DNA

damage-induced NF- κ B signaling are still not completely understood, and therefore additional unidentified essential pathway components could be potential new therapeutic targets.

3.3.2. Identification of specific inhibitors of genotoxic stress-induced NF- κ B

Previous work by our research group, spearheaded by Micheal Willenbrock (see Mucka et al., 2023), identified two distinct small molecule inhibitors through differential small molecule screening that specifically inhibit the activation of IKK/NF- κ B following DNA damage while leaving canonical IKK/NF- κ B activation triggered by cytokines like TNF α or IL-1 β unaffected¹¹². This was accomplished using a high-throughput screen quantifying p65 nuclear translocation, an essential step in NF- κ B activation, and was established through a collaboration between our group, the FMP Screening Unit, and the group of Marc Nazaré. A chemical library of over 32,000 compounds was screened and 138 small molecule inhibitors of etoposide-induced p65 nuclear translocation were identified (Figure 3-4). These hit compounds were used in a subsequent TNF α -induced counter-screen and 21 compounds that inhibited NF- κ B only after DNA damage were selected for IC₅₀ determination. Among them, two promising structurally distinct compounds, MW01 and MW05, inhibited p65 translocation at sub-micromolar concentrations following etoposide treatment, without affecting p65 translocation upon TNF α stimulation, were selected for further investigation.

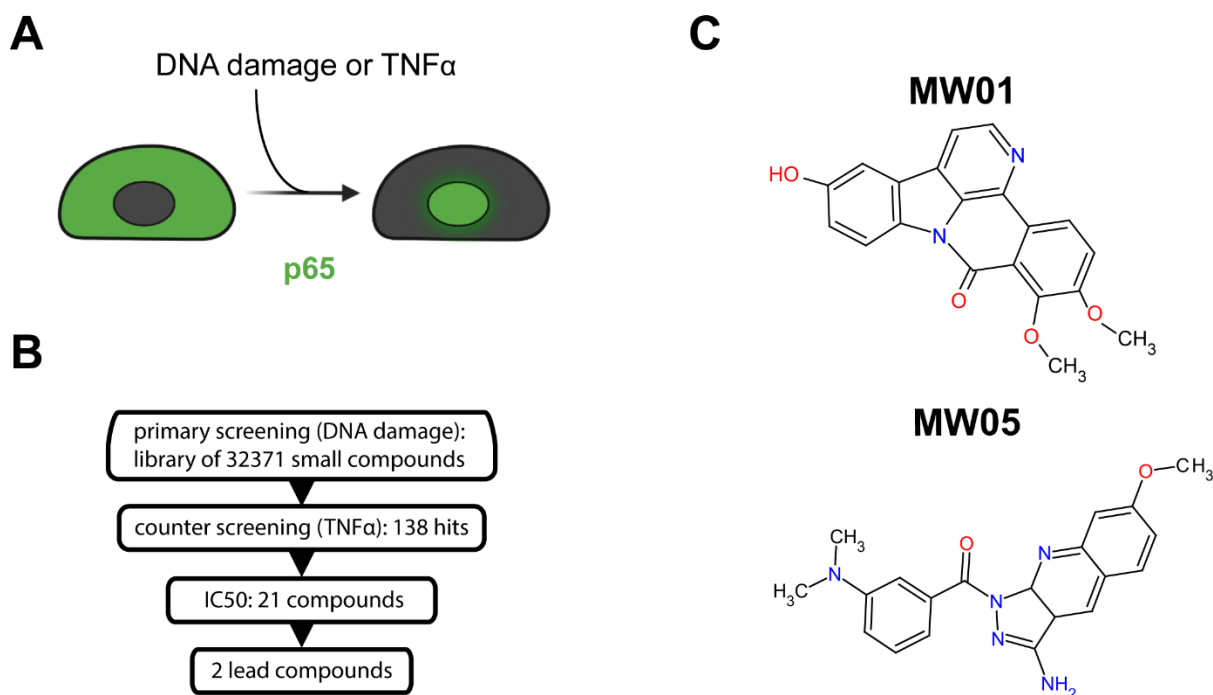


Figure 3-4: Summary of screen for small molecule inhibitors of DNA damage-induced NF- κ B.

(A) Schematic of p65 nuclear translocation, the main quantified readout during the chemical library screen. (B) Schematic summarizing number compounds passing each step of the screen. (C) Chemical structures of the two lead compounds MW01 (top) and MW05 (bottom).

The compounds were cell permeable with CaCo2 membrane permeability values of 12.60 ± 6.20 and $17.28 \pm 2.65 \times 10^{-6}$ cm/s and percent absorptions approximately 28% and 36% for MW01 and MW05 respectively (Table 3-1). Highly cell-permeable propranolol was included as a positive control.

Compound	Mean P_{app} ($\times 10^{-6}$ cm/s)	Percent absorption
MW01	12.60 ± 6.20	28.16 ± 4.10
MW05	17.28 ± 2.65	36.31 ± 3.28
Propranolol	33.43 ± 0.98	74.40 ± 6.48

Table 3-1: Permeability and percent absorption of MW01 and MW05 in CaCo2 cells.

3.4. Cancer therapeutics targeting DNA damage repair

Genotoxic stress-induced NF- κ B is the major mediator of anti-apoptotic signaling within the broader DNA Damage Response. The DDR is a coordinated cellular program regulating DNA repair, DNA damage signaling, and cell cycle progression, which has in recent years proven an effective target in for cancer therapeutics¹¹³. The inherent instability of the genome in rapidly dividing tumors creates potential avenues for therapeutic interventions targeting DDR pathways. This approach aims to selectively eliminate rapidly dividing cancer cells through increased replication stress, introduction of external DNA damage, and/or inhibition of DDR¹¹⁴. Due to the identification of specific genetic weaknesses in particular cancer types, the concept of synthetic lethality can be employed, where the loss of one cellular pathway leads to a heightened dependence on another pathway, which is non-essential under normal conditions¹¹⁵. Drugs can be used as monotherapy or adjuvant therapies with traditional radio- and chemotherapeutics¹¹⁵.

3.4.1. PARP inhibitors

This approach is best illustrated by the application of poly(ADP-ribose) polymerase (PARP) inhibitors, first approved for the clinic in 2014^{116,117}, in the context of tumors with deficiencies in the homologous recombination (HR) DNA repair factors breast cancer gene (*BRCA*)1 or 2, as well as tumors with impaired HR due to other factors^{118,119}. *BRCA*1/2 plays a crucial role in HR, and their deficiencies have been linked to cancer development¹²⁰. Additionally, it has been discovered that some tumors with intact *BRCA*1/2 genes can also exhibit heightened sensitivity to PARP inhibition, utilizing mechanisms that do not rely on HR inactivation, providing further evidence for targeting DDR elements¹²¹. However, the efficacy of combining chemotherapy with PARP inhibitors in the broader cancer population has not been definitively established, and the issue of PARP inhibitor resistance continues to pose a significant challenge across various patient groups.

Despite PARP inhibition's status as the proof-of-principle for DDR-targeting therapeutics, most small molecules in clinical trials for this synthetic lethality approach are kinase inhibitors of the DDR¹¹⁴. PARP inhibitors do not inhibit NF- κ B consistently, likely due to the unclear interregulation of PARP isoforms and varying isoform specificities of clinical PARP inhibitors or unknown off-target effects¹²². Considering the essential role of PARP1 in genotoxic stress-induced NF- κ B, problematic PARP inhibitor resistance, and NF- κ B's role in mediating PARP inhibitor radiosensitization, there is a strong case for inhibiting NF- κ B and downstream anti-apoptotic signaling through alternative, as-yet undescribed targets^{44,123,124}.

3.5. Kinase inhibitors in the treatment of cancer

Kinase inhibitors represent not just the most common class of small molecule DDR-targeting therapeutics in clinical trials, but also most numerous class of clinically approved cancer treatments^{114,125}. This abundance underscores the critical role kinases can play in tumorigenesis, which was described as early as 1978¹²⁶. The first protein-kinase inhibitors were developed in the early 1980s by Hiroyoshi Hidaka¹²⁷. Naphthalene sulphonamides, such as N-(6-amino-hexyl)-5-chloro-1-naphthalenesulphonamide (W7), which had already been developed as antagonists of the calcium-binding protein calmodulin, were also found (at higher concentrations) to inhibit several protein kinases. Structural derivatization generated a series of compounds which lost their calmodulin antagonist activity but displayed improved specificity for several kinases. These compounds were cell permeable and ATP competitive, suggesting their potential use *in vivo*. In the decades since, significant insight has been gained in the structure, function, and roles of kinases in physiological and pathological signal transduction, leading to intense interest in targeting these proteins pharmacologically^{128,129}. In 2001, years of progress in the field culminated in the rapid approval of Imatinib, the first kinase inhibitor rationally designed for a target, in this case the oncogenic fusion protein BCR-ABL, found in most cases of chronic myelogenous leukemia (CML)¹³⁰. Following this approval many in the field believed kinase inhibition would become a dominant therapeutic modality of the new millennium¹³¹.

The development of kinase inhibitors as cancer therapeutics has posed significant challenges due to high structural similarity of conserved kinase domains, which results in lack of target specificity and thus potentially toxic off-target effects¹²⁵. Advances in small molecule design and screening have allowed the identification of highly specific kinase inhibitors which greatly reduce these effects, although completely specific kinase inhibitors remain elusive¹²⁸. In fact, this lack of complete specificity has been observed to be beneficial in some cases with kinase inhibitors targeting multiple kinases, a phenomenon referred to as polypharmacology¹³². However, the diverse roles of kinases within signaling cascades and the crosstalk between other pathways present an additional layer of complication in selecting a promising kinase target or targets for rational drug design.

Due to the failure of IKK inhibitors and inhibitors of other kinases within the genotoxic stress pathway to reach the clinic, there is a critical need to develop and characterize novel kinase regulators of DNA damage-induced NF- κ B.

4. Aims

Following genotoxic stress, NF- κ B potently upregulates numerous pro-survival genes, which compete with apoptotic signaling from the p53 axis to determine cell fate. In a clinical context, this represents a form of therapeutic resistance in tumors following traditional chemotherapeutic treatments. Inhibition of DNA damage-induced NF- κ B activity and the resultant anti-apoptotic signaling is thus an attractive strategy in contexts of therapy-induced and on-going DNA damage, as found in numerous tumors. Previous work by our group identified two structurally distinct inhibitors, MW01 and MW05, of DNA-damage induced NF- κ B which spare NF- κ B activation by other physiological stimuli.

The primary aim of this study was to identify the functional target(s) of MW01 and MW05 and the localization of the target(s) in the signaling pathway. Based on the differential screen used to identify the inhibitors, the putative target was suspected to be a previously unidentified regulator of DNA damage-induced NF- κ B. Successful confirmation of a novel, druggable regulator of genotoxic stress-induced NF- κ B activity by a molecular biology approach would then illuminate a new therapeutic strategy in the treatment of tumors. Further molecular studies aimed to localize where the putative target(s) act in within the signaling cascade and provide a deeper understanding of the mechanistic basis for sub-pathway specificity. In addition, involvement of a novel regulator in the pathway could provide evidence for the repurposing of previously described inhibitors of the putative target as cancer therapeutics.

The second aim of the project was the characterization of MW01 and MW05 in various preclinical contexts. Co-treatment with DNA damaging agents, such as γ -radiation or chemotherapeutics, to induce DSBs would allow a proof of concept for the potentiation of DNA damage and apoptosis. Treatment with MW01 and MW05 in the context of defective DNA repair machinery, as in presence of Olaparib or in *BRCA*-deficient cells, would provide similar insight into the ability of the compounds to push cell fate decisions towards cell death. Additional testing in several tumor types based on differential target profiles for each compound would identify promising therapeutic contexts and future directions for the development of each lead.

Finally, synthesis of a derivative library would, in addition to aiding in target identification, improve potency and lay the basis for optimization of pharmacokinetic properties. Improvement of the pharmacokinetic parameters would pave the way for use in clinically relevant tumor models and support patent applications for future potential licensing opportunities.

5. Materials

5.1. Instruments and devices

137-Cs source for γ -irradiation	Eckert-Ziegler
Analytical balance	Sartorius AC 210 P
	Sartorius BP 310S
Brightfield light microscope	Zeiss Telaval 31
Cell culture incubator	Binder CB 220
Centrifuges	Eppendorf 5417R
	Eppendorf 5402
	Beckmann Coulter J6-HMI
CFX 96 Real-Time system	Biorad C-1000 Thermal cycler
Confocal microscope	Zeiss LSM 710
Flow Cytometer	BD Bioscience LSR II
Heat blocks	Techne DB3
Magnetic stirrer	Heidolph MR3000 and 3001
Microscope slides Superfrost Plus	Thermo Scientific
Overhead rotator	Fröbel Labortechnik
pH meter	Knick 766
Power supply	Biorad PowerPac 200/300
Protein gel chamber	Biorad
Roller mixer	Stuart scientific SRT1
Semidry transfer cell	Biorad Trans-Blot SD
Shaker	UniEquip Unitwister
Spectrophotomer, visible light	Amersham Biosciences Novaspec plus
Spectrophotometer, UV (ultraviolet) light	Peqlab Biotechnology ND-1000
Tissue culture hoods	BDK
Ultra-low temperature freezer	Binder UF V 700
Vortex mixer	Scientific Industries Vortex-genie 2
Water bath	Haake F3
Western blot membrane detection device	Vilber Lourmat Fusion Solo

5.2. Chemicals and Disposables

[α -32P] dATP	NEN (Perkin Elmer)
4',6-diamidino-2-phenylindole (DAPI)	Roche
Acrylamide/Bisacrylamide (30%)	Roth
Ammonium peroxodisulfate (APS)	Roth
Autoradiography films	Amersham Hyperfilm MP

Boric acid (H ₃ BO ₃)	Roth
Bovine serum albumin (BSA)	Sigma Aldrich, Roth
Bradford reagent	Biorad
Bromphenol blue	Biorad
Cell culture 6-well plates	Greiner
Cell culture dishes 10 cm	Greiner
Cell culture dishes 15 cm	Greiner
Cell culture dishes 6 cm	Greiner, TPP
Chemoluminescence films	Amersham Hyperfilm ECL
Complete protease inhibitor tablets -EDTA	Roche
Dulbecco's modified essential medium (DMEM)	Gibco
Dimethylsulfoxide (DMSO)	Sigma Aldrich
dNTPs	Biomol
1,4-Dithiothreitol (DTT)	Sigma Aldrich
ECL solutions	Millipore Immobilon Western HRP Substrate
Ethylenediaminetetraacetic acid (EDTA)	Amresco, Roth
Ethylene glycol-bis(β-aminoethyl ether)-N,N,N',N'-tetraacetic acid (EGTA)	Sigma Aldrich
Ethanol	Merck
Etoposide	Sigma Aldrich
Fetal calf serum (FCS)	Gibco
Filter papers for transfer	Roth
filtered, sterile pipette tips 10, 200, 1000 μl	Biozym
Glycerol	Merck
Glycine	Roth
HEPES	Roth
Hydrochloric acid (HCl)	Roth
Hydrogen peroxide (35%)	Roth
IGEPAL CA-630	Sigma Aldrich
IL-1β	Alexis
Isopropanol	Roth
KU-55933 (ATM inhibitor)	Selleckchem
Magnesium chloride (MgCl ₂)	Merck
Microseals for qRT-PCR plates	Biorad
Methanol	Roth
Mowiol	Calbiochem
Nonidet P-40 (NP-40)	Sigma Aldrich
Olaparib (PARP inhibitor)	Cayman chemical
OptiMEM	Sigma Aldrich
Paraformaldehyde (PFA)	Sigma Aldrich
Penicillin/Streptomycin	Gibco
PhosStop	Roche
Pipette tips 10, 200, 1000 μl	Sarstedt
Plastic tubes, sterile 15 ml	Falcon, Greiner

Plastic tubes, sterile 50 ml	Falcon, Greiner
Poly d(I-C)	Roche
Potassium chloride (KCl)	Roth
Precision cuvettes	Sarstedt
Prestained protein weight marker	Fermentas
PVDF membranes	Roth, Millipore
qRT-PCR plates (96 well)	Biozym
Restore PLUS WB Stripping buffer	Thermo Scientific
RNAse Zap	Ambion
RPMI 1640	Gibco
Safe lock tubes (1.5 and 2 ml)	Sarstedt
Shandon ImmuMount	Thermo Scientific
Skim milk powder	Fluka
Sodium chloride (NaCl)	Roth
Sodium dodecyl sulfate (SDS)	Roth
Sodium fluoride (NaF)	Sigma Aldrich
Sodium orthovanadate (Na ₃ VO ₄)	Sigma Aldrich
TEMED	Roth
TNF α	Abcam
Tris	Roth
Trypan blue	Sigma Aldrich
Trypsin-EDTA	Biochrom
Tween-20	Roth
β -Glycerophosphate	Calbiochem

5.3. Antibodies

Primary antibodies	Clone	Application	Company
CLK2	ab86147	WB	Abcam
CLK4	Ab67936	WB	Abcam
p65	C-20	WB, IF	Santa Cruz Biotechnology
p65 S536	93H1	WB	Cell Signaling Technology
p53	DO-1	WB	Santa Cruz Biotechnology
LDH-A	N-14	WB	Santa Cruz Biotechnology
PARP-1	CII10	WB	Santa Cruz Biotechnology
PAR (p(ADP)r)	10H	WB	Abcam
ATM S1981	10H11.E12	WB	Rockland Immunochemicals
H2AX S139 (γ H2AX)	JBW301	WB, IF	Millipore
I κ B α	C-21	WB	Santa Cruz Biotechnology
I κ B α S32/36	5A5	WB	Cell Signaling Technology
Tubulin	B-5-1-2	WB	Sigma Aldrich
IKK α / β S176/180	16A6	WB	Cell Signaling Technology
IKK γ	FL-419	WB, IP	Santa Cruz Biotechnology
IKK γ S85	ab63551	WB	Abcam

Secondary antibodies

Alexa-488-conjugated anti-rabbit	IF	Life Technologies
Alexa-546-conjugated anti-mouse	IF	Life Technologies
HRP-conjugated anti-rabbit	WB	JacksonImmunoResearch
HRP-conjugated anti-mouse	WB	JacksonImmunoResearch
HRP-conjugated anti-goat	WB	JacksonImmunoResearch

5.4. Buffers

Buffer for cell culture:

Phosphate buffered saline (PBS)

NaCl	137 mM
KCl	2.7 mM
Na ₂ HPO ₄	10 mM
KH ₂ PO ₄	1.7 mM

Buffers for protein biochemical methods:

Whole cell lysis buffer (Bäuerle buffer)

HEPES pH 7.9	20 mM
NaCl	350 mM
Glycerin	20%
MgCl ₂	1 mM
EDTA	0.5 mM
EGTA	0.1 mM
NP-40	1%
DTT	1 mM
complete proteinase inhibitors	

Buffer A (used for the generation of cytoplasmic extracts)

Tris-HCl pH 7.9	20 mM
MgCl ₂	1.5 mM
KCl	10 mM
β-Glycerophosphate	8 mM
NaF	20 mM
Na ₃ VO ₄	200 mM
DTT	1 mM
complete proteinase inhibitors	

Buffer C (used for the generation of nuclear extracts)

Tris-HCl pH 7.9	40 mM
Glycerol	25% (v/v)
NaCl	420 mM

MgCl ₂	1.5 mM
β-Glycerophosphate	8 mM
NaF	20 mM
DTT	1 mM
complete proteinase inhibitors	
<u>6x SDS sample buffer</u>	
Tris-HCl, pH 6.8	300 mM
EDTA	12 mM
Glycerol	40% (v/v)
SDS	12% (w/v)
DTT	10% (w/v)
Bromophenol blue	1% (w/v)
<u>SDS-running buffer</u>	
Tris-HCl pH 7.3	25 mM
SDS	0.1% (w/v)
Glycine	192 mM
<u>Western Blot Transfer Buffer</u>	
Tris pH 8.3	48 mM
Glycin	39 mM
SDS	0.037 (w/v)
Methanol	20% (v/v)
<u>TBS-T</u>	
Tris pH 7.5	25 mM
NaCl	150 mM
Tween 20	0.1% (v/v)
<u>Blocking solution</u>	
TBS-T	
skim milk powder	3-5% (w/v)
<u>H2K EMSA reaction buffer (2x)</u>	
HEPES pH 7.9	40 mM
KCl	120 mM
Ficoll	8%
BSA solution	10 mg/ml
Poly d(I-C)	2 mg/ml
<u>Tris borate EDTA (TBE)</u>	
Tris	50 mM
Borate	50 mM

5.5. Eukaryotic cell lines

Name	Cell type	Source
HEK293	human embryonic kidney epithelial cell line	DSMZ
NF-κB/293/GFP-Luc	HEK293 NF-κB GFP/luciferase reporter cell line	System Biosciences
U2-OS	human osteosarcoma cell line	DSMZ
U2-OS-PIP4K2C-KO	PIP4K2C CRISPR knockout U2-OS cells	see 6.3.5
U2-OS-PIP4K2A-KO	PIP4K2A CRISPR knockout U2-OS cells	see 6.3.5
U2-OS-PIP4K2A/2C-DKO	PIP4K2A/C CRISPR double knockout U2-OS cells	see 6.3.5
U2-OS-TRAF6-KO	TRAF6 CRISPR knockout U2-OS cells	Krappmann lab
U87	Glioblastoma cell line	Gargiulo lab
U251	Glioblastoma cell line	Gargiulo lab
NCH	Glioblastoma cell line	Gargiulo lab
GBM2	Patient-derived glioblastoma cell line	Gargiulo lab
GBM166	Patient-derived glioblastoma cell line	Gargiulo lab
GIC	Patient-derived glioblastoma cell line	Gargiulo lab

5.6. Oligonucleotides

Primer	Source	Sequence
<i>CLK2_Fw</i>	BioTeZ	5'-TTCGGCCGAGTTGTACAATG-3'
<i>CLK2_Rv</i>	BioTeZ	5'-AGCACGTTGATCTCAAGTCG-3'
<i>CLK4_Fw</i>	BioTeZ	5'-CGAGCTCGTTCAGAAATCCAAG-3'
<i>CLK4_Rv</i>	BioTeZ	5'-TAGCATCTGGACACATCGGAAG-3'
<i>NFKBIA_Fw</i>	BioTeZ	5'-TTGGGTGCTGATGTCAATGC-3'
<i>NFKBIA_Rv</i>	BioTeZ	5'-ACACCAGGTCAGGATTTTGC-3'
<i>GAPDH_Fw</i>	BioTeZ	5'-AATCCATGGCACCGTCAAG-3'
<i>GAPDH_Rv</i>	BioTeZ	5'-ATCGCCCCACTTGATTTTGG-3'
<i>B2M_Fw</i>	BioTez	5'-TACTGAATTCACCCCACTG-3'
<i>B2M_Rv</i>	BioTeZ	5'-TGCTGCTTACATGTCTCGATCC-3'

siRNA	Source	Sequence
<i>BRCA1</i> si 1	Santa Cruz I#12519	Not disclosed
<i>PIP4K2C</i> si 1	Eurogentec	5'-GCUCCUGUUACUAUAAUAA-3'
<i>PIP4K2C</i> si 2	Eurogentec	5'-GCAGUAUGGAUGUCUUCAU-3'

<i>PIP4K2C</i> si 3	Eurogentec	5'-CAGCAACCAUUGCUCUUUA-3'
<i>PIP4K2C</i> si 4	Eurogentec	5'-GCUCCAAGAUCAAGGUCAA-3'
<i>PIP4K2A</i> si 1	Eurogentec	5'-CGAGCCAUUUCAAGUUUAA-3'
<i>PIP4K2A</i> si 2	Eurogentec	5'-GAGACAGUUAUCAGAAUAA-3'
<i>PIP4K2A</i> si 3	Eurogentec	5'-CCGAGCCAUUUCAAGUUUA-3'
<i>NEDD4L</i> si 1	Eurogentec	5'-CCUCCACCCUCUACUUUAU-3'
<i>NEDD4L</i> si 2	Eurogentec	5'-GGAGACAGCAUUCUAUUUA-3'
<i>NEDD4L</i> si 3	Eurogentec	5'-CCAGAGAAAUCACCUUAAU-3'
<i>CLK2</i> si 1	Eurogentec	5'-CCUCCUGGCUCUCUAUAUA-3'
<i>CLK2</i> si 2	Eurogentec	5'-GCUGCAUCAUCUUUGAAUA-3'
<i>CLK4</i> si 1	Eurogentec	5'-GGGAGAAAGAGGAUUUGAU-3'

5.7. Kits and enzymes

Product	Manufacturer
GoTaq qPCR Master Mix	Promega
iScript cDNA synthesis Kit	Biorad
RNA 6000 Nano Assay Kit	Agilent
Klenow Fragment, DNA Polymerase I	New England Biolabs
Subcellular Fractionation Kit for Cultured Cells	Thermo Fisher
Lambda protein phosphatase	New England Biolabs
Qiaquick plasmid maxiprep kit	Qiagen
Qiaquick RNEasy RNA extraction kit	Qiagen
Qiaquick Nucleotide Removal Kit	Qiagen
PIP-Strip lipid binding assay	Echelon Biosciences

5.8. Software

Software and algorithms	Manufacturer
Bio-Rad CFX Maestro	Bio-Rad
Image-Lab 3.0	Bio-Rad
Prism 7.04	GraphPad
ImageJ	National Institutes of Health

6. Methods

6.1. Molecular biology methods

6.1.1. RNA isolation

For RNA isolation cells were washed with ice-cold PBS. Isolation of RNA was then performed using spin columns according to manufacturer's instructions (Qiagen, RNeasy RNA isolation kit).

6.1.2. Determination of nucleic acid concentration

Using a UV light spectrophotometer DNA/RNA concentration was measured at OD260. Protein or chemical contaminations were checked by measurement of ratios of OD260/280 and OD260/230. Further analyses were performed on samples with OD260/280 ratios of about 2.

6.1.3. Reverse Transcriptase-PCR

Complementary DNA (cDNA) was generated by reverse transcribing 500-1000 ng total RNA using the iScript cDNA synthesis Kit (Promega) following manufacturer's instructions.

6.1.4. Quantitative real-time PCR (qRT-PCR)

To quantitate specific mRNA (messenger RNA) species in samples, RNA was isolated, RNA concentration was measured, and mRNA was then transcribed into cDNA. The amount of mRNA transcripts of certain genes within a sample was quantified by employing gene specific primers and using a C-1000 Thermal cycler (Biorad). The expression of genes of interest was normalised against two or three reference genes (*GAPDH*, *RPL_13a*, and *B2M*) using the CFX manager software. The fold induction of mRNA was calculated over untreated sample levels by the $\Delta\Delta$ -Ct method.

6.1.5. Mutagenic PCR

New England Biolab's (NEB) Exchanger kit was used to generate single amino acid mutations in plasmids. Based on the published sequence information of the TRAF6 plasmid (AddGene #21624), the respective codon of the target lysine 388 and lysine 356 was changed to code for glutamate. The NEB

exchanger suggests an optimal codon and primer sequence for amplification, which were then synthesized by Biotech. Mutagenic PCR was then performed using the mutagenic primers based on the recommended PCR program from the NEB software. Wild-type plasmid was removed using methylation-dependent nuclease Dpn1, leaving only the mutant plasmids. Sanger sequencing was used to confirm the introduction of the intended mutation and the absence of frameshift or other problematic mutations

6.2. Protein biochemical methods

6.2.1. Whole cell lysis

Cell pellets were resuspended in 3 volumes of Bäuerle lysis buffer on ice and lysed for 20 min while shaking moderately at 4 °C. Samples were centrifuged at 20,000 × *g* for 10 min at 4 °C and the supernatant, representing the whole cell protein extract, was transferred into a new 1.5 ml reaction tube.

6.2.2. Subcellular fractionation

For the preparation of nuclear and cytoplasmic fractions, cells were lysed with buffer A (supplemented with 1 mM DTT, 10 mM NaF, 20 mM β-glycerophosphate, 250 nM NaVO₃, complete protease inhibitor cocktail (Roche) and 50 nM calyculin A. Lysates were adjusted to a final concentration of 0.2% NP-40, vortexed for 10 s and spun down. The supernatant, representing the cytoplasmic extract (CE), was transferred into a new 1.5 ml reaction tube. The pellet was washed with buffer A, was resuspended with buffer C and shaken for 20 min at 4 °C. Following 10 min of centrifugation at 14,000 rpm, the supernatant, representing the nuclear extract (NE), was transferred into a new reaction cap.

6.2.3. Determination of protein concentration

To determine protein concentration of cell lysates, 1-2 μl of protein extracts were mixed with 1 ml Bradford reagent diluted 1:5 with ddH₂O. Absorbance was measured in a spectrophotometer at a wavelength of 595 nm against a lysis buffer reference and was compared to a BSA standard curve.

6.2.4. SDS-PAGE

For preparation of cell lysates for SDS-PAGE 20-40 µg of protein lysates were mixed with 6x reaction buffer and heated to 95 °C for 4 min. After boiling samples were loaded into a poly-acrylamide gel. Gels were casted consisting of a separating gel and a stacking gel. The concentration of acrylamide within the separating gels was depending on the experiment and the desired separation between certain molecular weights, but generally ranged between 8% and 12%.

Stacking gel

Tris-HCl, pH 6.8	125 mM
Acrylamide	5%
SDS	0.1%
APS (ammonium persulphate)	0.1%
TEMED	0.1%

Separation gel

Tris-HCl, pH 8.8	375 mM
Acrylamide	8-12 %
SDS	0.1%
APS	0.075%
TEMED	0.05%

After sample loading a voltage of 80 V was applied to allow protein concentration at the border line of stacking and separating gel. Afterwards, voltage was increased to 140 V and proteins were separated for circa 2 h.

6.2.5. Western Blot

Proteins separated by SDS-PAGE (polyacrylamide gel electrophoresis) were immobilised by Western blotting (WB) to methanol-activated PVDF membrane using transfer buffer and a semi-dry blotting apparatus. Proteins were transferred to membranes by applying a constant current of 80 mA per 6x9 cm membrane for 90 min. For the transfer of small proteins (<30 kDa) the blotting time was reduced to 30 min. Membranes were blocked in 3-5% milk in TBS-T for 30 minutes – 1 hour. Primary antibodies were incubated in blocking solution, typically at 1:1000, overnight at 4 °C on a roller. Membranes were washed 3 x 5 min in TBS-T. Secondary antibodies were incubated 1:5000-1:10000 in blocking solution for 1 h at TR. Membranes were washed 5 x 5min in TBS-T, followed by 1 x 5min in PBS.

6.2.6. Electrophoretic Mobility Shift Assay

Nuclear or whole cell lysates were incubated with a ³²P-labeled NF-κB DNA-consensus sequence. The shift mixture was prepared following the shift mixture recipe:

Shift mixture for EMSA (H2K/NF-κB)

total lysate	3-5 µg
2x shift buffer	10.0 µl
BSA (10 ng/µl)	1.0 µl
DTT (100 mM)	0.4 µl
Poly dl-dC (2 µg/µl)	1.0 µl
³² P-labeled oligonucleotide	45,000 cpm
ddH ₂ O	ad 20 µl

The shift mixture was incubated for 30 min at 37 °C before the samples were loaded onto an EMSA gel:

EMSA gel recipe (native polyacrylamide gel)

ddH ₂ O	44 ml
10X TBE	6 ml
Acrylamide (30%)	10 ml
APS (10%)	450 µl
TEMED	45 µl

For electrophoresis, a current of 26 mA was applied for 2 h. After drying the gel onto a Whatman paper, signals were visualised on an autoradiography film (GE Healthcare) after overnight incubation at -80 °C in a radiography cassette.

All work using radioactive substances were done at a monitored workspace suitable for radioactive work.

6.2.7. PIP Strip

1 µL of secondary antibody was spotted directly onto open areas of the dry membrane as a control for the HRP conjugate and detection reagent and allowed to dry completely before proceeding. The membrane was blocked with 5 to 10 mL of blocking buffer PBS-T + 3% BSA and gently agitated for one

hour at room temperature (RT). Protein of interest was added after discarding blocking buffer at 0.5 µg/mL TRAF6 protein in 5 mL PBS-T + 3% BSA and incubated for 1 h at RT with gentle agitation. The membrane was washed with >5 mL PBS-T three times with gentle agitation for ten minutes each. Wash solutions were discarded and rabbit anti-TRAF6 (D21G3) (CST #8028) was added 1:1000 to 5 mL PBS-T + 3% BSA blocking solution and incubate for 1 h at RT with gentle agitation. Membrane was washed again as in previous wash. HRP-conjugated anti-rabbit secondary (JacksonImmunoResearch 711-035-152) was added 1:10000 in 5 mL PBS-T + 3% BSA blocking solution and incubate for 2 h at RT with gentle agitation. Membrane was washed again as before but five times rather than three. Signal was detected with ECL as described in the Western blotting protocol (6.2.5).

6.3. Cell biology methods

6.3.1. Cell culture

All cell lines were cultured in media supplemented with 10% FCS and penicillin/streptomycin (100 U/ml and 100 µg/ml) in 95% relative humidity and 5% CO₂ atmosphere. U2-OS and HEK293 cells were cultured in DMEM (Gibco).

For passaging, cells were washed with PBS, trypsinised with trypsin/EDTA solution at 37 °C until detachment from the plate and suspended in the corresponding medium. Splitting ratios were between 1:3 to 1:6 for U2-OS.

For cryo-conservation in liquid nitrogen cells were trypsinised at 37 °C, suspended in medium and pelleted by centrifugation at 320 × *g* for 5 min. Afterwards, cells were resuspended in freezing medium (corresponding medium supplemented with 20% FCS, 10% DMSO and penicillin/streptomycin) and were frozen in freezing boxes containing isopropanol in a -80 °C freezer. Cells were transferred to liquid nitrogen at the following day.

Thawing of cells was done in at 37 °C in a water bath. Partially-frozen cells were pipetted dropwise to 37 °C pre-warmed medium and centrifuged for 5 min at 300 × *g*. Finally, cells were resuspended in fresh complete medium.

6.3.2. Stimulation of cells with cytokines

For the activation of the canonical NF- κ B pathway cells were treated with recombinant human TNF α (10 ng/ml) or IL-1 β (10 ng/ml) for 20-30 min at 37 °C.

6.3.3. Induction of DNA damage

Genotoxic stress was applied by ionizing irradiation of cells with a Cs137 source (OB29 Irradiator, STS Braunschweig), or by inhibition of the topoisomerase II enzyme by administration of etoposide at concentrations between 20-50 μ M for 2 h.

6.3.4. siRNA transfection

2 x 10⁵ cells were seeded into each well of a 6-well plate one day before the transfection. 10 μ M of working solutions for each siRNA was prepared. 3 μ l of siRNA working solution was added to 150 μ l of OPTIMEM. 9 μ l of RNAimax was also added into 150 μ l OPTIMEM medium in a separate tube. The first tube containing the siRNA/OPTIMEM mix was then added to the second tube with RNAimax/OPTIMEM mix and was incubated at room temperature for 5 minutes. The mixture was then added to the cells in a dropwise manner. Subsequent experiments were done 72 hours post-transfection.

6.3.5. Generation of CRISPR knockout cell lines

Guide RNAs were selected from the GeCKOv2 library and cloned into the LentiCRISPRv2 plasmid, which was confirmed by Sanger sequencing. LentiCRISPRv2 vectors containing respective guide RNAs were transfected into HEK293T cells together with psPAX2, pCMV, pVSV-G plasmids containing viral packaging components using polyethyleneimine (PEI). Lentiviruses were harvested and transduced into U2-OS cells, which were then subjected to puromycin selection for 3 days. Surviving cells were trypsinized from the plate and clones were green fluorescent protein (GFP)-sorted into 96-well plates as a second round of selection for cells successfully expressing the LentiCRISPRv2 vector. The plates were monitored colony growth and expanded for downstream analysis. Clones were screened for protein knockout by loading 40ug of protein and analyzing target protein level by western blot.

6.3.6. Immunofluorescence staining and confocal microscopy

For immunofluorescence staining 0.95×10^5 cells were seeded in 6 well plates onto autoclaved cover slips. Cellular confluency dictated the beginning of the experiment (2-3 days from seeding). After conduction of experiments cells were washed with PBS and fixed with 4% PFA/double-distilled H₂O (ddH₂O) for 10 min at RT. Following two additional washing steps cells were incubated with a solution containing 0.12% glycine/0.2% saponin in PBS for 10 min and then blocked with a solution containing 10% FCS/0.2% saponin in PBS for 1 h. Primary antibody incubation was performed overnight at 4 °C (1:500 diluted in 0.2% saponin in PBS). The next day, cover slips were washed five times with a solution containing 0.2% saponin in PBS. Fluorophore-coupled secondary antibodies (1:1000 diluted in 0.2% saponin in PBS) were incubated for 1 h (hour) at RT. Nuclei were stained using 0.2 mg/ml DAPI in PBS for 5 or by directly mounting with DAPI/Mowiol. Finally, the cover slips were washed five times with 0.2% saponin in PBS and two times with ddH₂O. Confocal microscopy was performed using a Zeiss 710 LSM with a 40x or a 63x oil objective.

6.3.7. Cell Harvesting

Tissue culture plates of interest were washed with ice-cold PBS. The cells were scraped in PBS using cell scrapers and the cell suspension was transferred to 1.5 ml reaction tubes. Cells were pelleted by centrifugation at $20,000 \times g$ for 15 s at 4 °C. The supernatant was discarded and cells were snap frozen or lysed directly.

7. Results

7.1. Validation of DNA damage-specific NF- κ B inhibitors MW01 and MW05

I began the study by confirming the specific inhibition of DNA damage-induced NF- κ B by two small molecules previously identified by our group, MW01 and MW05. This was accomplished in a manner mirroring the original small molecule screen, wherein NF- κ B activation following either DNA damage or TNF α treatment was observed in the presence of compounds. U2-OS cells were used due to the low basal level and inducible nature of NF- κ B activation, as in the original screen, and multiple readouts of NF- κ B activity were used to confirm the effects of the compounds. At the protein level, western blotting was performed to confirm NF- κ B inhibition by MW01 and MW05 by quantifying phosphorylation of S536 of p65 (p-p65) following stimulation by either irradiation or TNF α treatment. A complete reduction of p-p65 levels upon treatment with either MW01 or MW05 only following irradiation was observed, while TNF α -stimulated p65 phosphorylation remained comparable to DMSO-treated controls (Figure 7-1A, B). Note that irradiation at 20 Gy generally causes a weaker induction of NF- κ B when compared to TNF α . Similarly, RNA expression analysis of the NF- κ B target gene *NFKB1A* revealed a reduction to basal levels upon treatment with MW01 or MW05 only following irradiation while TNF α -stimulated expression remained comparable to DMSO-treated controls (Figure 7-1C). Taken together, these results confirmed the DNA damage-specific inhibition of NF- κ B activity by MW01 and MW05 and expanded upon the results of the previous work performed in our group.

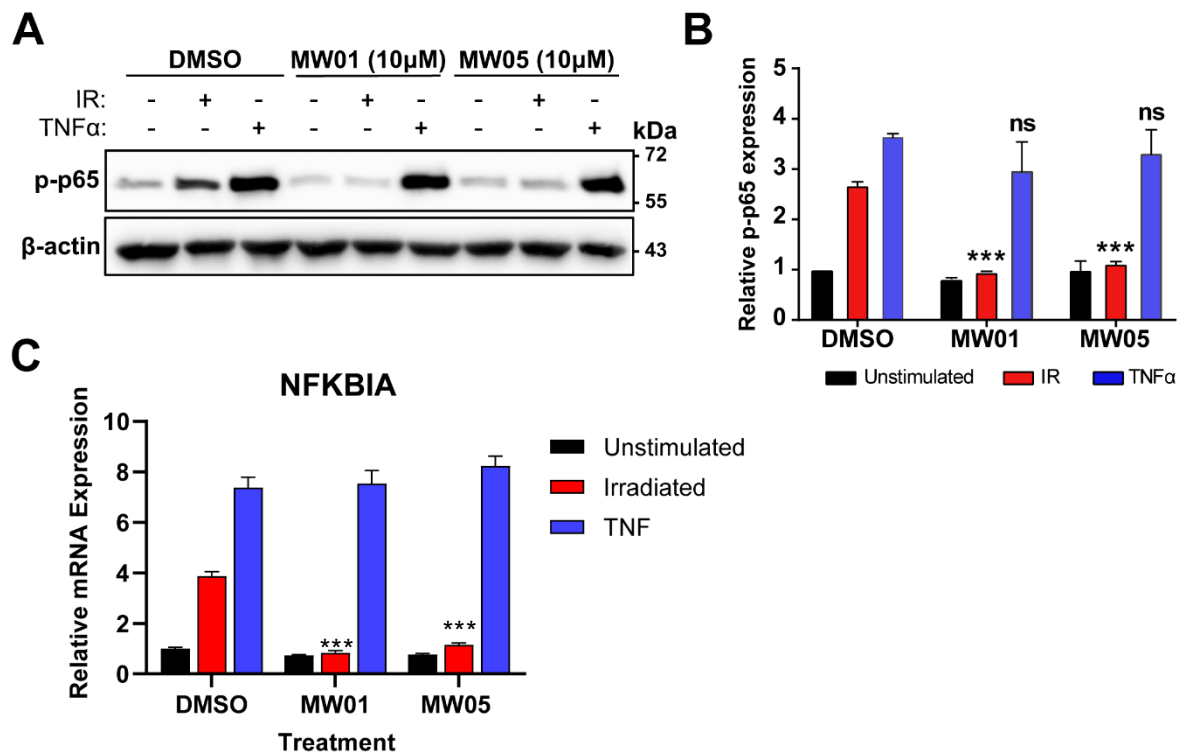


Figure 7-1: Validation of MW01 and MW05 inhibitory effect in primary NF-κB activity assays.

(A) Western blot analysis of NF-κB-p65 S536-phosphorylation following 1-hour pre-treatment with DMSO, MW01 (10 μM), or MW05 (10 μM), in unstimulated cells, after 90 min irradiation (IR, 20 Gy), or after 20 min TNFα (10 ng/mL) in U2-OS cells. β-actin was used as loading control. (B) Quantification of three independent replicates of experiment in (A). The p-p65 signal was normalized to β-actin per sample. Relative activation of NF-κB was compared to the unstimulated DMSO-treated condition with 2-way ANOVA. ns: not significant; ***: P<0.001. (C) RNA expression analysis for NF-κB target gene *NFKB1A* using same experimental setup as in (A), with 2-way ANOVA. ***: P≤0.001.

To examine cell-type specificity and in anticipation of later higher-throughput experiments, a dose-response experiment was performed for both MW01 and MW05 in an NF-κB luciferase reporter cell line, NF-κB/293/GFP-Luc. Maximal inhibition of irradiation-induced NF-κB-luciferase reporter activity was reached with 2.5 μM MW01 and with 10 μM MW05 (Figure 7-2A, B). TNFα-stimulated luciferase activity was not significantly changed at any tested concentration by MW01, but was reduced to some extent at 2.5, 5, and 10 μM by MW05, albeit much less so than irradiation-stimulated activity (Figure 7-2A, B). I suspect this was not due to inhibition of the initial TNFα-stimulated NF-κB signal cascade, but instead to regulatory processes that occurred during the 5-hour incubation period following stimulation that is required to synthesize the luciferase reporter protein during the assay. Considering the completely different structure of MW01 and MW05, it is possible that only MW05 interacts with a component of the signaling cascade activated by hours-scale TNFα exposure. From these data, I concluded that the NF-κB/293/GFP-Luc luciferase reporter assay was reliable to assess NF-κB activity

only following DNA damage and that further TNF α -stimulated reporter assay data would be considered secondary to p-p65 level or *NFKBIA* expression analysis. In addition, I confirmed the previous findings that the compounds inhibit genotoxic stress-induced NF- κ B in HEK293 cells in a manner comparable to the main cell-type used throughout the study, U2-OS.

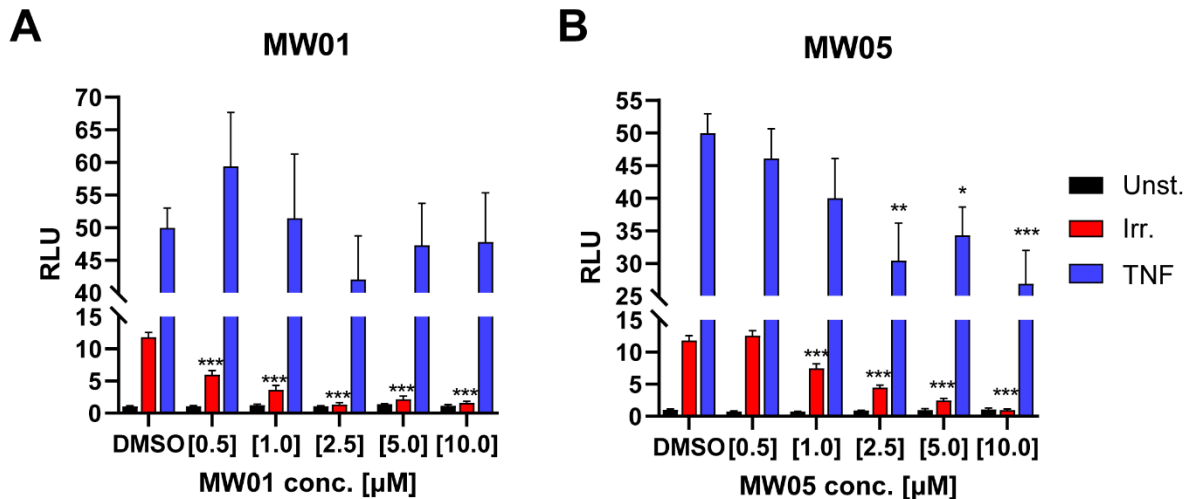


Figure 7-2: MW01 and MW05 inhibit NF- κ B reporter expression in a dose-dependent manner.

(A) Dose-response of MW01 in the HEK293-NF- κ B-Luc-GFP cell line in unstimulated, after 90 min irradiation (IR, 20 Gy), or after 20 min TNF α (10 ng/mL) condition. (B) Dose-response of MW05 in HEK293-NF- κ B-Luc-GFP cells in unstimulated, after 90 min irradiation (IR, 20 Gy), or after 20 min TNF α (10 ng/mL) condition. Statistical comparison with 2-way ANOVA. *: $P \leq 0.05$; **: $P \leq 0.01$; ***: $P \leq 0.001$; all other comparisons are not significant.

To better understand where a putative target could act within the pathway, several critical DNA damage-induced NF- κ B signaling events were analyzed following treatment with MW01 or MW05. IKK γ mono-ubiquitination, which is a prerequisite for IKK complex activation⁴⁴, was analysed by immunoprecipitation of IKK γ . The band corresponding to the mono-ubiquitinated form of IKK γ was exclusively observed in the DMSO-treated irradiated control, while pre-treatment of cells with MW01 or MW05 led to the abolishment of the IKK γ mono-ubiquitination (Figure 7-3A). In order to analyse the influence of MW01 and MW05 on the ATM-dependent IKK γ phosphorylation at S85, cells were pre-treated with the compounds and irradiated. MW01 and MW05 pre-treatment abolished the phosphorylation of IKK γ at S85 in a manner comparable to ATM inhibitor KU55933 (Figure 7-3B). In conclusion, MW01 or MW05 inhibited the formation of essential IKK γ post-translational modifications that are required for DNA damage-induced NF- κ B activation, thereby localizing the action of the compounds upstream of IKK.

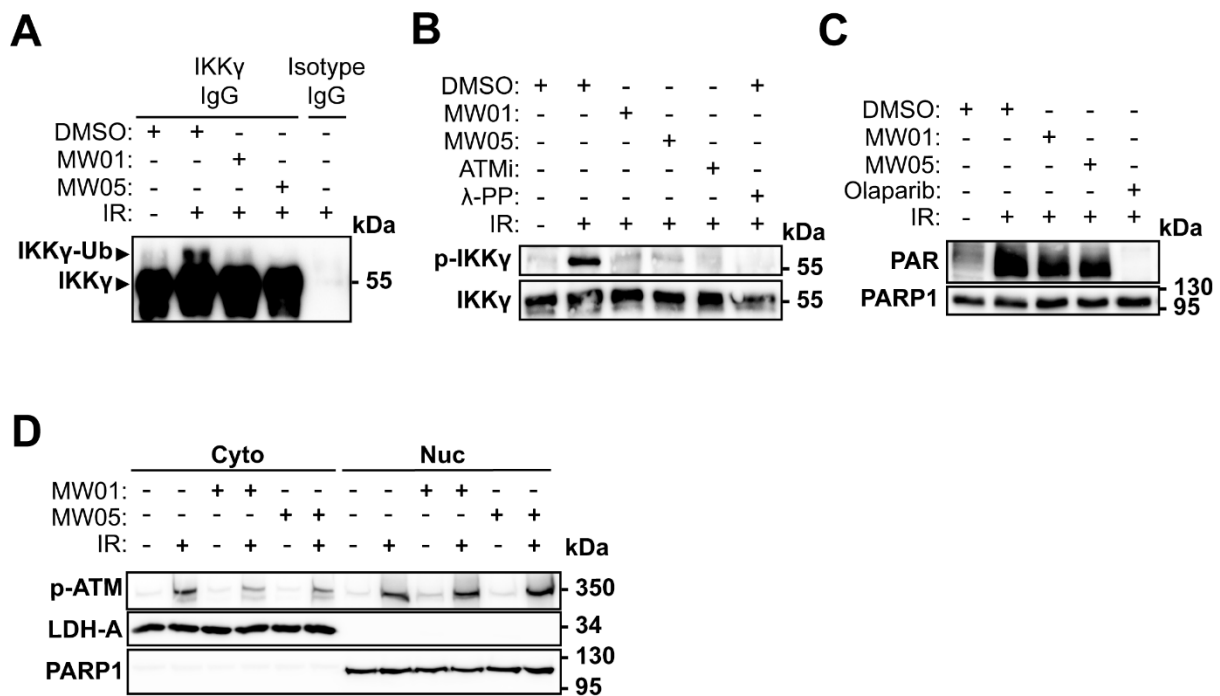


Figure 7-3: MW01 and MW05 inhibit critical genotoxic stress pathway steps.

Panels A-D are adapted from Mucka et al. 2023. Panels A-C were performed by Michael Willenbrock (A) HEK293 cells were pre-treated for 1 hour with the indicated substances, irradiated, and protein lysate obtained. Immunoprecipitation of IKKγ was performed on the lysates and subsequently used to detect the presence of IKKγ-Ub by immunoblot. (B) Western blot analysis for pS85-IKKγ and IKKγ in U2-OS cells were pre-treated for 1 hour with the indicated substances, irradiated, and lysed. (C) Western blot analysis of lysates from U2-OS cells detecting PAR and PARP1 treated as above with the indicated substances. (D) Western blot analysis of cytoplasmic (Cyto) and nucleoplasmic (Nuc) fractions of U2-OS cells treated with DMSO, MW01, or MW05 and irradiated. LDH-A and PARP1 were used as cytoplasmic and nuclear fraction markers, respectively.

Stilmann and colleagues described the enzymatic activity of PARP1 was essential for PARP1 signalosome formation and recruitment of other signaling components to initiate the DNA damage-induced NF-κB signaling cascade⁶². The effect of MW01 and MW05 on PARP1 enzymatic function was previously analyzed, revealing a strong band detected using a PAR chain specific antibody in DMSO, MW01, and MW05 pre-treated samples following irradiation in U2-OS cells, indicating PARP1 activity was not inhibited by either compound (Figure 7-3C). In contrast, pre-treatment of cells with the clinically approved PARP inhibitor Olaparib¹¹⁷ led to the inhibition of PAR chain formation, illustrating that MW01 and MW05 did not interfere with activation of PARP1 enzymatic activity (Figure 7-3C).

To investigate the effect of MW01 and MW05 treatment on pathway components still further upstream, ATM activation and cytoplasmic translocation were analyzed. Subcellular fractionation revealed the phosphorylation of S1981 on ATM (p-ATM), a critical DNA damage-induced ATM auto-

phosphorylation site, was unchanged in the nuclear fraction by pre-treatment with either MW01 or MW05 (Figure 7-3D). However, a notable reduction in irradiation-induced p-ATM levels in the cytoplasmic fraction was observed following treatment with either compound compared to DMSO-treated controls (Figure 7-3D). These data illustrate that MW01 and MW05 do not inhibit the enzymatic activity of ATM but do reduce cytoplasmic accumulation of p-ATM, which is a critical step in activating NF- κ B following DNA damage. Considered together with the abolishment of critical IKK post-translational modifications and un-affected PAR synthesis, these data suggest that the putative target of MW01 or MW05 is upstream of IKK and downstream of ATM activation, and thus is likely a nuclear protein.

7.2. Investigation of treatment contexts for MW01 and MW05

7.2.1. MW01 and MW05 potentiate apoptosis by unbalancing the NF- κ B/p53 axis

To determine possible treatment contexts for the compounds, I assessed the efficacy of MW01 and MW05 in inducing cell death in several *in vitro* models. Cell fate decisions depend on a balance of anti- and pro-apoptotic signals, of which NF- κ B and p53 are the major contributing transcription factors, respectively^{96,133}. To analyse the effect of MW01 and MW05 on apoptotic cell death after genotoxic stress in more detail, apoptotic marker cleaved PARP1 was detected by western blot (Figure 7-4A). The pre-treatment of U2-OS cells with MW01 or MW05 led to a slight increase of PARP1 cleavage in unstimulated cells (Figure 7-4A). After irradiation of cells, a marginal increase of PARP1 cleavage was detected in the irradiated control. In contrast, MW01 and MW05 pre-treatment strongly increased the cleavage of PARP1 following irradiation (Figure 7-4A).

To show that the inhibition of NF- κ B by MW01 and MW05 led to the downregulation of anti-apoptotic signaling, induction of anti-apoptotic NF- κ B target gene *BIRC3*, which encodes cIAP2, was analysed by quantitative real-time PCR. The pre-treatment of U2-OS cells with MW01 or MW05 did not significantly change the mRNA expression of the genes *BIRC3* in comparison to the DMSO control (Figure 7-4B). Irradiation of cells led to a nearly two-fold induction of *BIRC3* mRNA in the irradiated control, but *BIRC3* mRNA was downregulated in MW01 and MW05 pre-treated cells (Figure 7-4B). Taken together with the increased cleavage of PARP, these data illustrate that MW01 and MW05 increase apoptosis by inhibiting anti-apoptotic signaling by NF- κ B.

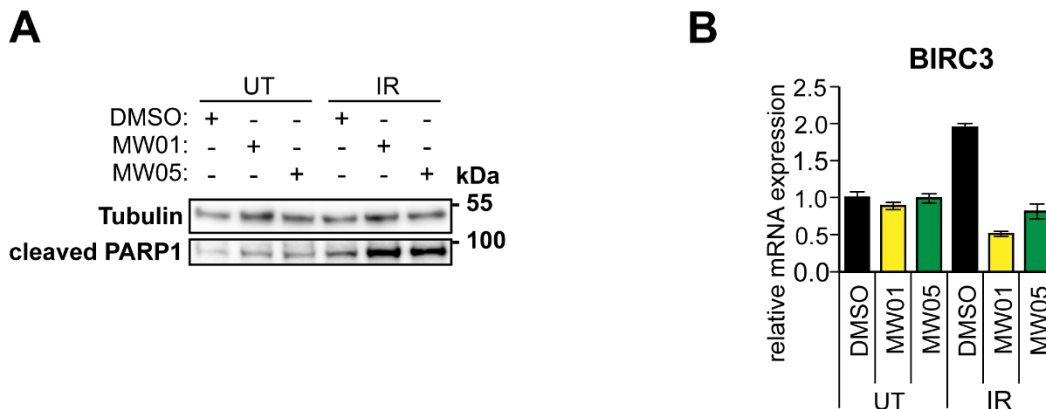


Figure 7-4: MW01 and MW05 increase apoptotic markers following irradiation.

Both panels adapted from Mucka et al. 2023 and performed by Michael Willenbrock (A) Western blot analysis of U2-OS cells treated with DMSO, MW01, or MW05 following irradiation. Apoptosis marker cleaved PARP1 and loading control Tubulin were detected. (B) RNA expression analysis of anti-apoptotic NF- κ B target gene BIRC3 in U2-OS cells treated with DMSO, MW01, or MW05 following irradiation.

Due to the important function of the DNA double strand break-induced IKK-NF- κ B pathway in anti-apoptotic signaling⁶², I hypothesized that both MW01 and MW05 should sensitize cells to DNA damaging agents, thus supporting their potential use to potentiate genotoxic therapies. To characterize the effect of MW01 and MW05 on cell viability, U2-OS cells were treated with each compound alone or in combination with etoposide. MW01 and MW05 alone slightly reduced cell viability after 6, 24, and 48 hours compared to DMSO-treated controls (Figure 7-5A). Importantly, at 48 hours, MW01 or MW05 treated cells did not display any obvious characteristics of cell death, suggesting that the compounds are not grossly toxic (Figure 7-5A, B). MW01 and etoposide co-treatment significantly reduced cell viability after 6 hours, while MW05 and etoposide co-treatment yielded a significant reduction after 24 hours, compared to etoposide alone (Figure 7-5A). Interestingly, 24 hours after co-treatment with either MW01 or MW05 and etoposide, attached cells were visibly distressed and the number of floating cells was drastically increased compared to etoposide alone (Figure 7-5B). This effect was greatly increased at 48 hours, with relatively fewer attached cells and more floating cells, indicating potentiated cell death upon MW01- or MW05-etoposide co-treatment (Figure 7-5B).

To investigate the underlying molecular causes of this phenotype, markers of NF- κ B and p53 activation, DNA damage, and apoptosis were analyzed after single and co-treatment with MW01, MW05, and

etoposide. MW01 and MW05 blocked etoposide-stimulated p65 phosphorylation, thereby validating inhibition of IKK and NF- κ B activity (Figure 7-5C). At 24 hours, a weak activation of γ H2AX in MW01 treatment alone was apparent compared to DMSO-treated controls (Figure 7-5C). Moreover, γ H2AX activation was persistent in MW01 and etoposide co-treatment as well as in MW05 and etoposide co-treatment compared to DMSO-treated controls, indicating an accumulation of DNA damage (Figure 7-5C). MW01 or MW05 treatment alone did not cause an increase in cleaved caspase-3 at 24 hours, suggesting again that the compounds alone are not grossly toxic. By contrast, this apoptosis marker was increased following MW01 and etoposide co-treatment as well as after MW05 and etoposide co-treatment (Figure 7-5C). A stabilization of p53 following MW01 treatment alone and in co-treatment of both lead compounds with etoposide was observed compared to DMSO (Figure 7-5C). I suspect the disparity in γ H2AX, p53, and cleaved caspase-3 levels between MW01 and MW05 in etoposide co-treatment is due to MW01 co-treated cells more quickly undergoing p53-mediated cell death compared to MW05. Thus, in the co-treatment at 24 hours, γ H2AX levels were comparatively lower and cleaved caspase-3 higher for MW01 than MW05 because the apoptotic cells are no longer repairing DNA damage. Considered with the cell viability and image data, these results indicate that MW01 and MW05 may be promising lead compounds for cancer therapeutics due to their reduction of pro-survival NF- κ B target gene expression and concomitant increase in apoptotic markers in co-administration with chemo- or radiotherapy.

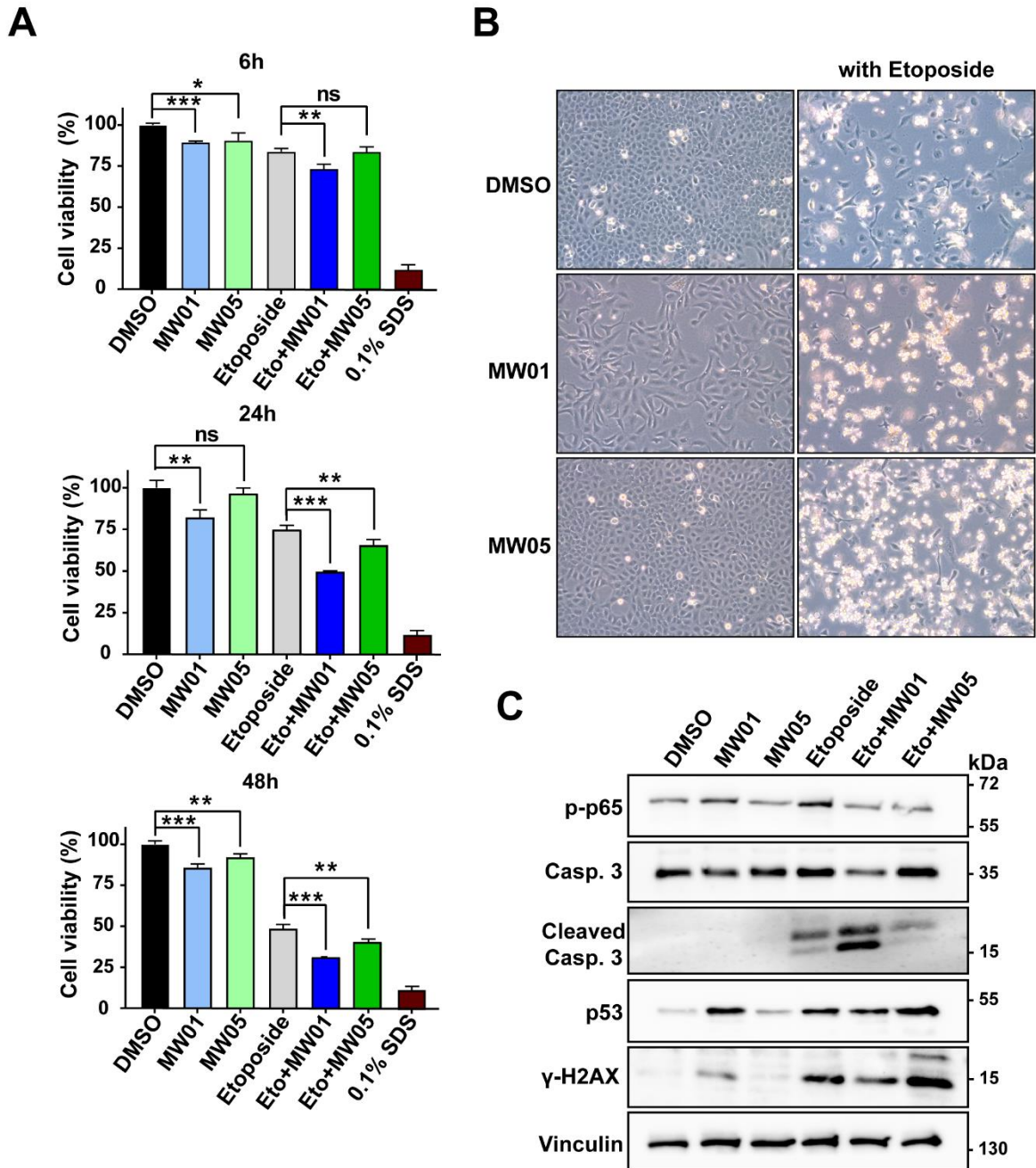


Figure 7-5: MW01 and MW05 reduce cell viability and induce markers of DNA damage and cell death in co-treatment with etoposide.

(A) Relative cell viability of U2-OS cells at 6, 24, and 48 hours following single treatment with either DMSO, MW01, MW05, or Etoposide (Eto), or co-treatment of either MW01 or MW05 with etoposide. Comparison with 2-way ANOVA. *: $P \leq 0.05$; **: $P \leq 0.01$; ***: $P \leq 0.001$; ns: not significant. (B) Light microscopy images of U2-OS cells following the same treatments as (A) at 48 hours. Single treatments on left and co-treatment with etoposide on right. (C) Western blot analysis of lysates from U2-OS following the same treatments as (C) at 24 hours.

7.2.2. MW01 and MW05 block NF- κ B activation from on-going DNA damage and potentiate the effects of PARP inhibitor Olaparib

BRCA1 is a tumor suppressor gene regulating DNA damage repair and gene transcription in response to double-strand breaks. Numerous kinases, including ATM, phosphorylate *BRCA1* in response to DSBs, which is then recruited to DNA damage foci where it initiates the homologous repair mechanism to repair DSBs. Without this critical repair mechanism, patients with inherited or acquired mutations in *BRCA1* or *BRCA2* are predisposed to breast and ovarian cancers due to subsequent genomic instability and tumorigenesis¹²⁰. Currently, these patients are treated with PARP inhibitors, which impair single-strand break repair and exploit a proposed synthetic lethality strategy aimed at further impairing DNA damage repair, leading to catastrophic genomic instability and tumor cell death. PARP inhibitor resistance is frequently observed in the clinic, thus there is dire need for alternative approaches to exploit similar synthetic lethality strategies^{114,123,134}. Previous work by our group illustrated that PARP1-dependent NF- κ B activation and apoptosis protection may be an alternative mechanistic explanation for the effect of PARP inhibitors and therefore that strategies targeting NF- κ B might be useful in similar contexts to PARP inhibitors⁶².

To investigate this hypothesis, MW01 and MW05 were tested in the context of on-going DNA damage, as in siRNA mediated *BRCA1* deficiency or in co-treatment with PARP inhibitor Olaparib. U2-OS cells were transfected with non-coding or *BRCA1*-targeting siRNAs and treated 24 hours later with MW01, MW05, Olaparib alone, or MW01 or MW05 in co-treatment with Olaparib. 48 hours following transfection, the cells were irradiated and whole cell lysates analysed by western blot at 24 hours after irradiation (Figure 7-6A, B). *BRCA1* knockdown was verified at protein level in both experiments and successful drug treatment was verified by observing reduction of p-p65 in MW01- or MW05-treated cells compared to DMSO-treated controls. In *BRCA1* knockdown conditions, both MW01 and MW05 alone increased DNA damage marker γ H2AX compared to DMSO-treated controls (Figure 7-6A, B). In addition, co-treatment with Olaparib in *BRCA1*-deficient cells led to a notable increase in γ H2AX, suggesting that under these conditions, the cells accumulate DNA damage faster than with either treatment alone. Further evidence of this effect is seen by comparing siNC-transfected single and co-treated γ H2AX levels, which are reduced compared to paired si*BRCA1* levels, likely due to the functional DNA damage repair mechanisms in those samples. p53 stabilization was observed in *BRCA1*-deficient cells following MW01 or MW05 alone at comparable levels to co-treatment with Olaparib. Considered together, these data suggest that MW01 and MW05 unbalance the p53/NF- κ B axis in favour of p53 and programmed cell death resulting from an accumulation of DNA damage.

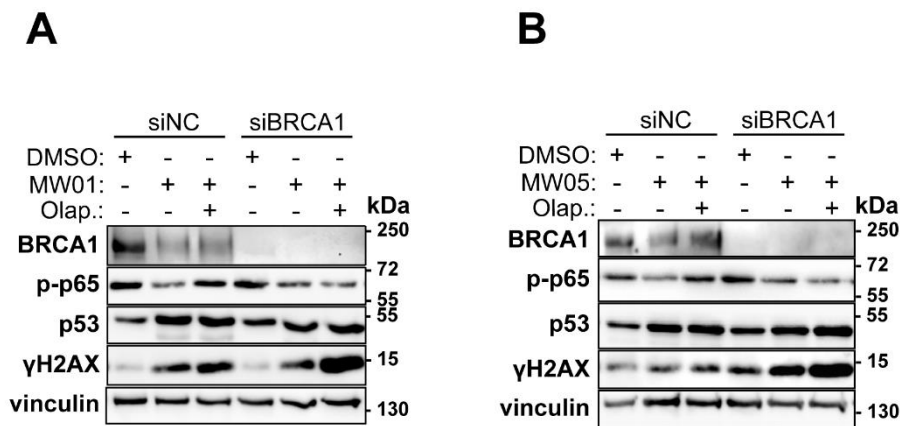


Figure 7-6: MW01 or MW05 pre-treatment leads to an accumulation of DNA damage in *BRCA1*-deficient cells.

(A) Western blot analysis of lysates from irradiated U2-OS cells transfected with non-coding or *BRCA1* siRNAs. Cells were treated with either DMSO, MW01, or Olaparib, or co-treated with MW01 and Olaparib. *BRCA1*, p-p65, p53, γ -H2AX, and vinculin were detected. (B) As in (A), with MW05 instead of MW01.

7.2.3. MW01 and MW05 reduce cell viability in glioblastoma cell lines

Glioblastoma is a lethal brain tumor that displays significant heterogeneity and therapeutic resistance, making successful treatment difficult and with average survival time of less than two years¹³⁵. Importantly, deregulated NF- κ B is critical driver of tumor progression and therapeutic resistance in glioblastoma¹³⁶⁻¹³⁸. Furthermore, several studies have shown that co-treatment with NF- κ B inhibitors can reverse therapeutic resistance observed with the current frontline treatment, temozolomide^{139,140}.

To determine if MW01 and MW05 could potentially be used to treat glioblastoma, several glioblastoma cell lines were treated with the compounds and cell viability was measured every 24 hours for 96 hours using a fluorescent cell viability assay. (Figure 7-7). In U87, U251, and NCH cell lines, MW01 treatment greatly reduced cell viability compared to DMSO-treated controls (Figure 7-7). However, no reduction below the initial 0-hour viability was observed in these cell lines, suggesting growth arrest rather than a cell killing effect of MW01. MW01 reduced cell viability of GBM2 patient-derived glioma cells to levels comparable to cell death control 0.1% SDS after 24 hours, suggesting the compound effectively killed the cells (Figure 7-7). In GBM166 and GIC cell lines, MW01 treatment slightly reduced cell viability compared at 24 and 48 hours to DMSO-treated controls and the initial viability reading, suggesting a weak cell killing effect (Figure 7-7). In GBM166 cells, the slight reduction continued at 72 and 96 hours compared to DMSO-treated controls, while in GIC cells the viability increased suggesting the cells recovered and continued growing (Figure 7-7). The effect of MW05 was similar to, but comparatively weaker than MW01 in all cell lines tested, except GBM2 (Figure 7-7). In these cells, no difference was

observed between MW05- and DMSO-treated controls, suggesting that the possible cell killing effect by MW01 might be due to a molecular target unique to that compound (Figure 7-7). Considering the weak effect of MW05 in most cases, MW01 appeared a more promising compound for continued testing in glioblastoma and further experimentation would investigate co-treatment with temozolomide or other chemotherapeutics.

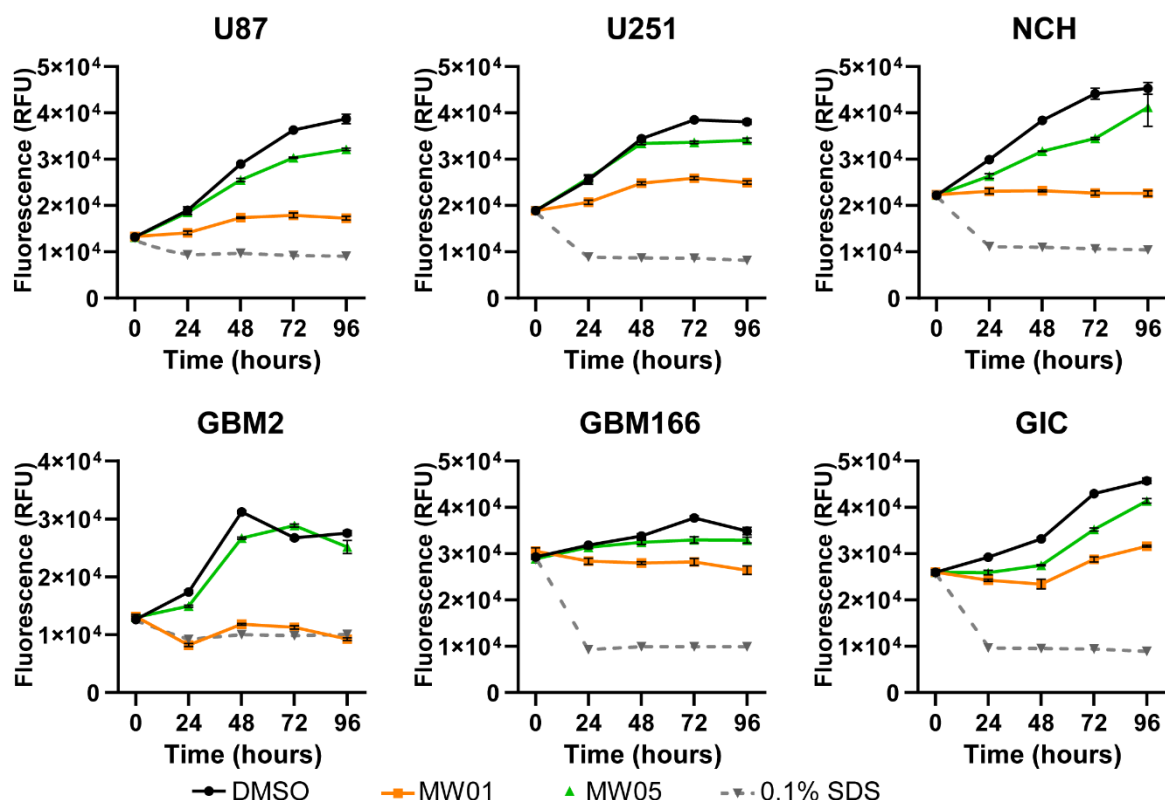


Figure 7-7: MW01 and MW05 reduce cell viability in glioblastoma cell lines.

Cell viability of several glioblastoma cell lines at 0, 24, 48, 72, 96 hours following treatment with DMSO, MW01, or MW05, measured using CellTiterFluor viability assay (Promega). Measurements expressed as relative fluorescence units (RFU). 0.1% SDS was included as a cell death control. Cell lines were generously provided by and cultured the Gargiulo lab.

7.3. Target Identification of MW01 and MW05

Based on their similar effects in the chemical library screen and signaling pathway analysis, MW01 and MW05 were used in comparative target identification studies seeking shared molecular targets. During the study, several target identification hypotheses were tested, each time leading to critical

information and allowing refinement of the approach. Broadly, preliminary target studies led to a mode of action and a high-throughput screen finding common hits between MW01 and MW05. Based on those results, several targets were systematically investigated, including notable off-targets, before finally identifying CLK2 and CLK4 as the true targets of the compounds.

7.3.1. PIP4K does not mediate the effect of MW01 or MW05

Previous work by our group in collaboration with the group of Mikhail Savitzki, EMBL, identified two isoforms of the lipid kinase Phosphatidylinositol 5-Phosphate 4-Kinase (PIP4K2), PIP4K2C and PIP4K2A, were bound by MW01 in a two-dimensional thermal proteome profiling (2D-TPP) with an IC50 of 45 nM and 290 nM, respectively, indicating high affinity for the protein. This profiling was carried out only on MW01 due to its better potency compared to MW05. The class II PIP4K family includes 3 members, PIP4K2A, PIP4K2B, and PIP4K2C, which catalyze the phosphorylation of phosphatidylinositol 5-phosphate to phosphatidylinositol 4,5-bisphosphate, are lipid signaling molecules with a range of functions within the cells¹⁴¹. Recent literature supports an important role for the PIP4K family in cancer as pharmacologic inhibition and genetic ablation have been shown to induce cell death in several tumor types^{142,143}. Based on this information, I investigated PIP4K2 as a potential target of MW01, with the intention of later confirming if these kinases are also shared targets of MW05.

To determine if PIP4K2C and A are required for DNA damage-induced NF- κ B activity, siRNA knockdown experiments were performed and NF- κ B-DNA binding assessed by EMSA (Figure 7-8A, B). Knockdown of PIP4K2C was robust for all siRNAs tested, but reduced irradiation-stimulated DNA binding in only 3 of 4 siRNAs (si's 1, 2, and 4) (Figure 7-8A). In addition, for TNF-stimulated DNA binding, a large reduction was observed with PIP4K2C si 4 and a moderate reduction for PIP4K2C si 2 (Figure 7-8A). Despite this violation of genotoxic stress specificity for MW01's molecular target, I remained open to the possibility that interregulation between PIP4K2 isoforms might confer such specificity¹⁴⁴. Knockdown of PIP4K2A was similarly efficient for all 3 PIP4K2A siRNAs tested and reduced irradiation-stimulated NF- κ B-DNA binding greatly for PIP4K2A si 2, moderately for PIP4K2A si 1, and weakly for PIP4K2A si 3 (Figure 7-8B). TNF α -stimulated NF- κ B-DNA binding was not reduced for any PIP4K2C siRNA, suggesting that PIP4K2A might be a genotoxic stress-specific target for MW01 (Figure 7-8B). Considered together, the overall trend following PIP4K2C and A knockdown was a greater reduction after irradiation than TNF α and therefore the pathway-specific reduction observed, especially with PIP4K2C si1 and PIP4K2A si2, warranted further investigation.

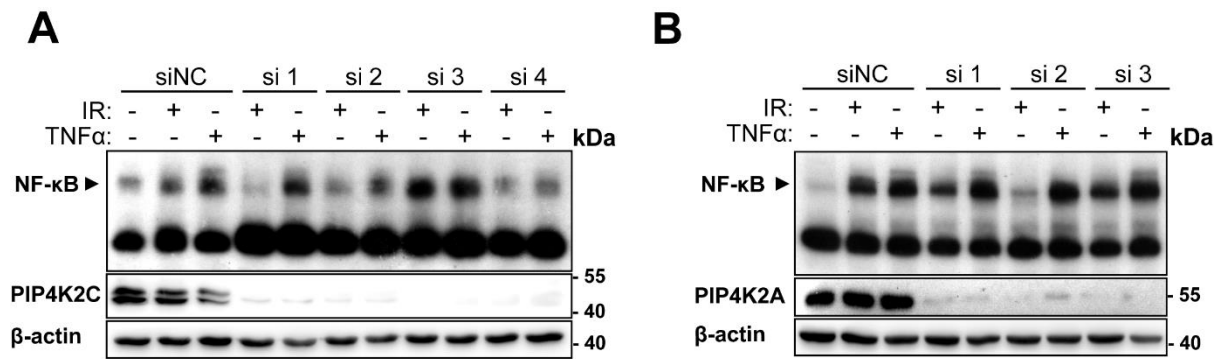


Figure 7-8: PIP4K2C and PIP4K2A knockdown reduces NF- κ B-DNA binding following irradiation.

(A) EMSA (top) and western blot (bottom) analysis of lysates from U2-OS cells transfected with non-coding or PIP4K2C siRNAs (si 1-4) and stimulated with either irradiation or TNF α . (B) EMSA (top) and western blot (bottom) analysis of lysates from U2-OS cells transfected with non-coding or PIP4K2A siRNAs (si 1-3) and stimulated with either irradiation or TNF α .

Due to the incomplete knockdown of PIP4K2A and C by siRNA and the very high catalytic activity of PIP4K2A, I decided to use CRISPR-Cas9 to generate U2-OS knockout cell lines for PIP4K2C, PIP4K2A, and a double-knockout for both PIP4K2C and A. The double-knockout was generated by serial knockdown of PIP4K2A in a PIP4K2C knockout clone following the same method.

To determine if the elimination of PIP4K2C and A via CRISPR could further clarify their role in genotoxic stress-induced NF- κ B activity, p-p65 levels and *NFKBIA* expression were examined following irradiation or TNF α treatment in each knockout cell line (Figure 7-9A, B, C). No reduction in p-p65 levels was found in any of the knockout cell lines following any stimulus compared to nt-gRNA-expressing controls (Figure 7-9A, B, C). In agreement with this finding, no change in *NFKBIA* expression was observed in any of the knockout cell lines compared to nt-gRNA-expressing controls (Figure 7-9A, B, C). Considered together with the siRNA knockdown data, I concluded the likelihood of involvement of these kinases in genotoxic stress-induced NF- κ B activity was low (Figure 7-9A, B, C).

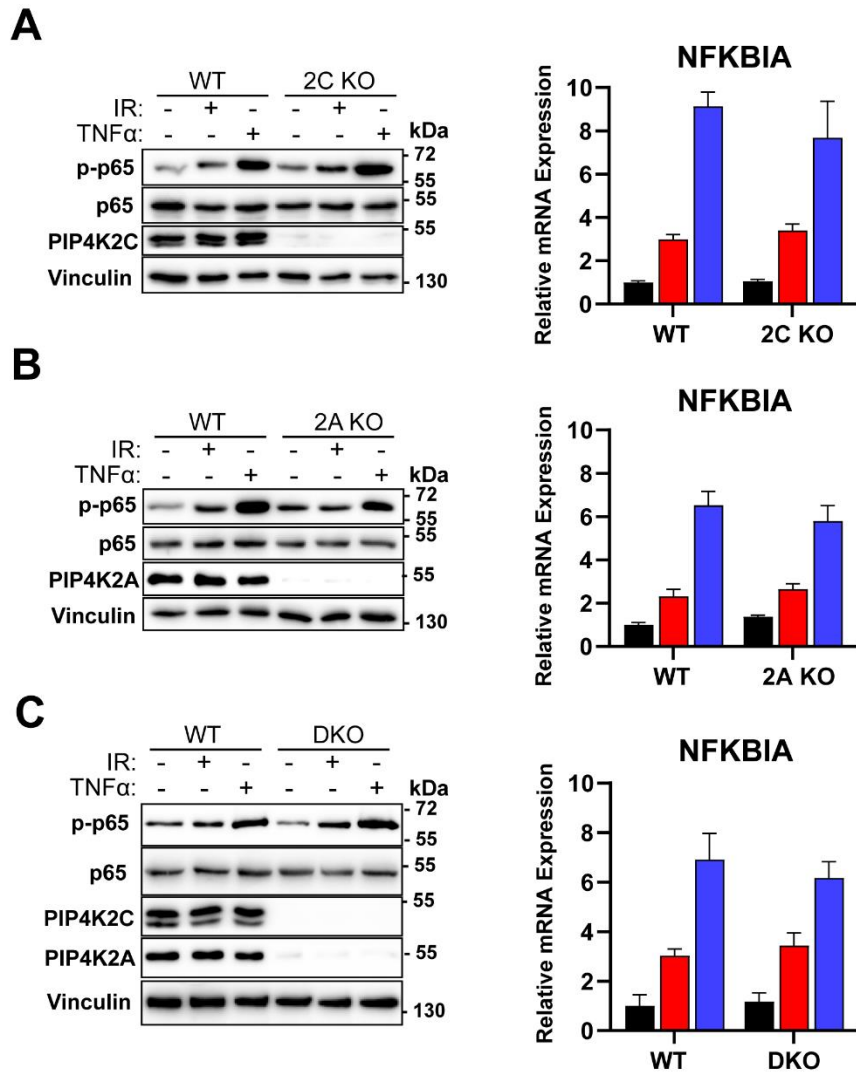


Figure 7-9: PIP4K2C, PIP4K2A, and PIP4K2C/2A knockout cells.

(A) Western blot and RNA expression analysis of U2-OS-PIP4K2C KO (2C KO) cells following either irradiation or TNF α stimulation. (B) Western blot and RNA expression analysis of U2-OS-PIP4K2A KO (2A KO) cells following either irradiation or TNF α stimulation. (C) Western blot and RNA expression analysis of U2-OS-PIP4K2A-PIP4K2C KO (DKO) cells following either irradiation or TNF α stimulation. "WT" cells expressed non-targeting gRNA. Comparison with 2-way ANOVA. All comparisons between WT controls and knockout cells, per treatment, were not significant.

Despite the lack of strong evidence from the silencing experiments, I nonetheless determined if MW01 and MW05 inhibited PIP4K2 catalytic activity and to that end, *in vitro* kinase activity assays for PIP4K2C and A were performed (Figure 7-10A, B). Purified kinase was incubated for 1 hour at 37 °C with ATP and substrate phosphatidylinositol-5-phosphate (PI5P) to generate ADP and phosphatidylinositol-4,5-phosphate (PI4,5P). The remaining ATP was quantified with a luminescent ATP detector molecule and compared to an ATP standard curve. Background signal was determined through inclusion of negative

controls lacking enzyme, substrate PI5P, or ATP and maximal catalytic activity was determined by incubating the kinase without DMSO or inhibitor. No PIP4K2C catalytic activity was detected above the no substrate control, in line with reports that this isoform has low or no catalytic activity and likely plays a scaffolding role for the catalytically active isoforms PIP4K2A and B^{145,146} (Figure 7-10A). The markedly higher PIP4K2A catalytic activity when compared to the negative controls and PIP4K2C was also in agreement with these studies¹⁴⁵, indicating that the assay conditions were acceptable to assess PIP4K2A kinase activity (Figure 7-10B). However, no change in relative luminescent signal was observed at any tested concentration of MW01 for either PIP4K2C or A, suggesting that MW01 does not inhibit PIP4K2A or 2C catalytic activity (Figure 7-10B).

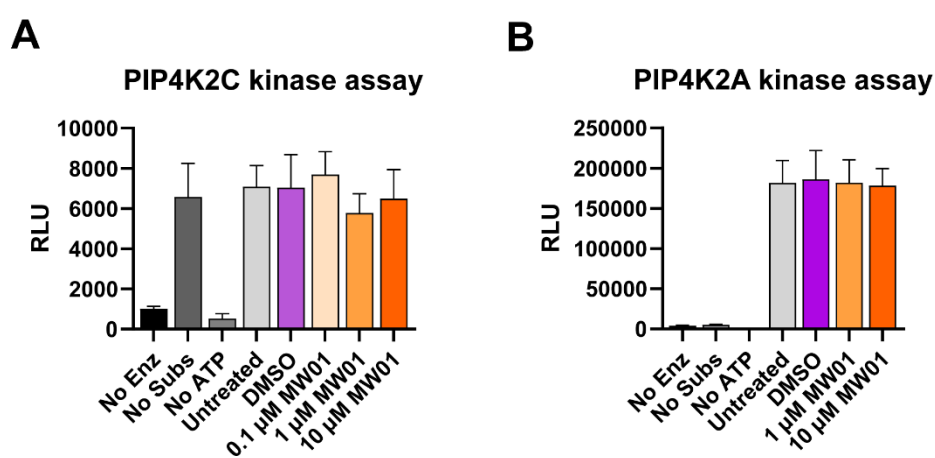


Figure 7-10: MW01 does not inhibit PIP4K2C or PIP4K2A *in vitro*.

(A) *In vitro* PIP4K2C kinase assay in the presence of DMSO, 0.1 μM, 1 μM, or 10 μM MW01. (B) *In vitro* PIP4K2A kinase assay in the presence of DMSO, 0.1 μM, 1 μM, or 10 μM MW01.

Considering the lack of PIP4K catalytic inhibition by the compounds and the unclear requirement for PIP4K2C and A for genotoxic stress-induced NF-κB activity based on, I determined it best to move on to other potential targets and identification strategies.

7.3.2. MW01 and MW05 are kinase inhibitors

Intrigued by the identification of these kinases nevertheless as potential interactors of MW01 in the 2D-TPP, I decided to perform a broad *in vitro* kinase activity panel with both compounds to confirm my PIP4K results and eliminate the possibility that MW01 and MW05 act on previously described kinases involved in genotoxic stress-induced NF-κB, most importantly IKK. 275 different kinases were tested

by ThermoFisher's SelectScreen kinase panel assay service, revealing that both MW01 and MW05 are kinase inhibitors with distinct kinase inhibition profiles (Figure 7-11, Table S1). Importantly, no previously known kinases within the DNA damage-induced NF- κ B pathway (such as TAK1 or IKK) were inhibited (Table S1). IC50 values were determined for all strongly inhibited kinases contained in the broad panel for both compounds (Fig. 7-12A). Interestingly, several hits shared by both lead compounds were found despite the more selective kinase inhibition profile of MW05, including various phosphatidylinositol phosphate kinases and CLK2 (Figure 7-12B).

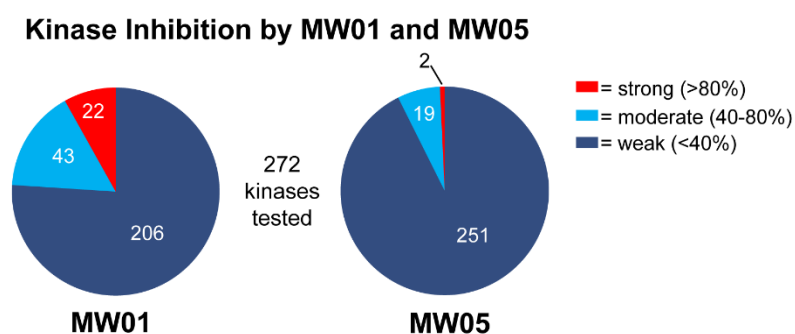


Figure 7-11 : MW01 and MW05 are kinase inhibitors with differing inhibition profiles.

In vitro kinase assay panel summary indicating the number of kinases inhibited strongly (>80%, red), moderately (40-80%, light blue), or weakly (0-40%, dark blue) by 10 μ M MW01 or 10 μ M MW05.

I next investigated if any of the shared kinase targets of MW01 and MW05 play a role in genotoxic stress-induced NF- κ B activity. Based on the CaCo2 recovery values (Table 3-1) and experimental treatment concentration of 10 μ M, the putative target kinase should have a low IC50 of, at most, 2000 nM for both lead compounds in the *in vitro* kinase panel (Figure 7-12A). Based on this criterion alone, I arrived at a relatively short list of potential targets for further analysis, leaving only Phosphatidylinositol 4,5-bisphosphate 3-kinases (PIK3) PIK3CG, PIK3C2G, and the unrelated CLK2 (Figure 7-12B). PIK3C2G was eliminated from further analysis since RNA expression data indicated high tissue specificity and lack of expression in our U2-OS model cell line¹⁴⁷. DNA-dependent protein kinase (DNA-PK) and mammalian target of rapamycin (mTOR) failed to meet the sub-2000 nM IC50 criteria for MW05 and MW01, respectively, but were nonetheless scrutinized experimentally in downstream experiments.

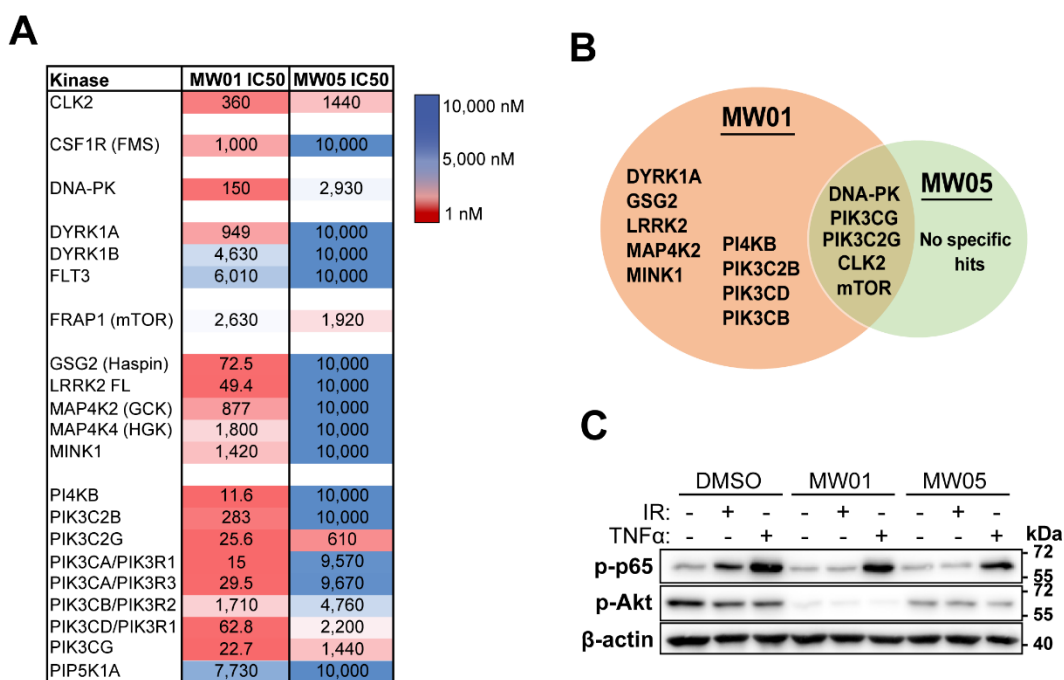


Figure 7-12: MW01 and MW05 share kinase targets and are active in cell-based assays.

(A) Comparison of IC₅₀s for indicated kinases with 10 μM MW01 or 10 μM MW05. Strength of inhibition indicated numerically and by color gradient (red indicates stronger, blue indicates weaker inhibition). (B) Diagram indicating shared targets of MW01 (orange) and MW05 (green) in the overlapping region. (C) Western blot analysis of lysates from U2-OS cells following 1 hour treatment with MW01 or MW05 and stimulated with either irradiation or TNFα.

To validate the lead compounds as kinase inhibitors in a cellular context, Akt-S473 phosphorylation was detected by western blot following treatment with MW01 and MW05. Serine 473 on Akt is a major phosphatidylinositol-dependent phosphosite downstream of phosphoinositide 3-kinases (PI3K) that is required for full activation of the kinase, and is therefore suggestive of overall phosphatidylinositol-3,4,5-trisphosphate (PIP₃) levels within the cell¹⁴⁸. In agreement with MW01's broader PI3K hit profile and lower IC₅₀'s compared to MW05, Akt-S473 phosphorylation was completely abolished by MW01 while MW05 instead partially reduced it, thereby confirming MW01 and MW05 as cell-active kinase inhibitors (Figure 7-12C). In addition, these results also suggested that MW01 and MW05 could affect the levels of PIP₃ and other phosphatidylinositols (PIs), which are critical signaling molecules frequently playing a role in membrane targeting and kinase activation^{149,150}.

Based on the determination of this mode of action for MW01 and MW05, I presumed that the target was likely a kinase involved, directly or indirectly, in the DNA damage-induced NF-κB signaling cascade. Since the kinases most strongly inhibited by MW01 and MW05 were mostly comprised of PI3K isoforms commonly targeted by other PI3K inhibitors, I surmised that the effect of our compounds

might be mediated via reduction in the phospholipid products of those kinases rather than inhibition of the kinases themselves. While PI3K/Akt and NF- κ B crosstalk has been described, a requirement for PI3K/Akt activity in NF- κ B activation appears cell-type and stimulus-specific and critically, has never been proven within genotoxic stress-induced NF- κ B¹⁵¹⁻¹⁵⁴. In consideration of the stronger comparative potency of MW01 in reducing both p-p65 and p-Akt levels, and the preliminary results of the PIP4K experiments, I hypothesized that there could be a phosphatidylinositols-phosphates (PIP)-dependent critical signaling event required for DNA damage-induced NF- κ B activity. To investigate this possibility, I examined a requirement for PIP-dependent activation of TRAF6, a previously described essential regulator, and of NEDD4L, a newly identified regulator, of genotoxic stress-induced NF- κ B.

7.3.3. TRAF6 does not undergo PIP-mediated translocations which could be affected by MW01 and MW05's PI3K inhibition

To determine if any known critical genotoxic stress-induced NF- κ B signaling molecules bind PIPs, I searched the literature for known pathway elements containing PIP-binding motifs. A previous study showed that the TRAF family of proteins contain a highly conserved PIP-binding motif within the TRAF domain that is required to target TRAF4 to tight junctions¹⁵⁵. Interestingly, TRAF6 was also shown to dynamically translocate from the membrane to the cytosol in response to IL-1, a canonical activator of NF- κ B¹⁵⁶. Since TRAF6 is essential for DNA damage-induced NF- κ B and physically binds to translocated ATM⁴⁴, I investigated if TRAF6 undergoes any translocation following genotoxic stress, if the translocation could be PIP-dependent, and if such a translocation could be inhibited by MW01 or MW05.

To determine if TRAF6 undergoes a genotoxic stress-induced translocation, sub-cellular fractionation of U2-OS cells was performed at 10, 20, and 45 minutes after irradiation and compared to unstimulated controls by western blot (Figure 7-13A). α -tubulin, plasma membrane calcium ATPase (PMCA1), and PARP1 were detected to determine purity of the cytosolic, membrane, and nuclear fractions, respectively, and showed little or no detectable cross-contamination (Figure 7-13A). ATM phosphorylation and cytosolic translocation was monitored to confirm activation of the genotoxic-stress-induced pathway. As previously established by our group, nuclear ATM phosphorylation was observed by 10 minutes, peaked at 20 minutes, with a minor reduction apparent by 45 minutes, indicating that ATM was successfully activated by irradiation (Figure 7-13A). The characteristic cytosolic translocation was observed, with p-ATM weakly detected in the cytosolic fraction at 10 minutes and further increasing thereafter to the peak at 45 minutes (Figure 7-13A). Interestingly, p-ATM was also

detected in the membrane fraction, with the time-course closely resembling p-ATM levels in the nuclear fraction, suggesting that p-ATM associates with the membrane or a membrane-bound compartment during the translocation (Figure 7-13A). Considered together with the good fraction purity, these results indicated that the genotoxic stress response was proceeding normally and therefore could be used to observe a possible genotoxic stress induced TRAF6 translocation. Despite this, TRAF6 levels appeared unchanged across the time-course when compared to unstimulated controls, suggesting that TRAF6 does not dynamically translocate following irradiation (Figure 7-13A).

Using the same sub-cellular fractionation method, I investigated whether MW01 and MW05 deplete TRAF6 in the various fractions, which could thereby inhibit NF- κ B (Figure 7-13B). Despite an observable increase in cytosolic p-ATM levels indicating genotoxic stress in the DMSO-treated controls and reductions in cytoplasmic p-ATM levels in MW01 and MW05-treated nuclear fractions, TRAF6 levels were unchanged in any drug-treated fraction compared to DMSO-treated controls (Figure 7-13B). p-ATM levels in the MW05-treated cytosolic fraction appeared comparatively high to other fractions, but comparison with α -tubulin loading controls revealed this was likely due to overloading of the sample (Figure 7-13B). Considered together with the fractionation time-course experiment, these results suggested that TRAF6 does not translocate dynamically in response to DNA damage and that MW01 and MW05 do not deplete TRAF6 in any investigated sub-cellular fraction.

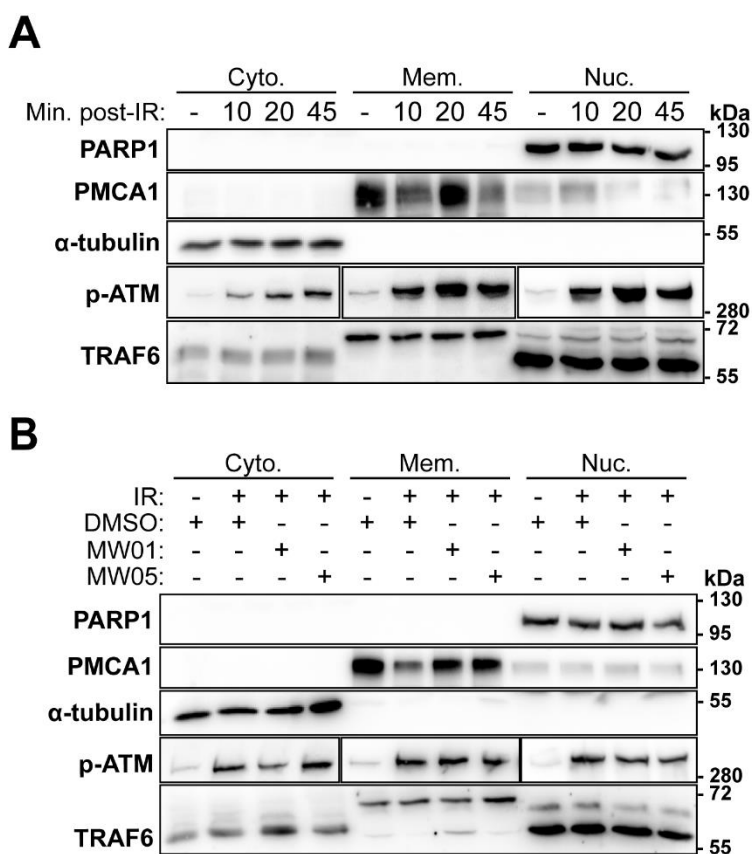


Figure 7-13: TRAF6 does not accumulate in cytoplasmic, nuclear, or membrane fractions following irradiation.

(A) Western blot analysis of cytoplasmic, nuclear, and membrane fractions from U2-OS cells at 10-, 20-, and 45-minutes post-irradiation. (B) Western blot analysis of cytoplasmic, nuclear, and membrane fractions from U2-OS cells treated with either DMSO, MW01, or MW05 at 45 minutes post-irradiation.

To confirm these results through an additional approach, immunofluorescent staining of TRAF6 in U2-OS cells was performed 45 minutes after irradiation on MW01 or MW05-treated cells (Figure 7-14). No notable difference in TRAF6 intensity or localization was observed between DMSO-treated unstimulated or irradiated cells, in agreement the results of the sub-cellular fractionation time-course experiment (Figure 7-14). In addition, TRAF6 appeared unchanged in unstimulated MW01 or MW05-treated cells compared to DMSO-treated controls, also in agreement with the drug-treated fractionation experiment (Figure 7-13B). Finally, TRAF6 was also unchanged in the MW01 or MW05-treated irradiated conditions, as in the DMSO-treated controls. Taken together, these results confirmed the sub-cellular fractionation experiments and strongly suggested that TRAF6 does not undergo genotoxic stress-induced translocations and therefore that MW01 and MW05 do not act by inhibiting such a process.

To investigate the role of the TRAF6-K356A and K388A mutations, a rescue-effect experiment was performed in U2-OS TRAF6-KO cells obtained from the Krappmann group. In agreement with previous findings by our group ⁴⁴, the cells are unable to activate NF- κ B following genotoxic stress to activate NF- κ B following genotoxic stress. I hypothesized that reconstitution of the TRAF6-KO cells with TRAF6-K388E would not be sufficient to activate NF- κ B after DNA damage compared to wild-type reconstituted controls. Such results would suggest an essential activation role mediated by the critical PIP-binding residue K388E. To that end, the TRAF6 KO cells were transfected with either vector, wild-type TRAF6, or TRAF6-K388E mutant PIP binding mutant and after 48 hours, TRAF6 levels were detected by western blot. TRAF6 was not detected in vector-expressing TRAF6-KO cells compared to wild-type, untransfected controls, confirming the TRAF6 knockout (Figure 7-16A). Wild-type TRAF6-transfected TRAF6-KO cells had higher levels of TRAF6 compared to wild-type, untransfected U2-OS controls, suggesting that the TRAF6-KO cells successfully expressed the wild-type TRAF6 plasmid (Figure 7-16A). However, very low levels of TRAF6 were detected in TRAF6-K388E-expressing cells compared to either TRAF6-WT-expressing or untransfected wild-type U2-OS controls, suggesting an issue with either K388E mutant expression or stability in the TRAF6-KO cell line (Figure 7-16A).

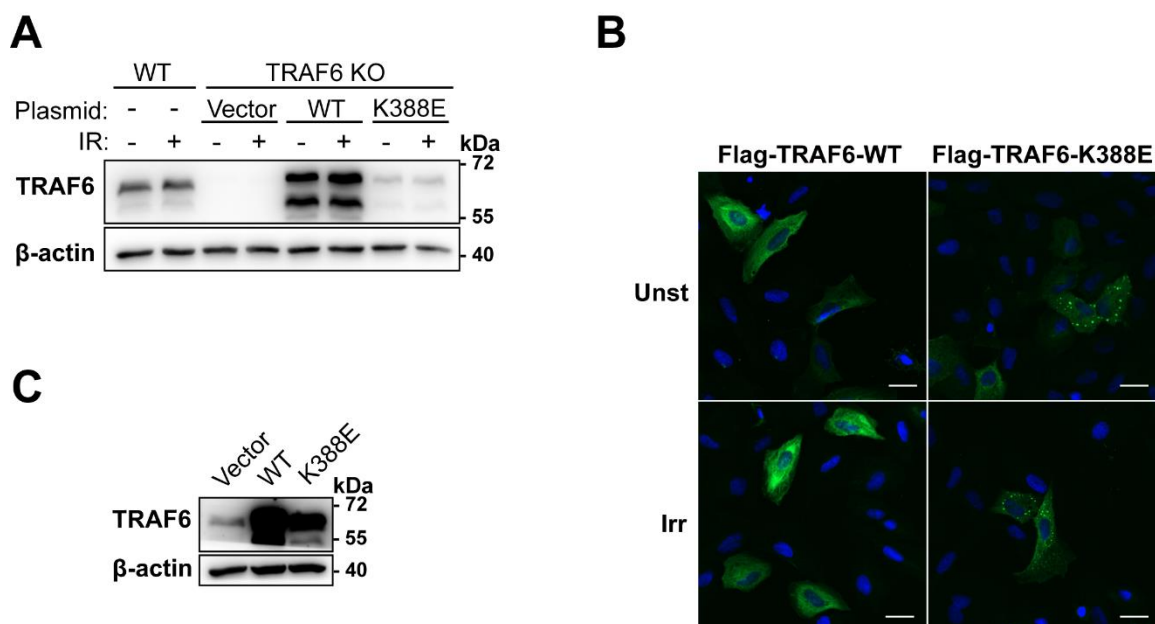


Figure 7-16: TRAF6-K388E mutant expression is poor and the protein likely unstable.

(A) Western blot analysis of U2-OS-nt-gRNA and U2-OS-TRAF6 knockout cells transfected with either vector, wild-type TRAF6, or TRAF6-K388E mutant plasmids in either unstimulated or irradiated conditions. (B) Immunofluorescence staining of FLAG (green, anti-FLAG M2 Sigma-Aldrich F3165) and DAPI counterstain (blue) in U2-OS cells transfected with either Flag-TRAF6-WT or Flag-TRAF6-K388E plasmids following irradiation. Scale bar: 20 μ M. (C) Western blot analysis of HEK293 cells transfected with vector, wild-type TRAF6, or TRAF6 K388E. β -actin was used as loading control.

As an alternative method to confirm TRAF6-K388E expression and to rule out possible expression issues in the TRAF6-KO cell line, immunofluorescent staining was performed in wild-type U2-OS cells. Since the TRAF6-WT plasmid used for K388E mutant generation contained a FLAG-tag, both WT and TRAF6-K388E were observed indirectly by staining FLAG to allow discrimination from endogenous TRAF6 (Figure 7-16B). FLAG staining in TRAF6-WT expressing cells appeared diffused throughout the cell, comparable to TRAF6 staining in the previous translocation experiments, suggesting a normal distribution of the tagged wild-type protein. (Figure 7-16B, Figure 7-14). By contrast, FLAG staining in TRAF6-K388E-expressing cells showed clearly defined puncta, indicative of an accumulation of the mutant TRAF6 protein and suggestive of possible lysosomal degradation (Figure 7-16B). Considered together with rescue-effect experiments, these results show that the TRAF6-K388E mutant is unstable in U2-OS cells and therefore is not suitable for comparison with the normally expressed TRAF6 wild-type.

To rule out the possibility of cell line specific degradation of the K388E mutant, TRAF6-WT and TRAF6-K388E were transfected in HEK293 cells and TRAF6 detected by western blot after 48 hours (Fig. 7-16C). While TRAF6 levels were higher in both TRAF6-WT and K388E-expressing cells than vector-expressing controls indicating successful transfection and expression, the level was much higher in the wild-type than the K388E-expressing cells, indicating the issue of K388E mutant stability was not limited to one cell line (Figure 7-16C). Having ruled out a DNA damage-induced TRAF6 translocation to membranes, or MW01 or MW05-mediated degradation of TRAF6 in a subcellular compartment, and unable to equally express the K388E mutant to assess an activation role for TRAF6-PIP binding, I reevaluated TRAF6 as an unlikely downstream target of the compounds and moved on to other targets.

7.3.4. NEDD4L is a potential new regulator of NF- κ B but does not mediate the effects of MW01 or MW05

A genome-wide screen for essential regulators of genotoxic stress-induced NF- κ B¹⁵⁷ recently identified numerous previously unknown proteins alongside well-described pathway elements. Among the previously undescribed hits was neural precursor cell expressed developmentally downregulated gene 4-like (NEDD4L), a E3 ubiquitin protein ligase with z-scores of -1.20, -1.07, and -0.11 for each of three individual siRNAs, which is comparable to -1.20, -0.94, and -0.45 for essential genotoxic stress pathway component ATM¹⁵⁷. Interestingly, NEDD4L was shown to interact with PIPs through its C2 domain,

which occurs in a calcium-dependent manner and is required for the full activation of E3 ligase activity¹⁵⁸. Considering this behaviour described an induced, PIP-dependent activation similar to my hypothesized model for TRAF6 and was a strong candidate hit from the genome-wide siRNA screen, I proceeded to investigate the role of NEDD4L in genotoxic stress-induced NF- κ B.

To confirm that NEDD4L is required for DNA damage-induced NF- κ B activity, U2-OS cells were transfected with NEDD4L-targeting siRNAs. All three NEDD4L siRNAs strongly reduced NEDD4L protein level compared to non-coding siRNA-expressing controls (Figure 7-17A). NF- κ B activation was monitored following irradiation or TNF α and reduced p-p65 levels following irradiation were observed in NEDD4L si 2- and si 3-expressing cells, while TNF α -stimulated p-p65 levels remained unchanged, suggesting a genotoxic stress pathway-specific role for NEDD4L (Figure 7-17A). This conclusion was confounded by the high knockdown efficiency of NEDD4L si 1 and concomitant lack of change in p-p65 in any stimulus condition (Figure 7-17A). Overall, the results agreed with the genome-wide siRNA screen¹⁵⁷, in which only 2 of 3 tested siRNAs were effective even for well-established pathway components and thus, I continued to investigate NEDD4L within the pathway.

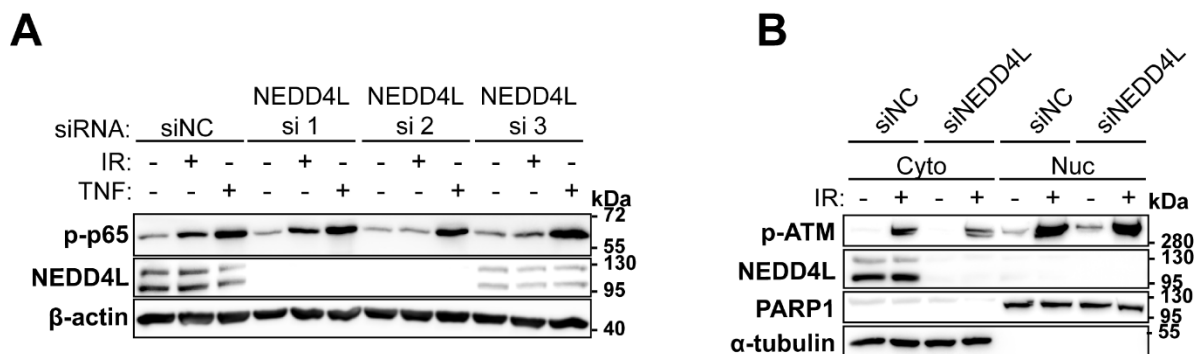


Figure 7-17: NEDD4L knockdown reduces p-p65 level and p-ATM nuclear export after irradiation.

(A) Western Blot analysis of lysates from U2-OS cells transfected with non-coding or NEDD4L siRNAs (si 1-3) and stimulated with either irradiation or TNF α . (B) Western blot analysis of cytoplasmic (Cyto) and nucleoplasmic (Nuc) fractions of U2-OS cells transfected with non-coding or NEDD4L siRNA.

To further assess where NEDD4L could act and if genotoxic stress pathway steps affected by NEDD4L knockdown mimic those inhibited by MW01 or MW05, U2-OS cells were transfected with NEDD4L siRNA 2, the most effective siRNA from Fig. 7-17A. After 48 hours, cells were irradiated, cytoplasmic and nuclear fractionation was performed, and protein levels detected by western blot (Figure 7-17B). α -tubulin and PARP1 were used to fraction purity and protein loading for the cytoplasmic and nuclear fractions respectively. p-ATM levels in the nuclear fraction were comparable in siNEDD4L-expressing

cells and non-coding-expressing cells, suggesting that NEDD4L is not required to activate ATM (Figure 7-17B). However, a reduction was observed in the cytoplasmic fraction of the siNEDD4L-expressing cells compared to controls, implicating NEDD4L in the poorly understood nuclear export of p-ATM and thereby suggesting a genotoxic stress-specific role for the protein (Figure 7-17B). In addition, these results represented the first instance within the study of molecular target studies producing pathway effect upstream of IKK/NF- κ B activation that matched the effect of MW01 or MW05 treatment, in this case the reduction of p-ATM in the cytoplasmic fraction (Figure 7-3D). Considering the similarity of the NEDD4L molecular studies to the drug treatment effect, the well-described requirement for NEDD4L-PIP binding for full catalytic activation¹⁵⁸, and the inhibition by MW01 and MW05 of targets synthesizing those critical phospholipids, I felt strongly that further investigation would reveal a link between the compounds and NEDD4L.

To prove this link, I intended to first confirm NEDD4L-PIP binding and to that end, a PIP-strip protein-lipid binding assay was performed. The assay was performed by incubating a purified protein of interest, in this case NEDD4L, with a membrane that has been spotted with various phospholipids. During the incubation, the protein of interest binds the spotted phospholipids, the interaction of which is determined by the structure of the protein, and the membrane is then washed and immunoblotted much the same as a western blot. Signal location from the immunoblot is then compared to the phospholipid legend, revealing the specific phospholipid bound by the protein of interest. In agreement with the structural study¹⁵⁸, blotting revealed that the primary phospholipid species bound by NEDD4L is PI4,5P, with weaker interactions for the two precursor species, PI3P and PI4P, and that overall phospholipid binding was calcium-dependent (Figure 7-18A).

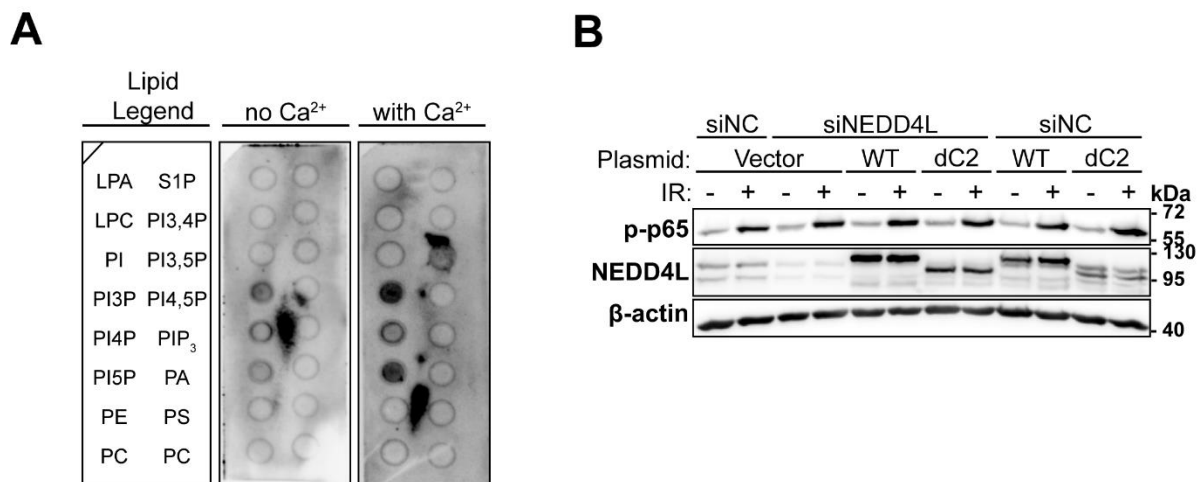


Figure 7-18: TRAF6 binds PI3P, PI5P, and PI3,P *in vitro*.

(A) Phospholipid binding of NEDD4L in the presence (right) or absence (middle) of Ca²⁺ detected using PIP-strips spotted with the phospholipids indicated in the legend (left). Lipid Legend: LPA: Lysophosphatidic Acid; LPC: Lysophosphocholine; PI: Phosphatidylinositol; PI3P: Phosphatidylinositol 3-phosphate; PI4P: Phosphatidylinositol 4-phosphate; PI5P: Phosphatidylinositol 5-phosphate, PE: Phosphatidylethanolamine; PC: Phosphatidylcholine; S1P: Sphingosine 1-phosphate; PI3,4P: Phosphatidylinositol 3,4-phosphate; PI3,5P: Phosphatidylinositol 3,5-phosphate; PI4,5P: Phosphatidylinositol 4,5-phosphate; PIP₃: Phosphatidylinositol 3,4,5-phosphate; PA: Phosphatidic Acid; PS: Phosphatidylserine. (B) Western Blot analysis of lysates from U2-OS cells transfected first with either non-coding siRNA or siNEDD4L, then transfected with either vector, wild-type NEDD4L, or NEDD4L-dC2.

Having experimentally confirmed NEDD4L-PIP interaction, I used a PIP-binding deficient mutant of NEDD4L lacking the critical C2 domain to investigate the role of this interaction in the pathway. I hypothesized that, were a NEDD4L-PIP interaction (mediated by the C2 domain) required to activate NF-κB, reconstitution of NEDD4L-depleted cells with NEDD4L-dC2 would not be sufficient to activate NF-κB following DNA damage. U2-OS cells were transfected first with either NEDD4L-targeting or non-coding siRNAs to deplete endogenous NEDD4L, and 24 hours later transfected with either vector, wild-type NEDD4L, or NEDD4L-dC2 to reconstitute NEDD4L. After an additional 24 hours (48 hours total), cells were irradiated, and NF-κB activation assessed via p65 phosphorylation by western blot. Comparison of NEDD4L levels in the vector plasmid-expressing, siNEDD4L-expressing cells was reduced compared to controls, indicating successful knockdown of NEDD4L. However, in conflict with the previous results, p-p65 levels of the irradiated samples of each vector-expressing sample were comparable, despite the observable reduction in NEDD4L levels in siNEDD4L-expressing cells (Figure 7-18B). Lack of the expected p-p65 reduction in these controls prevented further interpretation of this data, and due inability to reproduce the pathway-specific reduction in p-p65 by NEDD4L knockdown led me to reevaluate my overall approach to target identification.

7.3.5. Identification of CLK2 as a regulator of genotoxic stress induced NF- κ B by chemical pathway dissection

While pursuing the PIP interaction-oriented TRAF6 and NEDD4L hypotheses, I had begun to question whether the PI3K hits were off-targets of MW01 and MW05. Attempting to link inhibition of these kinases or their lipid products to the genotoxic stress pathway had proven extremely challenging and a path forward to interrogate TRAF6 or NEDD4L-PIP interaction was unclear. I devised several conceptual questions to challenge the PI3K/PIP-related target hypothesis, the most important of which was: do other PI3K inhibitors also inhibit NF- κ B? If the PI3Ks were the functional target of MW01 and MW05, any compound inhibiting them should also inhibit NF- κ B. By extension, I theorized that any drug inhibiting the true target should also inhibit NF- κ B. Therefore, using compounds with previously described IC₅₀s for the shared kinase hits of MW01 and MW05, I could perform a chemical dissection of the genotoxic stress induced NF- κ B pathway and discriminate between on and off-targets.

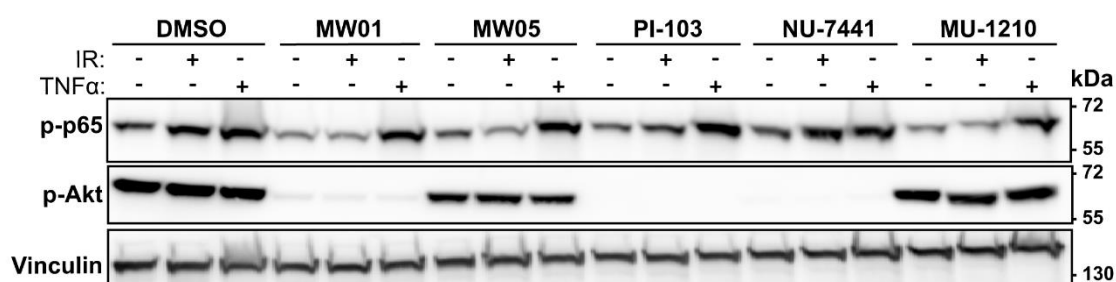


Figure 7-19: Chemical pathway dissection by inhibitors of shared kinase targets of MW01 and MW05.

Western blot analysis of lysates from U2-OS cells pre-treated with the indicated compounds for 1 hour, then stimulated with irradiation or TNF α .

A brief search revealed that PI-103, NU-7441, and MU-1210 could be used as PI3K, DNA-PK, and CLK inhibitors, respectively, based on similar or lower IC₅₀s for the shared target kinases of MW01 and MW05¹⁵⁹⁻¹⁶¹. In addition, PI-103 also inhibits DNA-PK and mTOR with low nanomolar IC₅₀s¹⁵⁹, and therefore, this compound can be used to test if PI3K, DNA-PK, or mTOR are involved in NF- κ B activation. As expected, based on the low nanomolar PI3K IC₅₀s of MW01 and PI-103, a complete reduction of p-Akt was observed following treatment with either compound (Figure 7-19). In addition, a partial reduction of p-Akt was observed following MW05 treatment, in agreement with the comparatively higher PI3K IC₅₀s (Figure 7-19). With the aforementioned compounds covering all

shared kinase targets of MW01 and MW05 except CLK2, only CLK inhibitor MU-1210 remained. Interestingly, treatment with this compound resulted in a reduction in p65 phosphorylation comparable to MW01 and MW05, suggesting experimentally for the first time that CLKs regulate irradiation-induced NF- κ B activity (Figure 7-19).

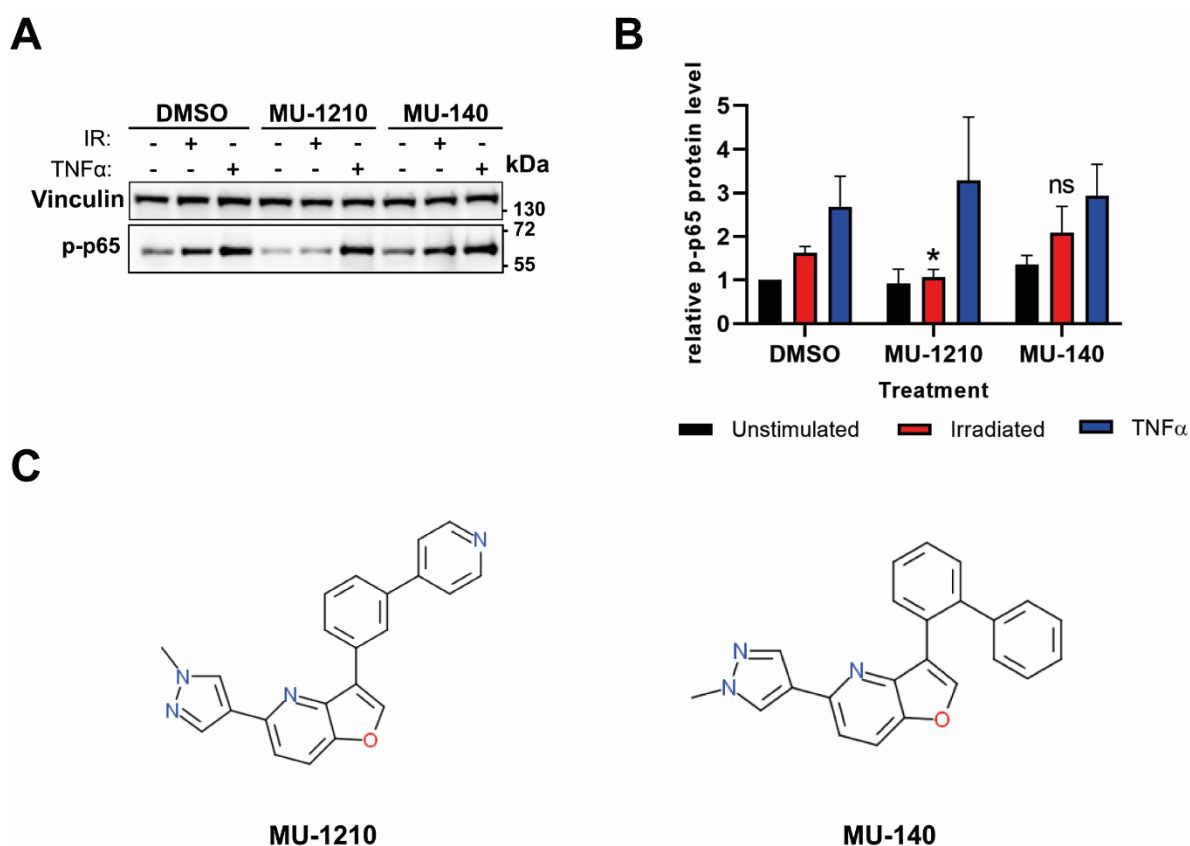


Figure 7-20: p-p65 phosphorylation is reduced by MU-1210 but not negative control MU-140 following irradiation.

(A) Western blot analysis of lysates from U2-OS cells pre-treated with the indicated compounds for 1 hour, then stimulated with irradiation or TNF α . (B) Quantification of relative p-p65 protein level from (A), Statistical comparison with 2-way ANOVA.. (C) Chemical structures of MU-1210 and it's negative control, MU-140. *: $P \leq 0.05$; ns: not significant.

To rule out the possibility of the observed NF- κ B inhibition being caused by a CLK inhibitor off-target, negative control CLK inhibitor MU-140 was tested under the same experimental conditions (Figure 7-20A-D). Lacking the CLK inhibition described by MU-1210, I expected that this compound would not affect p-p65 levels following either irradiation or TNF α stimulation. Fitting this expectation, no significant change in p-p65 level was observed following MU-140 treatment compared to controls, while MU-1210 treatment produced the characteristic irradiation-specific reduction (Figure 7-20A, B).

Considered together with the chemical dissection (Figure 7-19), these data implicate CLK2 as an essential regulator of genotoxic stress induced NF- κ B, leading me to further investigate CLKs.

7.3.6. CLK2 and CLK4 are regulators of genotoxic stress induced NF- κ B

CLKs are a family of four highly conserved dual-specificity kinases, CLK1-4, which have so far been described primarily in the context of spliceosome regulation. Since the initial kinase panel only contained CLK2, the potency and isoform specificity of all four CLKs for both MW01 and MW05 were determined using the same assay. The IC₅₀ data showed that MW01 is a CLK1, CLK2, and CLK4 inhibitor and MW05 is relatively less potent and displays selectivity toward CLK4, while both compounds largely spare CLK3 (Figure 7-21). Importantly, based on the CLK2 IC₅₀ of 360 nM for MW01, 1,440 nM for MW05 and the CaCo2 percent absorption values for the compounds (Table 3-1), sufficient intracellular levels MW01 and MW05 should be reached to inhibit CLK2 at 10 μ M in cell-based assays (Figure 7-21). However, the lower IC₅₀'s for CLK4 indicated that MW01 and MW05 are more selective toward CLK4 than CLK2, suggesting that CLK4 could also be involved and potentially contribute more to the pathway than CLK2 (Figure 7-21). With three structurally distinct compounds, MW01, MW05, and MU-1210, that inhibited CLK2 and CLK4 and inhibited NF- κ B selectively after DNA damage, I felt the pharmacological interrogation of the pathway provided strong evidence of the involvement of these kinases in the genotoxic stress pathway.

Kinase	MW01	MW05
CLK1	250	2,230
CLK2	360	1,440
CLK3	>3,300	>10,000
CLK4	14.1	307

Figure 7-21: MW01 and MW05 are CLK inhibitors with differing isoform specificity.

Comparison of IC₅₀s for CLK isoforms 1-4 of 10 μ M MW01 or 10 μ M MW05. Strength of inhibition indicated numerically and by color gradient (red indicates stronger, blue indicates weaker inhibition).

To investigate the role of CLK2 and CLK4 in the pathway, siRNA knockdown experiments were performed targeting CLK2 or CLK4 and NF- κ B activation monitored following irradiation or TNA α treatment. Recapitulating the effect of MW01 and MW05, CLK2 or CLK4 knockdown produced a significant irradiation-specific reduction in p-p65 level (Figure 7-22A, B). Furthermore, knockdown of CLK2 or 4 strongly reduced IKK γ -S85 phosphorylation, mirroring the ablation of this DNA damage-

specific, ATM-dependent IKK γ PTM by MW01 and MW05, thereby localizing CLKs upstream of IKK (Figure 7-22A, Figure 7-3B).

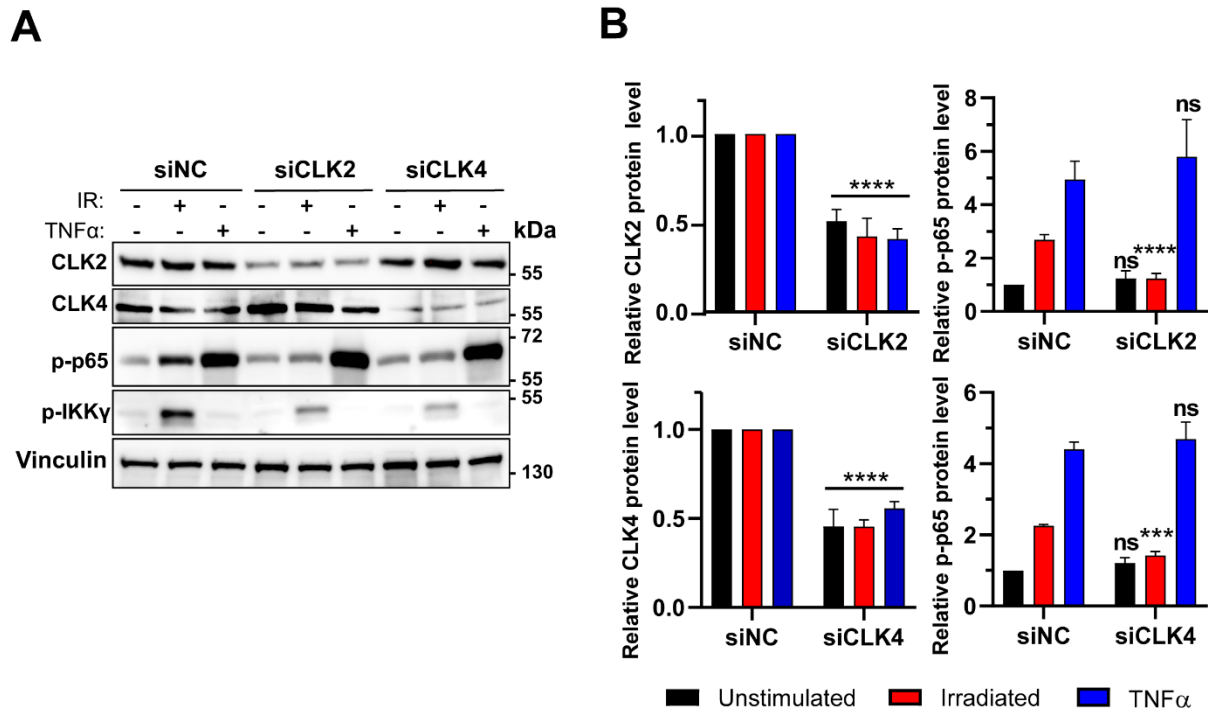


Figure 7-22: Knockdown of CLK2 or CLK4 reduces p-p65 only after irradiation.

(A) Western blot analysis of U2-OS cells transfected with either non-coding or CLK2 or CLK4-targeting siRNAs and stimulated with either irradiation or TNF α . (B) Quantification of CLK2 knockdown efficiency (top-left) and p65 phosphorylation under those conditions (top-right), quantification of CLK4 knockdown efficiency (bottom-left) and p65 phosphorylation under those conditions (bottom-right). Statistical comparison with 2-way ANOVA. ***: $P \leq 0.001$; ****: $P \leq 0.0001$; ns: not significant.

Under the same experimental conditions, mRNA expression analysis revealed a significant genotoxic stress pathway-specific reduction in *NFKBIA* expression in siCLK2 or siCLK4-targeting cells compared to controls (Figure 7-23A, B). As further confirmation of these data, CLK2 and CLK4 were also identified in the previously mentioned genome-wide siRNA screen¹⁵⁷ with z-scores of -1.21, -0.80, 0.60, and -1.22, -1.06, and 1.01 respectively, for each siRNA tested. Taken together, these data confirm CLK2 and 4 are the functional targets of MW01 and MW05.

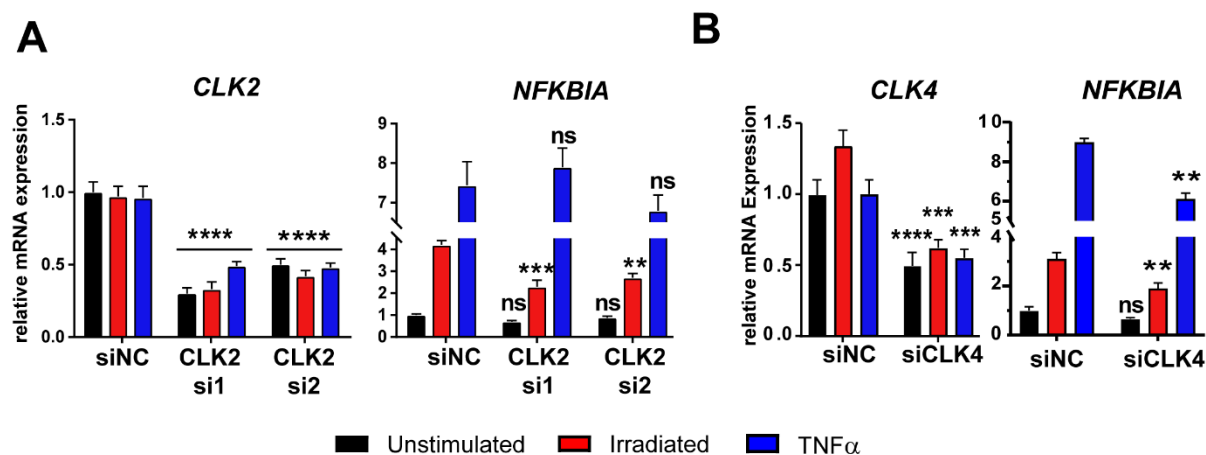


Figure 7-23: CLK2 and CLK4 knockdown reduces *NFKBIA* expression following DNA damage.

(A) RNA expression analysis of U2-OS cells transfected with either non-coding or CLK2 siRNA and stimulated with either irradiation or TNF α . (B) RNA expression analysis of U2-OS cells transfected with either non-coding or CLK2 siRNA and stimulated with either irradiation or TNF α . Statistical comparison with 2-way ANOVA. *: $P \leq 0.05$; **: $P \leq 0.01$; ***: $P \leq 0.001$; ****: $P \leq 0.0001$; ns: not significant.

7.3.7. Structural derivatives of MW01 and MW05 confirm CLK2 and CLK4 target identification

To validate the structural backbones of MW01 and MW05 as kinase inhibitors and leverage additional structures in discerning on- and off-target activity, a chemical library of derivatives of MW01 and MW05 was synthesized by Enamine, Ltd. (Table S2) and screened for similar NF- κ B inhibition compared to our lead compounds. In total 43 derivatives were synthesized, 28 derivatives of MW01 and 15 of MW05. In preparation of inhibitor activity screening the compounds were dissolved in DMSO at 5mM, the stock concentration of the lead compounds. Seven MW01 derivatives were insoluble at concentrations as low as 1mM DMSO, even when shaken at 50 °C and homogenized with a syringe and were excluded from further analysis due their exceptionally poor solubility, leaving 21 MW01 derivatives for downstream analysis. In agreement with the comparatively better solubility of MW05 to MW01, all MW05 derivatives were soluble at 5mM and were screened for inhibitor activity.

To determine if any derivatives of MW01 or MW05 specifically inhibited genotoxic stress-induced NF- κ B activity, U2-OS cells were incubated with the compounds, stimulated by either irradiation or TNF α and p-p65 detected by western blot (Figure 7-24A, B; Figure 7-25A, B). Due to the large number of samples and gels required, each set of derivatives was split in two. DMSO controls confirmed

successful activation of NF- κ B by irradiation or TNF α and the same control samples were loaded on each gel to facilitate direct comparison to derivative-treated samples. MW01 and MW05 were included on the first gel of each set to confirm successful drug treatment, which was apparent in all experimental groups. Blots shown are representative, but the experiments were repeated several times to clarify discrepancies between replicates. Active derivatives of each lead compound were identified which reduced p-p65 in an irradiation-specific manner, while most of the derivatives were inactive or weakly active (Figure 7-24A, B; Figure 7-25A, B).

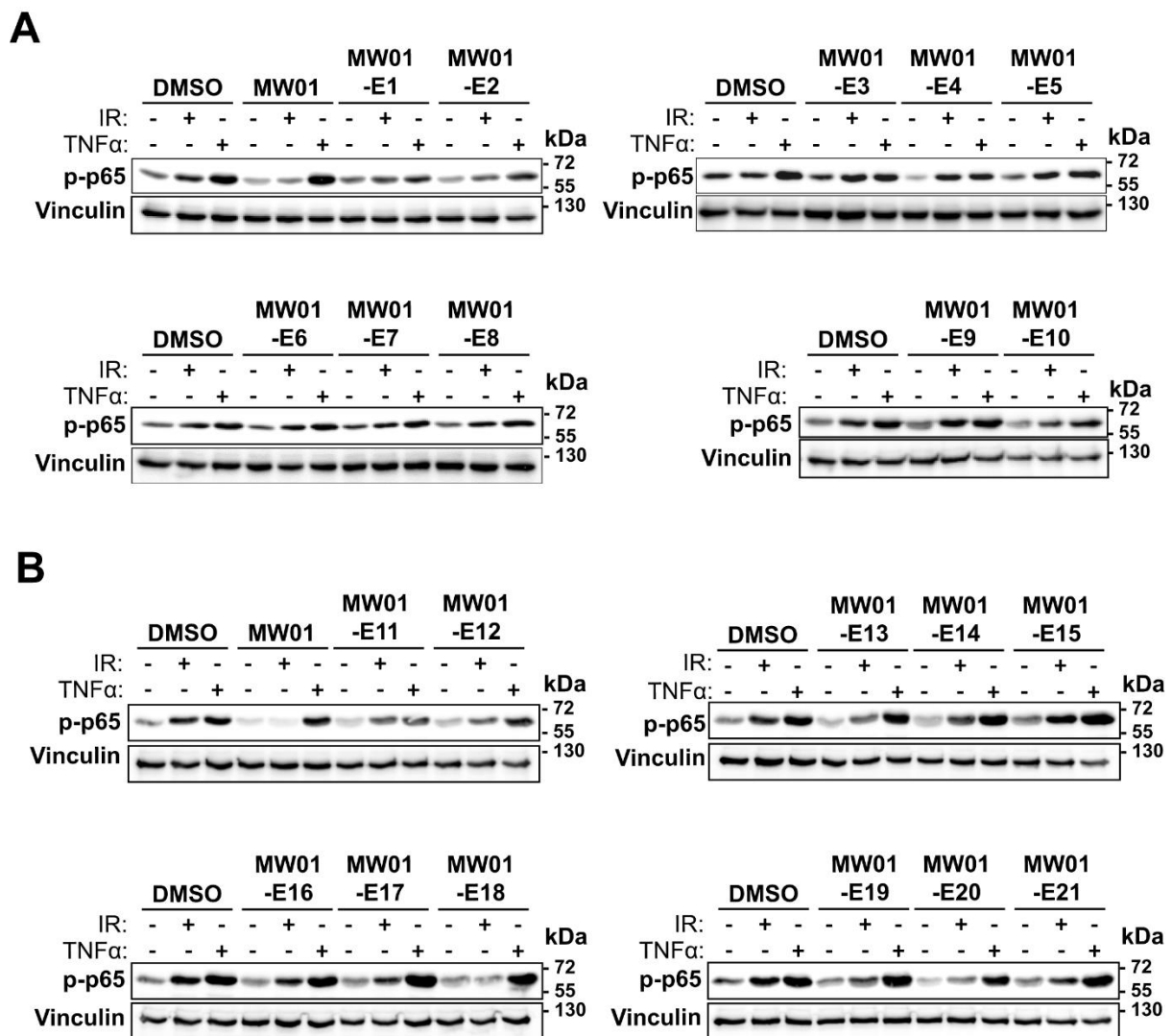
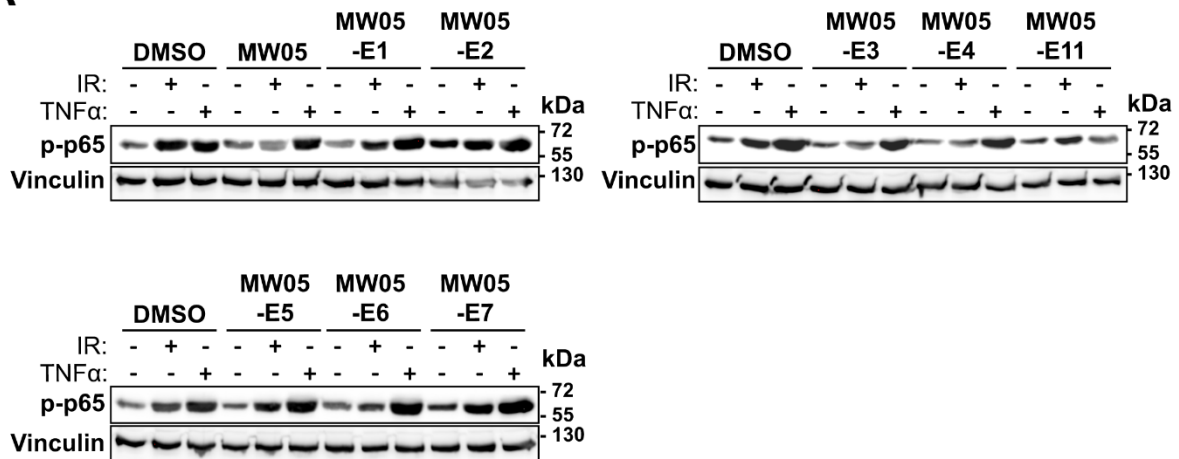


Figure 7-24: Screening of MW01 derivative library for active inhibitors.

(A) Western blot analysis of U2-OS cells pre-treated with the indicated MW01 derivatives and stimulated with either irradiation or TNF α . (B) Second set of MW01 derivatives, same experimental conditions as (A).

In the presented western blot data MW01-E2, -E10, -E11, -E12, -E18, -E19, and -E20 reduced p-p65 following irradiation (Figure 7-24A, B). However, MW01-E11 appeared to reduce TNF-stimulated p-p65 as well and was therefore excluded from further analysis (Figure 7-24A, B). Upon repeated interrogation, MW01-E18 and MW01-E10 were the most robust and reproducible inhibitors and were selected for downstream CLK inhibition analysis.

A



B

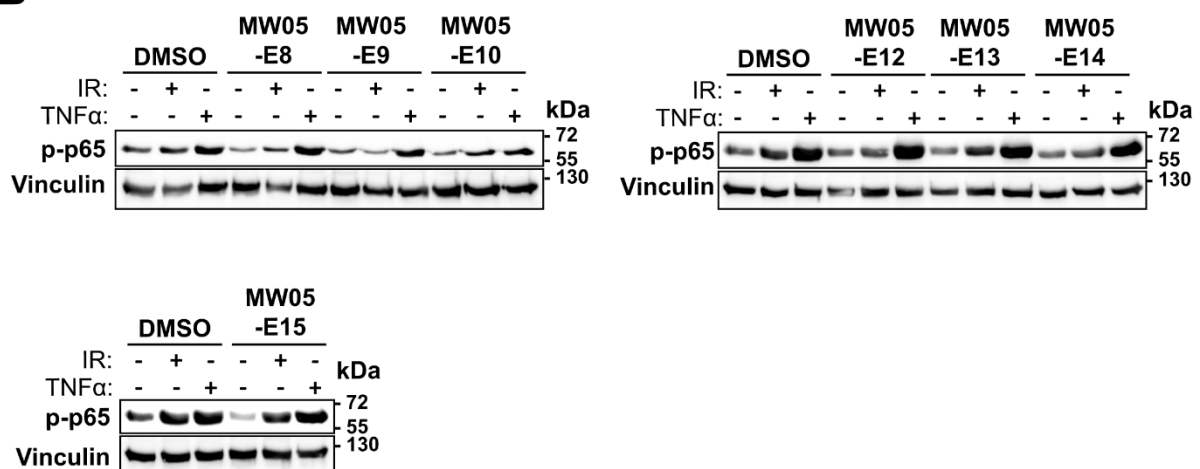


Figure 7-25: Screening of MW05 derivative library for active inhibitors.

(A) Western blot analysis of U2-OS cells pre-treated with the indicated MW05 derivatives and stimulated with either irradiation or TNF α . (B) Second set of MW01 derivatives, same experimental conditions as (A).

In the presented western blot data MW05-E3, -E4, -E6, -E8, and -E9, reduced p-p65 following irradiation (Figure 7-25A, B). Upon repeated interrogation, MW05-E9 and MW05-E3 were the most robust and reproducible inhibitors and were selected for downstream CLK inhibition analysis.

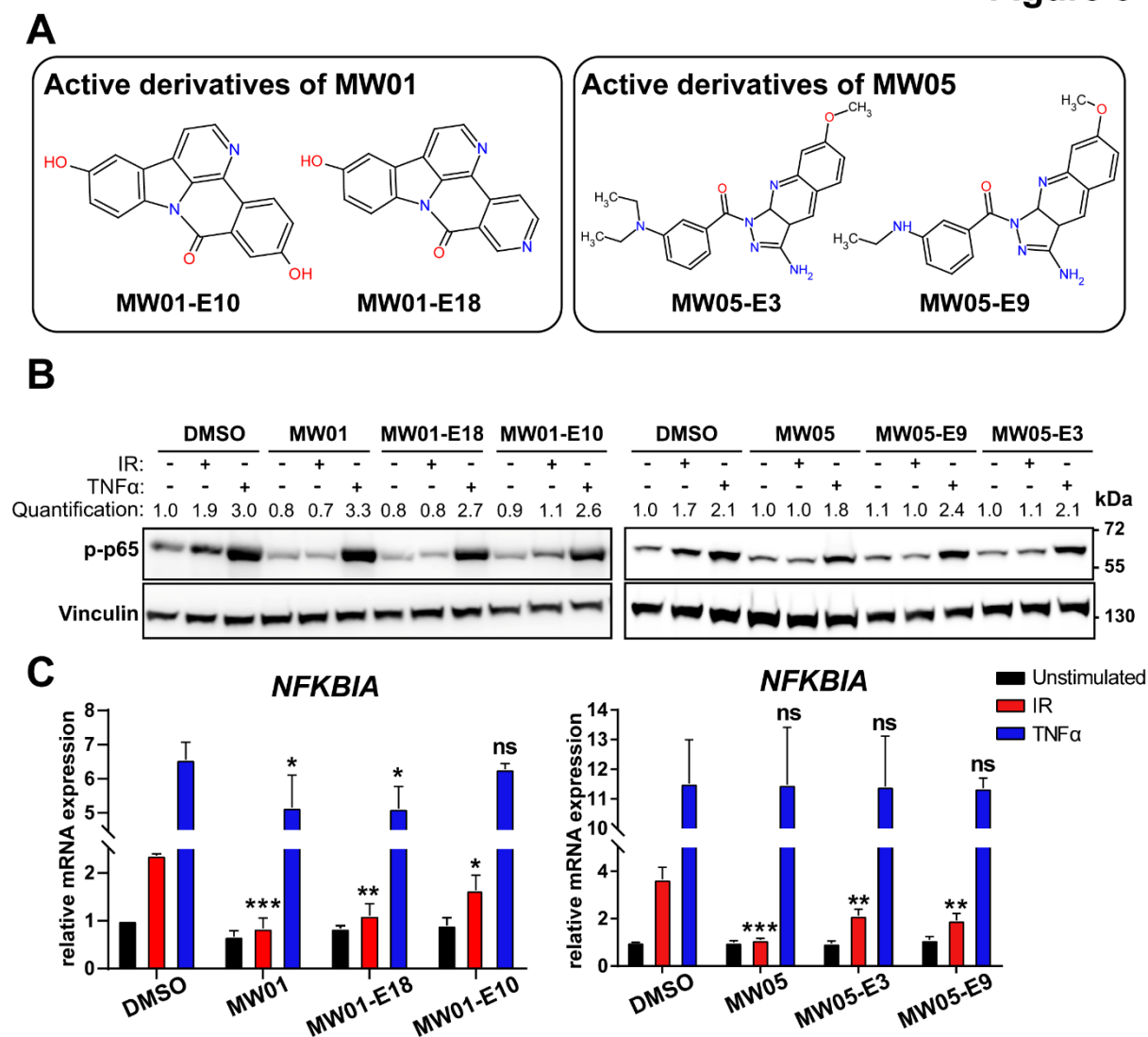


Figure 7-26: Active derivatives of MW01 and MW05 DNA damage-induce NF- κ B activation.

(A) Structures of identified active derivatives of 10 μ M MW01 (left), MW01-E10 and MW01-E18, and MW05 (right), MW05-E3 and MW05-E9. (B) Western blot analysis of lysates from U2-OS cells pre-treated with the indicated compounds for 1 hour, then stimulated with irradiation or TNF α . (C) RNA expression analysis using same experimental setup as in (B) for MW01 and derivatives (left) and MW05 and derivatives (right). *: $P \leq 0.05$; **: $P \leq 0.01$; ***: $P \leq 0.001$; ns: not significant.

Inhibition by the indicated active derivatives for both MW01 and MW05 was then further confirmed with repeated western blots and *NFKBIA* expression analysis (Figure 7-26A, B, C). Significant reductions in *NFKBIA* expression were observed for all selected active derivatives of each lead compound (Figure 7-26C; Figure 7-27C). Using the same experimental setup, lack of activity was confirmed for two inactive derivatives of each compound (Figure 7-27A, B, C). Phosphorylation of p65 was unchanged

after pre-treatment with any of the indicated derivatives and no significant change in *NFKBIA* was observed in any condition.

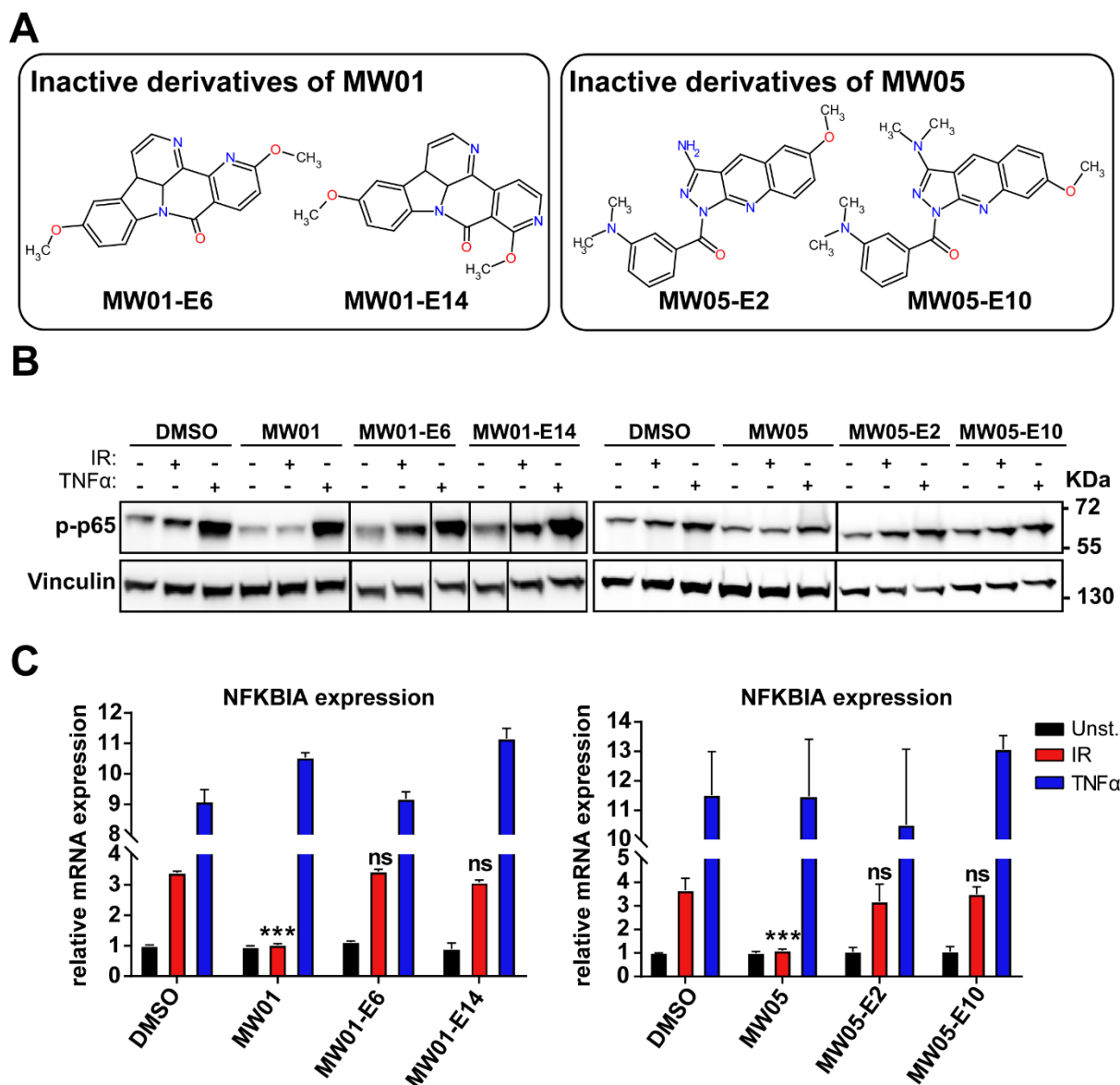


Figure 7-27: Inactive derivatives of MW01 and MW05 do not affect NF- κ B activation.

(A) Structures of identified inactive derivatives of 10 μ M MW01 (left), MW01-E6 and MW01-E15, and MW05 (right), MW05-E2 and MW05-E10. (B) Western blot analysis of lysates from U2-OS cells pre-treated with the indicated compounds for 1 hour, then stimulated with irradiation or TNF α . (C) RNA expression analysis using same experimental setup as in (B) for MW01 and derivatives (left) and MW05 and derivatives (right). Statistical comparison with 2-way ANOVA. ***: $P \leq 0.001$; ns: not significant.

To leverage these active and inactive derivatives in confirming CLK as the functional target of the lead compounds, the derivatives were subjected to an *in vitro* kinase panel containing all kinases strongly

inhibitable by MW01 and MW05 (Table S3). The profiles of active derivatives were similar to the respective lead compounds, validating the chemotypes of each as kinase inhibitors. However, inhibition of several kinases, except CLKs, was lost in the active derivatives of MW01 and MW05 including PI3K isoforms, providing further evidence that the NF-κB inhibitory effect is not caused by the inhibition of the phospholipid kinases (Table S3).

A

Lead	MW01 (IC50)		MW05 (IC50)	
	MW01-E18	MW01-E10	MW05-E3	MW05-E9
CLK1	581	438	1,810	2,700
CLK2	649	549	1,310	1,620
CLK3	>3,300	>3,300	>10,000	>10,000
CLK4	64.4	27.1	240	259

B

Lead	MW01		MW05		Percent inhibition
	MW01-E14 (10μM)	MW01-E6 (10μM)	MW05-E10 (10μM)	MW05-E2 (10μM)	
CLK1	6	10	35	16	= low, 0-40% = moderate, 40-70% = high, 70-100%
CLK2	20	18	28	74	
CLK3	7	9	2	5	
CLK4	67	58	92	75	

Figure 7-28: Active derivatives of MW01 and MW05 target CLK2 and 4.

(A) Comparison of IC50s for CLK isoforms 1-4 of MW01 derivatives MW01-E18 and MW01-E10, and MW05 derivatives MW05-E3 and MW05-E9. Strength of inhibition indicated numerically and by color gradient (red indicates stronger, blue indicates weaker inhibition). (B) Comparison of percent inhibition for CLK isoforms 1-4 of MW01 derivatives MW01-E6 and MW01-E15, and MW05 derivatives MW05-E2 and MW05-E10. Strength of inhibition indicated numerically and by color gradient (red= 100-70%, white= 40-70%, blue=0-40% inhibition).

Based on the high percent inhibition observed for CLK2 and 4 by active derivatives of MW01 and MW05, IC50 values for CLK1-4 were determined for the selected active derivatives. Crucially, all active compounds inhibited CLK2 with IC50 values of less than 2000 nM and CLK4 with IC50 values less than 300 nM, while three of four inactive compounds very weakly inhibited CLK2 (Figure 7-28A, B). The fourth inactive compound, MW05-E2, inhibited both CLK2 and CLK4 despite lacking activity in cell-based NF-κB activation assays, likely due to poor cellular uptake, an issue absent under *in vitro* kinase assay conditions (Table S3). Moderate CLK4 inhibition was noted for three of four inactive derivatives

while one, MW05-E10, inhibited CLK4 comparably to the active compounds. However, none of the inactive compounds share a combined CLK2 and 4 inhibition profile comparable to the leads or their active derivatives. Considering the similarity of NF- κ B pathway effects between the structurally distinct lead compounds, the agreement of all active derivatives with our kinase IC50 criteria, and significant results following siRNA knockdown of CLK2 and CLK4, I concluded that CLK2 and 4 are the functional targets of MW01 and MW05 and are therefore newly described regulators of genotoxic stress-induced NF- κ B.

8. Discussion

8.1. MW01 and MW05 are the first identified inhibitors of genotoxic stress-induced NF- κ B

NF- κ B's wide-reaching physiological role and its deregulation in numerous disease states suggest NF- κ B as an attractive therapeutic target, a view discussed repeatedly in the literature^{90,162}. However, relatively few therapeutics targeting NF- κ B have reached the clinic, particularly considering the nearly 40-year history of NF- κ B research. Targeting the ligands, cell surface receptors, or receptor adaptor proteins for various other NF- κ B activators, where the signaling cascade is initiated, is an effective therapeutic strategy in several contexts, including cancer, but specific inhibition of genotoxic stress-induced NF- κ B has not been previously reported¹¹⁰.

In this study, I first confirmed the activity of MW01 and MW05, novel specific small molecule inhibitors of genotoxic stress-induced NF- κ B activity previously identified by differential chemical library screen. Those compounds were then used to identify novel kinase regulators of DNA damage-induced NF- κ B activity, CLK2 and 4, through a combination of comparative kinase profiling, molecular characterization, and structural derivatization. In doing so, this study further characterized the first reported pathway-specific inhibitors of the genotoxic stress-induced NF- κ B activity, provide evidence of the compound's effects in potentiating cell death in tumor models, and implicate a new target to achieve this strategy.

8.2. MW01 and MW05 target the DNA damage response to potentiate apoptosis

The significance of the DNA damage response in human physiology is underscored by the presence of mutations in genes responsible for DDR enzymes. These mutations are not only detected in cancer cells but also in the inherited genetic makeup of individuals predisposed to cancer and genomic instability stemming from deficiencies in the DDR process, and are a defining characteristic of cancer⁸⁹. This instability contributes to a higher load of mutations, thereby escalating the likelihood of activating oncogenes and losing genes that restrain tumor growth, ultimately fostering the development of tumors. Additionally, the genetic diversity present within a tumor population can give rise to resistant subgroups following treatments like radiotherapy or chemotherapy and represents a type of therapeutic resistance.

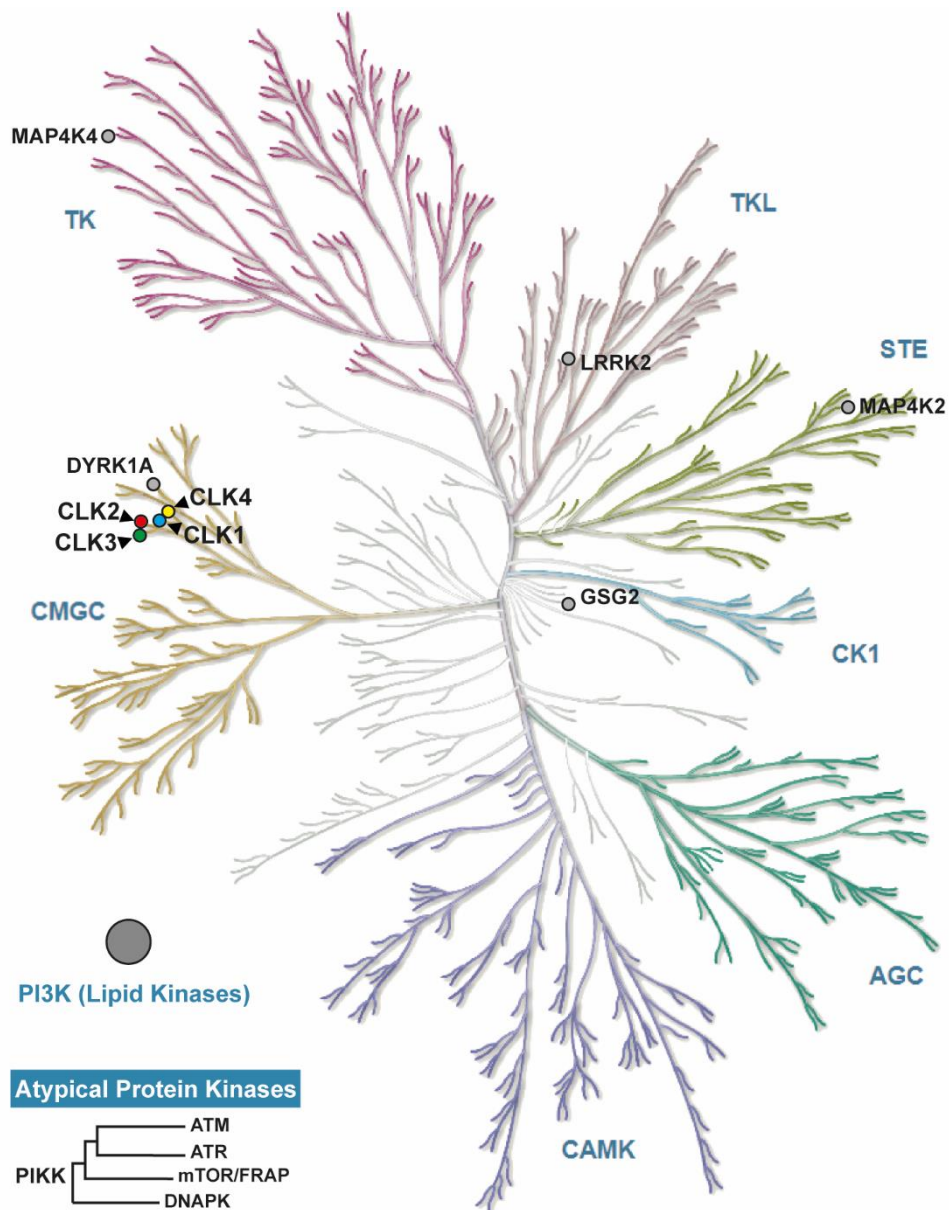
Previous work by our lab identified PARP1 as a critical component of the genotoxic stress-induced NF- κ B pathway⁶². Considering the essential role of PARP1 in those molecular studies, PARP inhibition would appear a promising avenue to achieve DNA damage-specific NF- κ B inhibition. Despite this, PARP inhibitors do not reliably inhibit NF- κ B following DNA damage. Olaparib, the first clinically approved PARP inhibitor, does not inhibit p65 phosphorylation following DNA damage while another clinically approved compound, Niraparib, has been shown to radiosensitize tumors by inhibiting NF- κ B¹²⁴. The causes of this discrepancy may be due to the unclear interregulation of the seventeen PARP isoforms and the diverse isoform specificity of investigational and clinical PARP inhibitors¹²². Thus, despite their noted clinical efficacy, PARP inhibitors cannot be used to inhibit NF- κ B following standard chemo- and radiotherapies and therefore may lack the tumor-killing effect resulting from abolished NF- κ B-mediated anti-apoptotic and pro-survival target gene expression.

MW01 and MW05 do not inhibit PARP activity and as such represent a new therapeutic avenue to inhibit DNA damage-specific NF- κ B activity and target the broader DDR. The results of the MW01/MW05 co-treatment with Olaparib in *BRCA* deficient cells presented in this study are preliminary in nature but there are several observations which warrant further study. (Figure 7-6). In these experiments, Olaparib was incubated overnight on *siBRCA1*-expressing cells before MW01/MW05 co-treatment was added the following day and cells lysed the next day, 48 hours total after the initial Olaparib treatment (Figure 7-6). Critically, a large increase in γ H2AX was observed in *siBRCA1*-expressing cells co-treated with MW01/MW05 and Olaparib compared to MW01 or MW05 treated cells, suggesting an accumulation of DNA damage which could lead to a genetic stability collapse and subsequent cell death. Furthermore, p-p65 levels in *siBRCA1*-expressing cells were low in the co-treatment condition, suggesting that NF- κ B activation due from impaired DNA repair, resulting from *BRCA1* knockdown and Olaparib treatment, was blocked by MW01 or MW05. This should lead to improved tumor cell killing in the co-treatment compared to Olaparib alone, which does not block DNA damage-induced NF- κ B activity. Several parameters including, length of each single treatment, co-treatment timing, and timepoints should be optimized to further interrogate this effect of the compounds. The experiment could also be run in a *BRCA1*- or *BRCA2*-deficient breast cancer cell line with wild-type p53, which would then mediate apoptosis once MW01 or MW05 inhibit NF- κ B, thereby unbalancing the NF- κ B/p53 axis. With further optimization of these parameters, I am confident a potentiation of DNA damage and apoptosis markers would be observed upon MW01/MW05 and Olaparib co-treatment.

8.3. CLK2 and CLK4 are the functional targets of MW01 and MW05

With the successful characterization of our inhibitors MW01 and MW05, our focus moved to target identification. Despite our observation of effects on several known DNA damage-induced NF- κ B pathway elements following treatment with MW01 or MW05 (Figure 7-3), we could not identify interaction or inhibition by our compounds with any known pathway elements. This was strongly suggestive of a previously unidentified DNA damage-specific regulator of NF- κ B as the shared target of our compounds. Once MW01 and MW05 were confirmed as kinase inhibitors and in consideration of the critical role of phosphorylation in signal transduction, it seemed highly likely that our functional target was a kinase. The inhibitory activity of both compounds MW01 and MW05 was determined at two different ATP concentrations and an ATP concentration-dependent inhibition was observed for both inhibitors, which is indicative of ATP competitive behavior (Table S1). In general, the structural diversity of ATP competitive kinase inhibitors is surprisingly large and therefore it might be difficult to match the ATP pharmacophore with a given inhibitor. However, both MW01 and MW05 inhibit several other, unrelated kinases which is further evidence that the compounds bind to the conserved ATP pocket and do not bind to, for example, an allosteric pocket, since this domain is highly conserved across the kinome (Figure 7-12, Figure 8-1, Figure 8-2, Table S1). Determination of the residues responsible for the suspected interaction within the ATP binding pocket of our compounds with CLK2 and 4, either by co-crystallization or *in silico* docking, would help direct further structural derivatization and lead optimization efforts (Figure 8-2).

Since kinase inhibitor promiscuity is a problem endemic to kinase inhibitors as a drug class¹²⁵, discerning on- and off-targets for compounds relies on an understanding of the physiological roles of putative drug targets. In general, on-targets are the functional targets which are responsible for mediating the intended effect of a drug, while off-targets are targets which do not mediate those effects and, in some cases, may also cause toxicity¹⁶³. In the case of MW01 and, to a lesser extent MW05, the kinase inhibition profile presents notable PI3K isoform off-targets, which initially seemed attractive as on-targets since I had previously investigated PIP4Ks, which had been identified in the 2D-TPP, and the well-described crosstalk between PI3K/Akt and NF- κ B (Figure 7-12, Figure 8-1). However, despite several published studies about the relationship between these pathways, it must be noted that these studies focussed on canonical NF- κ B stimuli other than DNA damage^{151,164,165}.



"Illustration reproduced courtesy of Cell Signaling Technologies Inc. (www.cellsignaling.com)"

Figure 8-1: Kinome tree map of targets of MW01 and MW05.

Schematic of phylogenetic kinome tree with on- and off-targets of MW01 and MW05 indicated. CLK1-4 are indicated with colored dots (blue, red, green, yellow respectively) and identified off-targets are marked with grey circles. Atypical protein kinase targets (bottom left) and lipid kinase (grey circle marked PI3K) are not phylogenetically related to the other targets and are therefore not part of the kinome tree itself. DYRK1A, MAP4K4, MAP4K2, LRRK2, and GSG2 are targets only of MW01.

While the PIP-based activation hypotheses for TRAF6 and NEDD4L produced negative data regarding the functional target identification for MW01 and MW05, they nonetheless produced some data which provided insights into these proteins. For example, the lack of translocation or constitutive membrane association of TRAF6 indicated that PIP binding should not have the hypothesized function to anchor

the assembly to membranes with ATM (Figure 7-13, Figure 7-14). However, the instability of the TRAF6-K388E PIP-binding mutant did not permit further study of any other potential PIP-dependent functions *in vitro* (Figure 7-16). From the preliminary studies presented here, it is unclear whether this is due to misfolding resulting in structural instability or insolubility or if the protein is structurally sound but requires PIP interaction for its stability. The latter case would represent a new finding regarding the functioning of TRAF6. To clarify this point, I would attempt to generate, purify, and further characterize the K388E mutant and repeat the PIP-strip experiment to confirm that PIP-binding by the mutant TRAF6 is abolished. This would help clarify if the poor stability *in vitro* is artefactual or a genuine biological insight.

In the end, adhering to a strict analysis of the kinase screening data for our two lead compounds ultimately led to the identification of CLK2 and CLK4 as the functional targets of MW01 and MW05. To guide my analysis, I established several criteria to narrow our selection of potential targets from the common kinases between MW01 and MW05 before moving on to biochemical analysis of the candidate target kinases. I hypothesized first that, considering the similar NF- κ B inhibition phenotypes of both compounds, the target should be shared by both lead compounds. Second, based on the CaCo2 recovery values for MW01 and MW05 respectively, and an experimental treatment concentration of 10 μ M, the putative target kinase should have a low IC₅₀ of, at most, 2000 nM for both lead compounds in the *in vitro* kinase panel (Figure 7-12). Based on these criteria alone, I arrived at a relatively short list of potential targets for further analysis, leaving only PIK3CD, PIK3CG, PIK3C2G, CLK2. IC₅₀ values for PIK3C2G by both lead compounds agreed best with these criteria, but RNA expression analysis indicates high tissue specificity as well as lack of expression in U2-OS, which was then eliminated from further analysis¹⁴⁷. DNA-pk and mTOR failed to meet the sub-2000nM IC₅₀ criteria for MW05 and MW01 respectively and were therefore likely out of dosage range in cell-based assays, but I decided to move forward with these targets to exclude their role experimentally. Of the remaining possible targets, CLK2 shared the most similar and second-lowest combined IC₅₀, suggesting that strong inhibition is likely reached with a treatment concentration of 10 μ M in cell-based assays. However, PIK3CD and PIK3CG also have IC₅₀s of similar magnitude for each respective compound, so I carried out further analysis on PIK3CD, PIK3CG, CLK2, DNA-PK, and mTOR.

```

CLK1_HUMAN      1  -----
CLK2_HUMAN      1  -----
CLK3_HUMAN      1  MPVLSARRRELADHAGSGRRSGPSPARTARSGPHLSALRAQPARAAHLSGRGTYVRRDTAGG
CLK4_HUMAN      1  -----

CLK1_HUMAN      1  0-----
CLK2_HUMAN      1  0-----
CLK3_HUMAN      61 60GPGQARPLGPPGTSLLLGRGARRSGEGWCPGAFESGARAARPPSRVEPRLATAASREG
CLK4_HUMAN      1  0-----

CLK1_HUMAN      1  -- 0-----MRHSKRTYCPDWDDD- -DYGK RSSSS
CLK2_HUMAN      1  -- 0-----MPHP RYHSS-RGSRGS RE-H RSRKH
CLK3_HUMAN      118 AGL 120PRAEVAAGSGRGARSGEWGLAAAAGAWETMHHCKRYRSPEDPYLSYR-----
CLK4_HUMAN      1  -- 0-----MRHSKRTYCPDWDSR S GHES- -RGS

CLK1_HUMAN      28 HKR 31KRSHSSAQENRCKYN--HS-KM-CDSHY---LESRS NE DYHSRRY DEYR
CLK2_HUMAN      28 KRR 31SRSWSS S-RTRRRRREDS HVRSRSSYDDRSDRRY RRY- - -CGSYR
CLK3_HUMAN      169 -- RRR 172S--YSREHEGLRYPSPR EPPRRS---RSRSHDLRYPQRRYRERRDS
CLK4_HUMAN      27 HKR 30RSHSS QENRHCKPH--HQ KE-SDCHY---LEARS NERDYRDRY DEYR

CLK1_HUMAN      78 N-DYTQG 83CEP HQRDHESTRYQNHSSKSSGRSGRSSYKSKHRIHHS SHRRSHGKSH
CLK2_HUMAN      79 RNDYSRD 85RGD YDIDYRHSYEQRENSSYRSQRSSRKHRRRRRRTFSRSSSQH
CLK3_HUMAN      216 DTYRCERSPS 226GEDYGPSRHRHRSRERGPYRTKHAHHCRRTRSCSSAASS
CLK4_HUMAN      78 N-DYCEG 83YVPRHYHRDI ESGYRI HCSKSSVRSRRSSPARKRNRHC--SSHQSRKSH

CLK1_HUMAN      134 RRKR RSVED 143DEEGLH CQSGDVL SARYEIVDTL GEGAFGKVECI DHKAGGRHVA
CLK2_HUMAN      136 SSRA RSVED 145DAEGLH YHVGDLQERYEIVSTL GEGTFG VVQC DHRRGGARVA
CLK3_HUMAN      272 RSQSSKRSSRSVED 286DKEGHLVCRID LQERYEIVGNLGEFTFGKVVVECLDHAR
CLK4_HUMAN      132 RRKR RSV ED 141DEEGLH CQSGDVL SARYEIVDTL GEGAFGKVECI DHGMDGMHVA

CLK1_HUMAN      190 VKI VKNV RYCEAA 203RSEI QVLEHLN TDPNSTFRVQMLEWF HGH C VPELLG
CLK2_HUMAN      192 KI KNV RY EAA 205RLEI VLEK NEKDPDNKLVQMF WFDYHGH C SFELLG
CLK3_HUMAN      328 KSQVALKI RNV KYREAA 346RLEI NVLKKI KEKD ENKFLCVLMSDFWNFHGHMCA
CLK4_HUMAN      188 VKI VKNVGRY EAA 201RSEI QVLEHLN TDPNSVFRVQMLEWF DHHGVCI VPELLG

CLK1_HUMAN      246 LSTYDFI KENGF L PFR ID 263HIRK MAYQI CKSVNFLHSNKLTHTDLKPENI L FV SDY
CLK2_HUMAN      248 LSTDFI KINN L PPI H 265QRHMA QICQAVKFL HDNKLTHTDLKPENI L FVNSDY
CLK3_HUMAN      384 FELLGKNTFEFLKEN FQPYPLP 406HVRHMAYQLCHALRFLHENQLTHTD KPENI L
CLK4_HUMAN      244 LSTYDFI KENS F L PFI D 261HIRQMAYQI CQS NFLH HNKLTHTDLKPENI L FV KSDY

CLK1_HUMAN      302 TEAYNPK KRDER L L NPD KV 323VDFGSAT DDEHHSTLVSTRHYRAPEV LALGWS
CLK2_HUMAN      304 E YNLEK KRDER KSTA V 325VDFGSAT DDEHHSTLVSTRHYRAPEV LELGWS
CLK3_HUMAN      440 VNSEFET YN H K CEEKS KNTSIRV 466AD GSATFDHEHHTI I VATRHYRPEV L
CLK4_HUMAN      300 VYKYN SK KRDER L KNTD KV 321VDFGSAT DDEHHSTLVSTRHYRAPEV LALGWS

CLK1_HUMAN      358 QPCDVWSI GCI L EYLLGFTVFQTHD 383SK EHLAMMERI LGPI PKHMI QKTRKRYFYH
CLK2_HUMAN      360 QPCDVWSI GCI L FEYLLGFTVFQTHD 385N EHLAMMERI LGPI PSRMI RKTRKQKYFY
CLK3_HUMAN      496 ELGWAQPCDVWSI GCI L FEYLRGFTL FQTHE 526NREHL VMEKI LGPI PSHMI HTRK
CLK4_HUMAN      356 QPCDVWSI GCI L EYLLGFTVFQTHD 381SK EHLAMMERI LGPI PQHMI QKTRKRYFYH

CLK1_HUMAN      414 HDRLDWDEHSSAGRYVSRRCPLKEFMLSQ 443DVEHE LFDL Q MLEYDPAKRI TLR
CLK2_HUMAN      416 RGRLDWDEN SAGRYVRENCKPL RY TSE 445AEEHQLFDL ESMLEYPAKR TLG
CLK3_HUMAN      552 QKYFYKGGLVWDENSSDGRYVKENCKPL KSYMLQD 586SLEH QLFDL MRRMLEFDPAQ
CLK4_HUMAN      412 HNQLDWDEHSSAGRYVRRRCPLKEFMLCH 441DEEHE LFDL V R MLEYDPTQRI TLD

CLK1_HUMAN      470 EALKHPFFDLLKKS I ----- 484
CLK2_HUMAN      472 EALQHPFFARL AEPNKLWSSRDI SR 499
CLK3_HUMAN      608 RITLAEALLHPFFAGLTPEE- -RSFHTSRNPSR 638
CLK4_HUMAN      468 EALQHPFFDLLK K- ----- 481

```

Figure 8-2: Sequence alignment of CLK isoforms 1-4.

Box-shade alignment of CLK isoforms 1-4. Highly conserved amino acids are indicated in black, while partly conserved are shaded in grey. ATP binding pocket region marked in green and “LAMMER” motif marked in red.

Finally, to address any other potential on- or off-targets, a kinome-wide inhibition profile for both MW01 and MW05 should be performed to identify any further targets that cannot yet formally be excluded as contributing to the pathway inhibitory effect, based on the kinase panel presented here.

8.4. CLK2 and CLK4 are novel regulators of genotoxic stress induced NF-κB

The identification of CLK2 and 4 as the shared target of our active compounds and their active derivatives was surprising, since the kinases have no previously reported role in NF-κB activation. In particular, confirmation of CLK2 and 4 as regulators of DNA damage-induced NF-κB challenges the prevailing narrative that CLK2 and 4 are primarily responsible for phosphorylating SR proteins that modulate RNA splicing¹⁶⁶⁻¹⁶⁹. As part of the “LAMMER” sub-family of CGMC kinases, CLK2 and 4 regulate serine-arginine (SR) proteins, affecting SR protein binding to pre-mRNA and subsequent spliceosome assembly (Figure 8-2)¹⁷⁰. This phosphorylation can either enhance or inhibit specific splicing events, thus influencing the production of different protein variants from the same gene. CLK-mediated splicing regulation is crucial for the development, differentiation, and proper physiological functioning of various cell types¹⁷⁰. However, this mode of action can be excluded for our compounds based on the previously established 30-minute pre-incubation required to block NF-κB prior to DNA damage, which is likely too short to observe the effects of alternate splicing on our pathway.

As further confirmation of CLK2 and 4 as functional targets of the lead compounds, work by our group also identified both kinases in a genome-wide siRNA screen for regulators of genotoxic stress-induced NF-κB with values between those reported for IKK and ATM, two well-described required DNA damage-induced NF-κB pathway elements¹⁵⁷. In addition, a recent study identified an interaction between CLK2 and HPV16 oncogene E6 that conferred increased radiosensitivity in HPV-positive cancers resulting from hijacking of the host’s DDR machinery, providing further evidence of CLK2’s role in the broader DDR¹⁷¹. CLK2/CLK3 was also identified as an interactor of E6, suggesting there may be interregulation between CLK isoforms that could confer specificity, especially given that CLKs are known to heterodimerize^{171,172}.

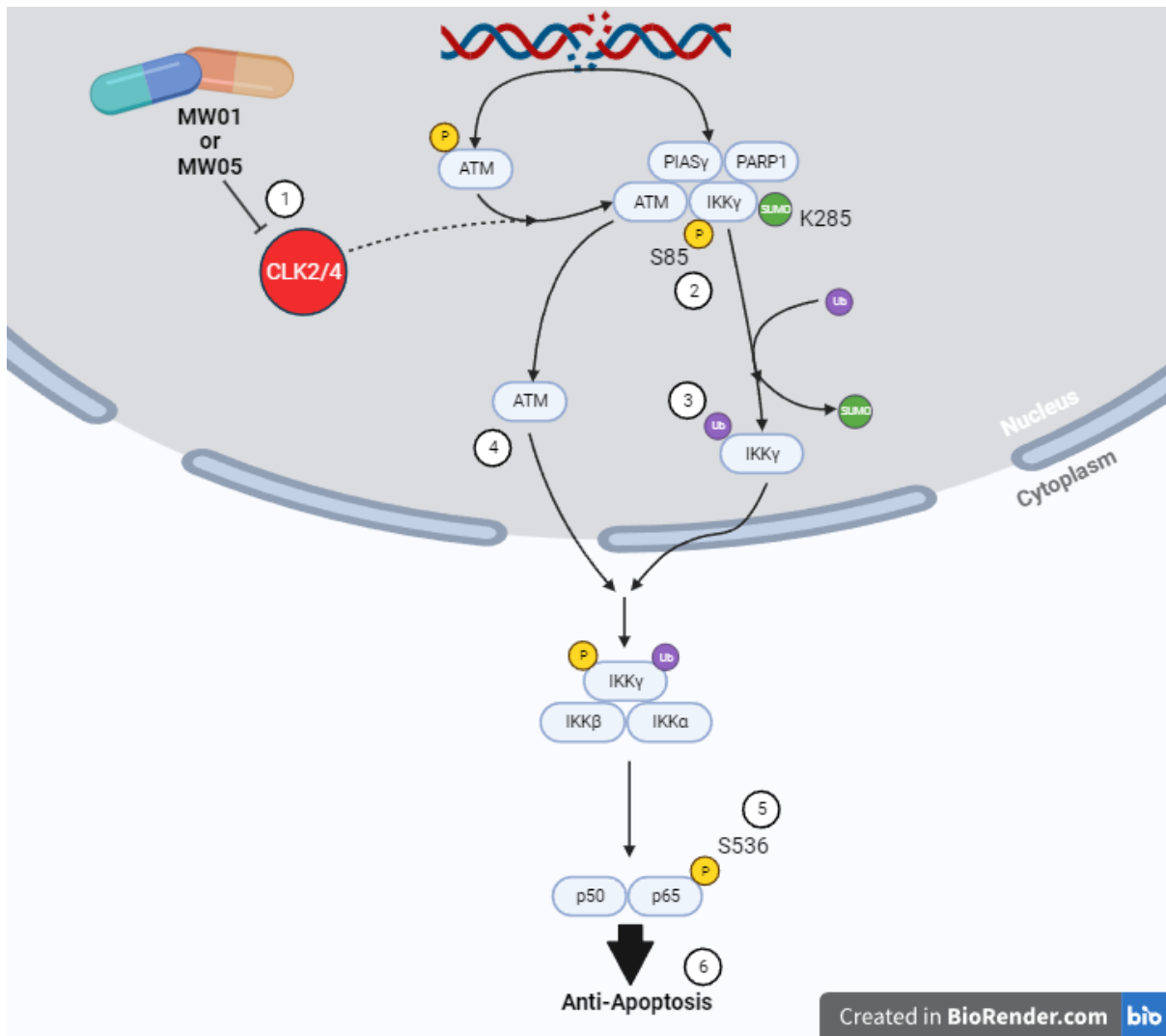


Figure 8-3: CLK2 and 4 are targeted by MW01 and MW05 and act between ATM and IKK in the genotoxic stress-induced NF-κB pathway.

Schematic of CLK2 and 4's possible input point into the genotoxic stress-induced NF-κB pathway, with effects of MW01 and MW05 treatment indicated by numbered white circles. (1) MW01 and MW05 inhibit CLK2 and CLK4. (2) IKKγ-S85 phosphorylation is lost. (3) IKKγ-K285 mono-ubiquitination is lost. (4) ATM nuclear export is reduced. (5) p65-S536 phosphorylation is blocked. (6) Downstream anti-apoptotic signaling is blocked.

When considered alongside the data presented in this work, these studies point to an expanding role for CLK2 and 4 which warrants further investigation. To that end, the mechanism by which CLK2 and 4 regulate NF-κB should be determined, potentially using a phospho-proteomic approach to identify DNA damage-inducible functional interactions with downstream effectors of CLK2 and 4, which should be abolished by treatment with our compounds. One possibility for CLK input into the genotoxic stress-induced NF-κB pathway could be to introduce a priming phosphorylation to IKKγ which would promote subsequent interaction with ATM upon DNA damage. Additional functional genomic approaches such

as CRISPR knockout or kinase-dead mutants would also be helpful in further exploring CLK2 and 4 mechanistically.

8.5. CLK2 and CLK4 are promising, druggable therapeutic targets in cancer

Dysregulation of CLKs and the alternative splicing processes they control have been implicated in various diseases, including cancer and neurodegenerative disorders, and the clinical implications of this have been illuminated by numerous recent studies¹⁷⁰. CLK2 has a proposed oncogenic role in many cancers such as colorectal cancer, non-small cell lung cancer, glioblastoma, and breast cancer and elevated CLK2 expression has been claimed to be associated with their occurrence, progression, and poor prognosis¹⁷³⁻¹⁷⁵. In addition, inhibition of CLK2 by small molecules has been shown to inhibit tumor xenografts *in vivo* in breast cancer models^{167,168,176}. Two compounds, SM08502 and CTX-712, have recently entered clinical trials for the treatment of advanced or refractory solid tumors and were well tolerated in phase I studies^{177,178}. Taken together, these data suggest that CLK2 is a promising target for the development of future small molecule inhibitors of genotoxic stress-induced NF- κ B in a wide array of tumours. CLK4 is comparatively less well understood, but it has been shown to be overexpressed in invasive breast cancers and associated with poor prognosis in triple negative breast cancer patients¹⁷⁹.

Several CLK inhibitors have been recently reported in the literature in addition to the novel inhibitors we identified here, providing multiple chemotypes as starting points for further pharmacokinetic optimization^{170,180-182}. One such inhibitor, MU-1210, blocked p-p65 in a genotoxic stress specific manner despite being structurally distinct from MW01 and MW05 (Figure 7-19). MU-1210 is a highly potent inhibitor of CLK1, 2, and 4, with IC50 values of 8, 20, and 12 nM for CLK1, 2, and 4, respectively¹⁸², which agrees with the finding that both CLK2 and CLK4 are regulators of DNA damage. Both MW01 and MW05 had IC50's for CLK4 which were an order of magnitude smaller than those for CLK2, suggesting that CLK4 more may be the more critical isoform, or that CLK2 and CLK4 work in concert together to regulate genotoxic stress-induced NF- κ B (Figure 7-21). Better chemical probes with improved isoform specificities will help untangle the distinct roles within the NF- κ B pathway and, to that end, selective inhibitors of CLK2 and 4 have recently been described, although as with any kinase inhibitor true single-kinase specificity remains elusive^{176,178,183-186}.

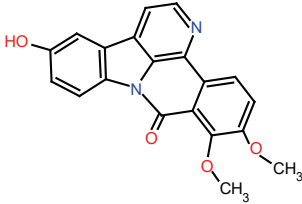
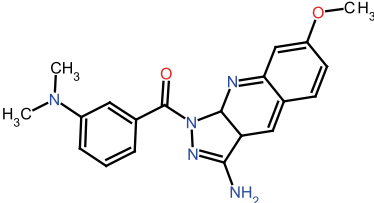
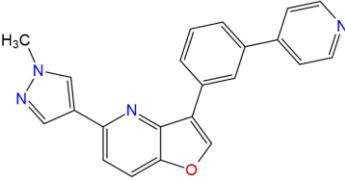
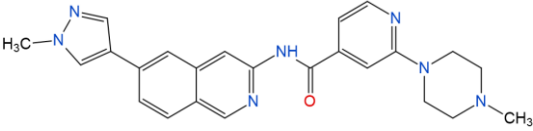
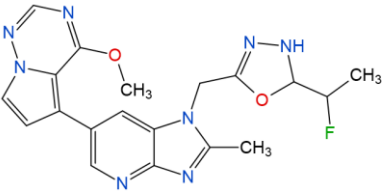
Name	Structure	CLK IC50s (nM)	Clinical Trial
MW01		1: 250 2: 360 3: >3,300 4: 14.1	-
MW05		1: 2,230 2: 1,440 3: inactive 4: 307	-
MU-1210		1: 8 2: 20 3: inactive 4: 12	-
SM08502		1: 8 (K _d) 2: 1 (K _d) 3: 22 (K _d) 4: 1 (K _d)	Phase 1
CTX-712		1: not disclosed 2: 1.4 3: not disclosed 4: not disclosed	Phase 1

Table 8-1: Structure and CLK isoform specificities of CLK inhibitors.

Considered together with the expanding physiological role of CLKs, their demonstrated relevance in cancer, and the rapid development of drugs targeting these kinases, I expect a bright future for CLK-targeting therapies. This promising prospect also warrants detailed analysis of the potential future development of MW01 and MW05 for clinical and investigational purposes.

8.6. Future directions for the development of MW01 and MW05

The successful identification of CLK2 and 4 as novel regulators of genotoxic stress-induced NF- κ B by is indicative of the validity of MW01 and MW05 as drugs, and of the analytical power of comparative target deconvolution using two structurally distinct lead compounds. MW01 and MW05, as with many small molecules, have characteristics such as solubility, cell permeability, and serum stability that

should be improved through derivatization to achieve to better pharmacokinetics. To that end, these parameters should be determined for the derivative library synthesized by Enamine Ltd., especially for the selected active derivatives MW01-E10, MW01-E18, MW05-E3, and MW05-E9 (Table S2, Figure 7-26, Figure 7-28). Critically, the affinity of further derivatives for CLK2 and CLK4 should also be improved to have a comparable magnitude to other published CLK inhibitors, such as MU-1210¹⁸². To guide further lead optimization efforts, structure activity relationships should be determined for the selected active and inactive derivatives. However, it should be noted that some characteristics, such as poor solubility, are common to other CLK inhibitors and are therefore not unique hurdles to the further development of MW01 and MW05¹³¹. Despite these challenges, the structural backbones of MW01 and MW05 offer differing possibilities for therapeutic development, and a patent was recently submitted regarding the MW05 derivatives described in this study (C. Scheidereit, P. Mucka et al., (2023) Selective inhibitors of Genotoxic Stress Induced IKK-NF-κB Pathways for Cancer Therapy”, Europäisches Patentamt, EP 23175081.1)¹⁸⁷.

The future direction of each lead compound and the derivatives should be guided by the differential kinase specificities characterized here (Table 8-2, Table 8-3, Table S3). Of the two lead compounds, MW01 is overall less specific than MW05, yet is more potent against most of their shared targets. While the field has generally aimed to produce highly specific single kinase inhibitors, there is growing interest in compounds which target multiple proteins, a phenomenon termed polypharmacology¹³². From this perspective, off-targets (targets not responsible for a drug’s intended effect) could potentially be beneficial if the context also warrants inhibiting those kinases. For example, the sub-100 nM IC50s of MW01 for various PI3K isoforms and resultant inhibition of downstream signaling (Figure 7-19) might be favorable depending on the treatment context. Numerous PI3K inhibitors inhibiting the same isoforms as MW01, such as PIK3CD, with similar potency, have been approved as combinatorial therapies for breast cancer, chronic lymphocytic leukemia, and follicular lymphoma^{188,189}. As such, MW01 also represents a newly identified PI3K inhibitor that also blocks anti-apoptotic signaling from DNA damage-induced NF-κB and therefore may have improved tumor killing effect when compared to standard PI3K inhibitors. Since the active derivatives of MW01, MW01-E10 and -E18, largely preserve the PI3K inhibition observed with MW01 (Table 8-2, Table S3), the pharmacokinetic parameters of these compounds should be determined so that a preferred structural backbone for further derivatization can be identified.

NF-κB inhibition Kinase	Percent Inhibition				
	active	active	active	inactive	inactive
	MW01 (10μM)	MW01-E18 (10μM)	MW01-E10 (10μM)	MW01-E14 (10μM)	MW01-E6 (10μM)
CLK1	88	61	69	6	10
CLK2	91	70	70	20	18
CLK3	53	35	35	7	9
CLK4	91	98	99	67	58
DNA-PK	96	94	62	43	9
DYRK1A	90	65	56	12	14
DYRK1B	82	68	81	23	20
FRAP1 (mTOR)	80	43	42	26	12
GSG2 (Haspin)	83	88	80	24	29
IKKB (IKK beta)	12	16	31	16	10
IRAK1	67	69	71	9	56
IRAK4	50	2	-186	-15	-9
LRRK2	87	75	86	-4	64
MAP4K2 (GCK)	77	93	98	81	70
PI4K2A (PI4K2 alpha)	25	30	13	35	22
PI4K2B (PI4K2 beta)	20	24	22	21	11
PI4KB (PI4K beta)	23	81	90	36	12
PIK3C2A (PI3K-C2 alpha)	100	44	31	23	26
PIK3C2G (PI3K-C2 gamma)	43	81	81	50	35
PIK3CA/PIK3R1	68	90	90	80	38
PIK3CA/PIK3R3	94	94	90	59	10
PIK3CB/PIK3R1	49	62	34	26	13
PIK3CB/PIK3R2	96	63	35	12	12
PIK3CD/PIK3R1	97	77	87	84	34
PIK3CG	86	99	93	49	-1
PIP4K2A	96	-1	-2	53	-4
PIP5K1A	67	28	5	11	20
PIP5K1B	66	-3	5	26	14
PIP5K1C	89	27	33	8	14
PRKCN (PKD3)	88	52	74	-1	-8

Table 8-2: Percent inhibition of selected kinase targets of MW01 and derivatives.

NF- κ B inhibition Kinase	Percent Inhibition				
	active	active	active	inactive	inactive
	MW05 (10 μ M)	MW05-E9 (10 μ M)	MW05-E3 (10 μ M)	MW05-E10 (10 μ M)	MW05-E2 (10 μ M)
CLK1	73	79	81	35	16
CLK2	86	87	86	28	74
CLK3	72	38	41	2	5
CLK4	94	84	99	92	75
DNA-PK	61	64	67	8	16
DYRK1A	60	36	76	20	53
DYRK1B	69	46	58	14	84
FRAP1 (mTOR)	81	71	52	2	5
GSG2 (Haspin)	20	23	83	19	36
IKKB (IKK beta)	5	7	23	10	12
IRAK1	-7	6	37	-19	2
IRAK4	2	-11	-13	-6	-3
LRRK2	5	-1	37	-6	8
MAP4K2 (GCK)	10	0	51	5	2
PI4K2A (PI4K2 alpha)	-1	-7	4	-3	-4
PI4K2B (PI4K2 beta)	0	-6	3	1	8
PI4KB (PI4K beta)	-1	-14	24	1	9
PIK3C2A (PI3K-C2 alpha)	43	-6	17	6	10
PIK3C2G (PI3K-C2 gamma)	1	41	72	10	27
PIK3CA/PIK3R1	12	21	51	-9	26
PIK3CA/PIK3R3	87	16	47	-3	8
PIK3CB/PIK3R1	4	19	40	4	1
PIK3CB/PIK3R2	68	22	34	2	7
PIK3CD/PIK3R1	61	25	55	6	28
PIK3CG	52	40	56	-7	2
PIP4K2A	63	-6	2	-14	-6
PIP5K1A	67	-16	-2	-8	-9
PIP5K1B	64	33	29	-8	-12
PIP5K1C	77	-5	39	-4	-2
PRKCN (PKD3)	70	14	31	5	7

Table 8-3: Percent inhibition of selected kinase targets of MW05 and derivatives.

In the case of MW05, the more specific kinase profile of the lead compound and improved specificity of equally active derivatives points toward the possibility of a specific CLK inhibitor with selectivity towards CLK2 and CLK4 (Table 8-3, Table S3). Interestingly, while the active derivatives MW05-E3 and -E9 show similar potency and CLK isoform specificity to MW05, the inactive derivatives MW05-E10 and -E2 retain potent inhibition of CLK4 or CLK2 and 4, respectively, and therefore may serve as starting points for the development of isoform specific CLK inhibitors. MW05-E10 strongly inhibited CLK4, with a percent inhibition of 92% while CLK1 and 2 were only weakly inhibited with percent inhibitions of 35% and 28% respectively, suggesting that further derivatives based on this structure could yield an

isoform-specific CLK4 inhibitor (Table 8-3). The apparent disagreement of this inhibition profile with the CLK4 knockdown experiment (Figure 7-22), which showed single knockdown of CLK4 was sufficient to abolish NF- κ B activity, could be explained by the more potent effect of genetic ablation or by potential interregulation between isoforms. Further studies with CLK4-specific (and CLK2-specific) inhibitors could help clarify potential isoform-specific roles for CLKs within the pathway. In the case of MW05-E2, specificity for CLK2 and 4 was improved over the MW05 compound since inhibition of CLK1 was lost, with 15% inhibition compared to 86% inhibition for MW05 (Table 8-3). However, the percent inhibition of CLK2 and 4 (74% and 75% inhibition, respectively) was slightly reduced compared to MW05 (86% and 94%), suggesting a loss of potency for those isoforms (Table 8-3). Despite the inhibition of CLK2 and CLK4 in the kinase panel, MW05-E2 was inactive in cell-based assays, which could potentially be due to poor cellular permeability (Figure 7-27, Figure 7-28). Further structural derivatives of MW05-E2 could regain activity in cell-based assays and improve the potency for CLK2 and 4 or could be used as a chemical probe and would then be useful in elucidating the specific roles of the CLK isoforms.

9. Supplemental Information

Table 9-1: Broad kinase inhibition panel of MW01 and MW05.

Broad *in vitro* kinase inhibition panel using SelectScreen service by Thermo Fisher using ADAPTA or Z'-lyte assays.

Kinase	MW01 (10000nM)	MW01 (1000nM)	MW05 (10000nM)	MW05 (1000nM)
ABL1	27	15	6	4
ABL1 E255K	11	7	5	6
ABL1 F317I	19	8	-1	6
ABL1 F317L	13	8	4	6
ABL1 G250E	32	9	0	12
ABL1 T315I	34	9	5	8
ABL1 Y253F	30	9	7	-2
ABL2 (Arg)	21	9	2	5
ACVR1B (ALK4)	-3	-9	-8	1
ADRBK1 (GRK2)	17	8	4	-1
ADRBK2 (GRK3)	5	0	-3	2
AKT1 (PKB alpha)	10	5	3	3
AKT2 (PKB beta)	9	1	-8	10
AKT3 (PKB gamma)	18	7	-6	4
ALK	40	18	-2	0
AMPK (A1/B2/G2)	5	-6	4	-10
AMPK (A1/B2/G3)	19	3	-6	0
AMPK (A2/B1/G2)	10	-12	-16	-12
AMPK (A2/B1/G3)	12	-2	-3	0
AMPK (A2/B2/G3)	18	8	-4	4
AMPK A1/B1/G1	14	4	-3	6
AMPK A2/B1/G1	32	8	0	5
AURKA (Aurora A)	18	8	-5	7
AURKB (Aurora B)	19	15	-6	8
AURKC (Aurora C)	10	8	9	9
AXL	80	51	-8	4
BLK	26	8	-1	0
BMX	6	-8	4	-10
BRSK1 (SAD1)	6	0	-6	-1
BTK	23	11	8	5
CAMK1 (CaMK1)	-2	-12	-5	-11
CAMK1D (CaMKI delta)	9	5	-1	1
CAMK2A (CaMKII alpha)	39	12	16	9
CAMK2B (CaMKII beta)	37	9	3	5
CAMK2D (CaMKII delta)	60	13	13	3
CAMK4 (CaMKIV)	16	-3	-9	2
CDC42 BPA (MRCKA)	15	11	2	9
CDC42 BPB (MRCKB)	5	0	-6	5
CDC42 BPG (MRCKG)	5	1	0	0
CDK1/cyclin B	46	20	57	19

CDK17/cyclin Y	9	3	21	8
CDK18/cyclin Y	15	5	55	13
CDK2/cyclin A	37	14	25	12
CDK4/cyclin D1	-4	-8	-1	-3
CDK4/cyclin D3	-6	-2	-8	-6
CDK5/p25	12	4	8	4
CDK5/p35	14	17	7	5
CDK6/cyclin D1	-8	1	0	2
CDK7/cyclin H/MNAT1	4	3	29	2
CDK9/cyclin T1	20	11	57	19
CHEK1 (CHK1)	13	4	27	16
CHUK (IKK alpha)	21	19	18	7
CLK1	88	n.d.	73	n.d.
CLK2	91	78	86	40
CLK2	91	78	72	40
CLK4	91	n.d.	94	n.d.
CSF1R (FMS)	51	36	-6	5
CSK	18	11	13	9
CSNK1A1 (CK1 alpha 1)	17	5	1	2
CSNK1A1L	11	1	1	1
CSNK1D (CK1 delta)	39	13	-1	-1
CSNK1E (CK1 epsilon)	32	6	0	2
CSNK1E (CK1 epsilon) R178C	64	23	6	0
CSNK1G1 (CK1 gamma 1)	12	5	6	3
CSNK1G2 (CK1 gamma 2)	41	22	13	4
CSNK1G3 (CK1 gamma 3)	12	4	9	1
CSNK2A1 (CK2 alpha 1)	18	9	5	9
CSNK2A2 (CK2 alpha 2)	29	16	4	7
DAPK1	14	8	3	3
DAPK3 (ZIPK)	9	2	-3	2
DNA-PK	96	86	61	30
DYRK1A	90	80	60	22
DYRK1B	82	62	69	28
DYRK3	43	17	7	5
DYRK4	0	-2	4	4
EEF2K	37	11	5	3
EGFR (ErbB1)	0	17	5	13
EGFR (ErbB1) C797S	11	4	-14	1
EGFR (ErbB1) G719S	14	5	-5	4
EGFR (ErbB1) L858R	5	3	16	6
EGFR (ErbB1) L861Q	8	-9	-18	-6
EGFR (ErbB1) T790M	19	8	0	4
EGFR (ErbB1) T790M C797S L858R	12	2	2	1
EGFR (ErbB1) T790M L858R	29	9	10	-5
EPHA1	16	9	-5	11
EPHA2	14	6	-15	13
EPHA5	7	-4	-16	-8
EPHA8	21	4	-9	-1
EPHB1	9	-3	-6	-3

EPHB2	17	10	1	6
EPHB3	11	1	5	6
EPHB4	7	5	2	-3
ERBB2 (HER2)	4	2	-19	-5
ERBB4 (HER4)	4	-3	-11	5
FER	25	11	0	7
FES (FPS)	15	0	-1	1
FGFR1	5	6	-7	-1
FGFR2	11	13	-5	0
FGFR2 N549H	13	0	-22	-4
FGFR3	8	4	-8	1
FGFR3 K650E	16	6	-3	8
FGFR3 V555M	11	5	-9	-30
FGFR4	37	13	-4	13
FGR	26	10	15	5
FLT3	86	61	6	2
FLT3 D835Y	92	81	15	10
FLT4 (VEGFR3)	31	13	-3	7
FRAP1 (mTOR)	80	31	81	31
FRK (PTK5)	22	15	6	9
FYN	15	3	5	4
GRK4	12	8	2	-1
GRK5	0	-3	0	-2
GRK6	5	0	3	6
GRK7	0	-2	5	-2
GSG2 (Haspin)	83	77	20	4
GSK3A (GSK3 alpha)	55	25	18	3
GSK3B (GSK3 beta)	52	27	14	6
HCK	22	13	9	10
HIPK1 (Myak)	47	21	-6	-4
HIPK2	74	48	13	4
HIPK4	62	42	8	12
IGF1R	31	11	-12	-1
IKBKB (IKK beta)	12	4	5	6
IKBKE (IKK epsilon)	17	11	6	8
INSR	11	1	-7	8
IRAK1	67	57	-7	17
IRAK4	50	19	2	0
ITK	-2	0	-6	-10
JAK2	48	15	-20	-3
JAK2 JH1 JH2 V617F	29	15	-28	1
JAK3	20	9	-6	4
KDR (VEGFR2)	54	24	-15	7
KIT T670I	13	1	-13	-1
KIT V559D	25	11	15	13
KIT V559D V654A	-12	-10	-37	-16
KIT V560G	7	12	2	11
KSR2	8	5	-2	7
LCK	37	12	5	8
LRRK2	87	83	5	-3

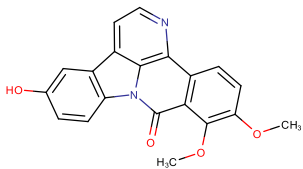
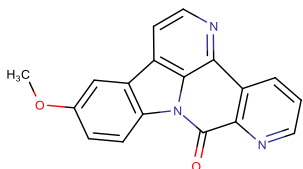
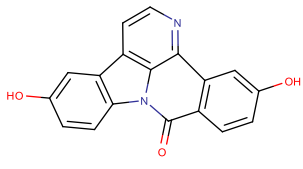
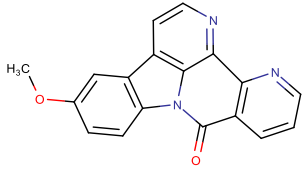
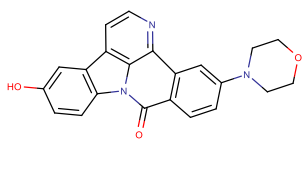
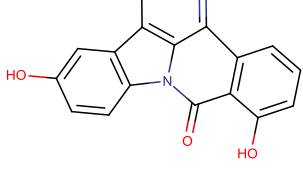
LRRK2 FL	90	85	6	-6
LRRK2 G2019S	93	90	16	-2
LRRK2 G2019S FL	90	87	11	-1
LRRK2 I2020T	90	83	5	-3
LRRK2 R1441C	86	83	3	-2
LTK (TYK1)	44	19	-9	7
LYN A	18	5	-6	1
LYN B	23	6	0	6
MAP3K19 (YSK4)	17	4	-5	-3
MAP4K2 (GCK)	77	50	10	13
MAP4K4 (HGK)	80	64	11	9
MAP4K5 (KHS1)	68	39	4	15
MAPK1 (ERK2)	9	4	7	5
MAPK12 (p38 gamma)	11	8	4	4
MAPK13 (p38 delta)	11	13	9	8
MAPK3 (ERK1)	4	14	11	14
MAPK7 (ERK5)	1	9	-7	2
MAPKAPK2	3	3	-6	4
MAPKAPK3	24	8	3	10
MAPKAPK5 (PRAK)	18	8	7	7
MARK1 (MARK)	6	4	-5	3
MARK2	5	10	5	3
MARK3	7	0	-5	3
MARK4	15	9	-10	-3
MATK (HYL)	2	14	13	13
MELK	54	26	48	28
MERTK (cMER)	86	54	11	4
MET (cMet)	35	14	-8	5
MET (cMet) Y1235D	4	-2	-44	1
MET M1250T	42	19	-15	1
MINK1	73	60	9	20
MST1R (RON)	39	22	-16	-1
NEK1	58	23	6	-1
NEK2	0	-4	1	-3
NEK6	-4	4	-4	1
NEK9	9	4	5	6
NIM1K	13	7	2	7
NTRK2 (TRKB)	68	35	42	13
NTRK3 (TRKC)	66	42	11	10
NUAK1 (ARK5)	66	48	11	6
PAK1	22	10	2	16
PAK2 (PAK65)	7	14	4	14
PAK3	15	10	15	26
PAK4	20	13	15	11
PAK6	-10	5	3	11
PAK7 (KIAA1264)	11	2	13	15
PDGFRA (PDGFR alpha)	47	20	6	7
PDGFRA D842V	35	3	-2	-4
PEAK1	16	-1	0	2
PHKG1	12	8	-11	3

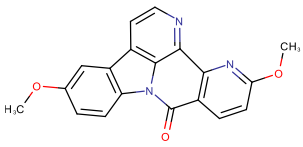
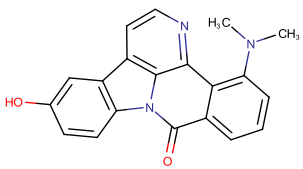
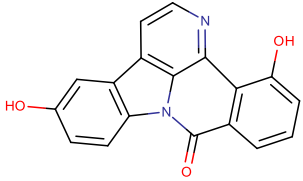
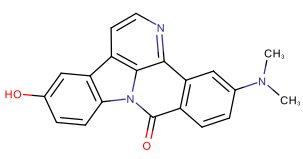
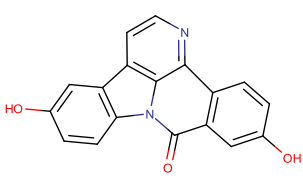
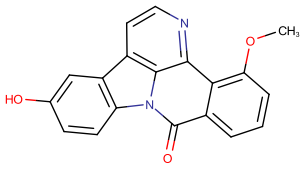
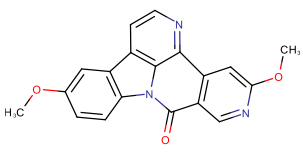
PHKG2	8	6	-3	6
PI4K2A (PI4K2 alpha)	25	7	-1	-7
PI4K2B (PI4K2 beta)	20	3	0	9
PI4KA (PI4K alpha)	23	13	-1	1
PI4KB (PI4K beta)	100	94	43	-2
PIK3C2A (PI3K-C2 alpha)	43	26	1	-5
PIK3C2B (PI3K-C2 beta)	68	53	12	2
PIK3C2G (PI3K-C2 gamma)	94	92	87	56
PIK3C3 (hVPS34)	49	23	4	4
PIK3CA E542K/PIK3R1	96	94	68	22
PIK3CA E545K/PIK3R1	97	91	61	15
PIK3CA/PIK3R1	86	81	52	14
PIK3CA/PIK3R3	96	92	63	16
PIK3CB/PIK3R1	67	30	67	21
PIK3CB/PIK3R2	66	24	64	15
PIK3CD/PIK3R1	89	79	77	40
PIK3CG	88	81	70	20
PIM1	24	11	-9	8
PIM2	13	6	-3	-1
PIM3	42	22	2	11
PIP4K2A	-3	-8	-9	-10
PIP5K1A	43	25	5	-6
PIP5K1B	21	4	7	-13
PIP5K1C	69	54	26	-1
PKN1 (PRK1)	16	9	4	15
PLK1	3	5	6	6
PLK2	-2	-1	-2	3
PLK3	23	6	12	5
PRKACA (PKA)	17	6	-15	12
PRKCA (PKC alpha)	18	11	-1	4
PRKCB1 (PKC beta I)	-17	1	-7	5
PRKCB2 (PKC beta II)	14	11	-5	9
PRKCD (PKC delta)	17	6	0	14
PRKCE (PKC epsilon)	8	9	-12	6
PRKCG (PKC gamma)	16	13	-3	11
PRKCH (PKC eta)	7	1	-9	-3
PRKCI (PKC iota)	-8	4	6	20
PRKCN (PKD3)	57	34	15	17
PRKCQ (PKC theta)	21	4	-15	2
PRKCZ (PKC zeta)	10	18	-4	16
PRKD1 (PKC mu)	49	28	9	5
PRKD2 (PKD2)	71	38	10	11
PRKG1	59	27	-11	5
PRKG2 (PKG2)	72	47	0	7
PRKX	16	22	-2	8
PTK2B (FAK2)	9	2	-7	-2
RET	34	15	12	9
RET A883F	24	10	3	7
RET S891A	30	-3	-18	-15
RET V804E	17	5	-7	1

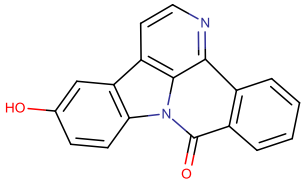
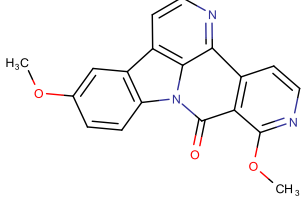
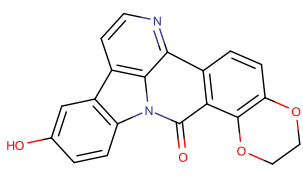
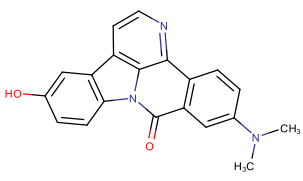
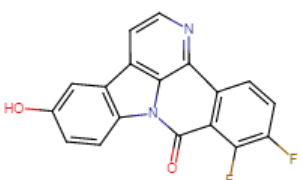
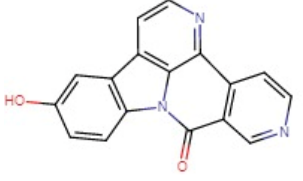
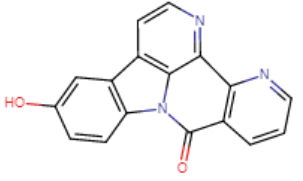
RET V804L	38	15	0	2
RET Y791F	32	17	7	5
ROCK1	13	0	-5	-4
ROCK2	18	14	4	14
RPS6KA1 (RSK1)	19	12	3	10
RPS6KA2 (RSK3)	11	6	6	5
RPS6KA3 (RSK2)	10	5	2	3
RPS6KA4 (MSK2)	24	12	4	-3
RPS6KA5 (MSK1)	25	5	-14	2
RPS6KA6 (RSK4)	17	5	4	2
RPS6KB1 (p70S6K)	15	19	7	12
RPS6KB2 (p70S6Kb)	1	7	15	3
SBK1	3	3	-26	-7
SGK (SGK1)	15	-4	-12	-2
SGK2	14	6	-11	-3
SGKL (SGK3)	10	12	6	8
SNF1LK2	12	5	-2	4
SPHK1	-3	-7	1	-2
SPHK2	-8	-16	-4	-7
SRC	16	0	3	6
SRC N1	25	15	14	16
SRPK1	15	12	10	8
SRPK2	0	-2	10	4
STK22B (TSSK2)	20	11	2	11
STK22D (TSSK1)	22	11	5	2
STK25 (YSK1)	-3	-9	-11	-3
STK4 (MST1)	11	4	3	4
SYK	37	16	7	5
TBK1	17	8	-8	11
TEK (Tie2)	5	19	12	-2
TEK (TIE2) Y897S	-10	-14	-11	-18
TXK	29	12	-13	4
TYRO3 (RSE)	29	11	2	7
YES1	16	17	20	15
ZAP70	16	12	11	15

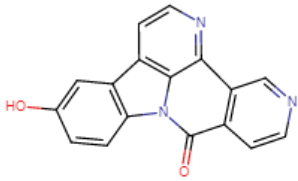
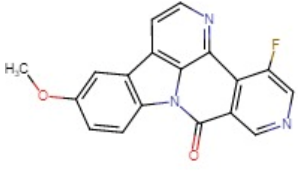
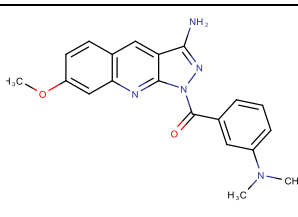
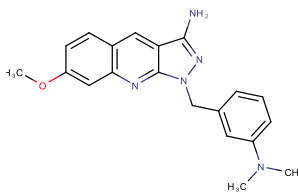
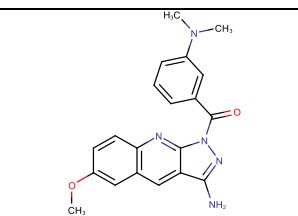
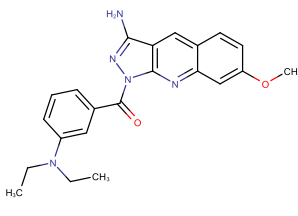
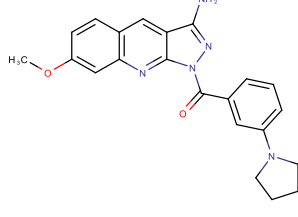
Table 9-2: MW01 and MW05 derivative library.

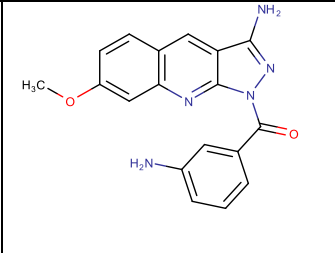
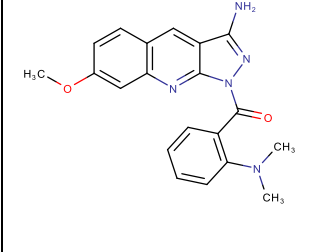
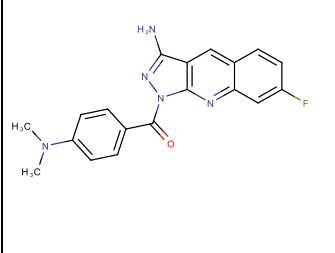
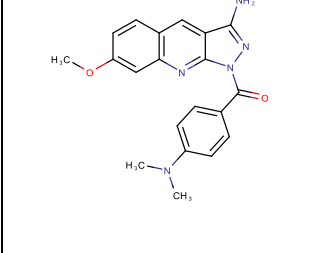
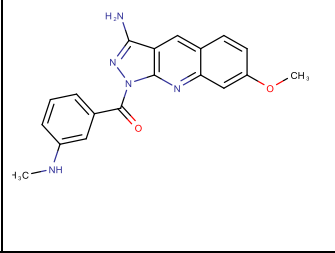
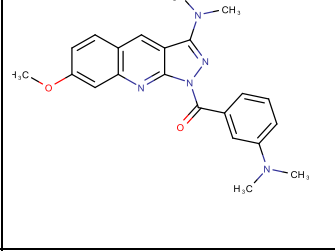
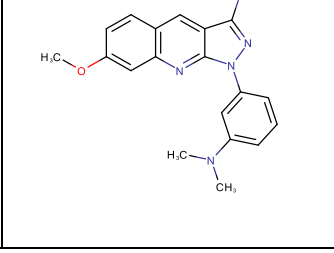
Structural derivative library of lead compounds MW01 and MW05 synthesized by Enamine Ltd.

Name	Structure	SMILE	Enamine ID	Purity %
MW01		<chem>COC1=C(OC)C2=C(C=C1)C1=C3N(C4=C(C=C(O)C=C4)C3=CC=N1)C2=O</chem>	Z3244953667	95
MW01-E1		<chem>COC1=CC2=C(C=C1)N1C3=C2C=CN=C3C2=C(N=CC=C2)C1=O</chem>	Z4613513986	98
MW01-E2		<chem>OC1=CC2=C(C=C1)N1C3=C2C=CN=C3C2=C(C=CC(O)=C2)C1=O</chem>	Z4623297010	98
MW01-E3		<chem>COC1=CC2=C(C=C1)N1C3=C2C=CN=C3C2=C(C=CC=N2)C1=O</chem>	Z4613515656	100
MW01-E4		<chem>OC1=CC2=C(C=C1)N1C3=C2C=CN=C3C2=C(C=CC(=C2)N2CCOCC2)C1=O</chem>	Z4613448788	100
MW01-E5		<chem>OC1=CC2=C(C=C1)N1C3=C2C=CN=C3C2=C(C(O)=CC=C2)C1=O</chem>	Z4623297025	97

MW01-E6		<chem>COC1=CC2=C(C=C1)N1C3=C2C=CN=C3C2=C(C=CC(OC)=N2)C1=O</chem>	Z4613838256	100
MW01-E7		<chem>CN(C)C1=C2C3=NC=CC4=C3N(C3=C4C=C(O)C=C3)C(=O)C2=CC=C1</chem>	Z4613449330	96
MW01-E8		<chem>OC1=CC2=C(C=C1)N1C3=C2C=CN=C3C2=C(C=CC=C2O)C1=O</chem>	Z4623297004	100
MW01-E9		<chem>CN(C)C1=CC2=C(C=C1)C(=O)N1C3=C2C=CN=C3C1=O</chem>	Z4613448981	97
MW01-E10		<chem>OC1=CC2=C(C=C1)N1C3=C2C=CN=C3C2=C(C=C(O)C=C2)C1=O</chem>	Z4623297012	98
MW01-E11		<chem>COC1=C2C3=NC=CC4=C3N(C3=C4C=C(O)C=C3)C(=O)C2=CC=C1</chem>	Z4623297038	100
MW01-E12		<chem>COC1=CC2=C(C=C1)N1C3=C2C=CN=C3C2=C(C=NC(OC)=C2)C1=O</chem>	Z4613897071	98

MW01-E13		<chem>OC1=CC2=C(C=C1)N1C3=C2C=CN=C3C2=C(C=CC=C2)C1=O</chem>	Z3243812160	100
MW01-E14		<chem>COC1=CC2=C(C=C1)N1C3=C2C=CN=C3C2=C(C1=O)C(OC)=NC=C2</chem>	Z4613898542	100
MW01-E15		<chem>OC1=CC2=C(C=C1)N1C3=C2C=CN=C3C2=C(C1=O)C1=C(OCCO1)C=C2</chem>	Z4615451237	100
MW01-E16		<chem>CN(C)C1=CC2=C(C=C1)C1=NC=CC3=C2N(C1=C3C=C(O)C=C1)C2=O</chem>	Z4613449794	97
MW01-E17		<chem>OC=1C=CC2=C(C1)C=3C=CN=C4C3=N2C(=O)C=5C(F)=C(F)C=CC45</chem>	EN300- 27707803	95
MW01-E18		<chem>OC=1C=CC2=C(C1)C=3C=CN=C4C3=N2C(=O)C=5C=NC=CC54</chem>	EN300- 27707927	95
MW01-E19		<chem>OC=1C=CC2=C(C1)C=3C=CN=C4C3=N2C(=O)C=5C=CC=NC54</chem>	EN300- 27716224	95

MW01-E20		<chem>OC=1C=CC2=C(C1)C=3C=CN=C4C3 N2C(=O)C=5C=CN=CC54</chem>	Z4905255295	100
MW01-E21		<chem>COC=1C=CC2=C(C1)C=3C=CN=C4C 3N2C(=O)C=5C=NC=C(F)C54</chem>	Z4905255587	100
MW05		<chem>COC1=CC2=C(C=C1)C=C1C(N)=NN(C(=O)C3=CC(=CC=C3)N(C)C)C1=N2</chem>	Z2027896743	91
MW05-E1		<chem>COC1=CC2=C(C=C1)C=C1C(N)=NN(CC3=CC(=CC=C3)N(C)C)C1=N2</chem>	Z4619432587	100
MW05-E2		<chem>COC1=CC2=C(C=C1)N=C1N(N=C(N) C1=C2)C(=O)C1=CC(=CC=C1)N(C)C</chem>	Z4619442527	100
MW05-E3		<chem>CCN(CC)C1=CC(=CC=C1)C(=O)N1N =C(N)C2=C1N=C1C=C(OC)C=CC1=C 2</chem>	Z4619437296	97
MW05-E4		<chem>COC1=CC2=C(C=C1)C=C1C(N)=NN(C(=O)C3=CC(=CC=C3)N3CCCC3)C1 =N2</chem>	Z4619437299	100

MW05-E5		<chem>COC1=CC2=C(C=C1)C=C1C(N)=NN(C(=O)C3=CC(N)=CC=C3)C1=N2</chem>	Z4619437298	97
MW05-E6		<chem>COC1=CC2=C(C=C1)C=C1C(N)=NN(C(=O)C3=C(C=CC=C3)N(C)C)C1=N2</chem>	Z4619437297	96
MW05-E7		<chem>CN(C)C1=CC=C(C=C1)C(=O)N1N=C(N)C2=C1N=C1C=C(F)C=CC1=C2</chem>	Z4619443254	95
MW05-E8		<chem>COC1=CC2=C(C=C1)C=C1C(N)=NN(C(=O)C3=CC=C(C=C3)N(C)C)C1=N2</chem>	Z4619437300	99
MW05-E9		<chem>CNC1=CC(=CC=C1)C(=O)N1N=C(N)C2=C1N=C1C=C(OC)C=CC1=C2</chem>	Z4619432589	100
MW05-E10		<chem>COC1=CC2=C(C=C1)C=C1C(=NN(C(=O)C3=CC(=CC=C3)N(C)C)C1=N2)N(C)C</chem>	Z4619432582	97
MW05-E11		<chem>COC1=CC2=C(C=C1)C=C1C(N)=NN(C1=N2)C1=CC(=CC=C1)N(C)C</chem>	Z4619432588	99

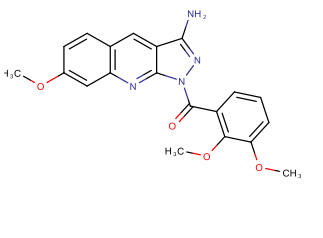
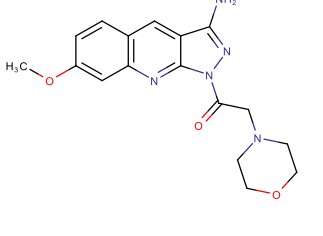
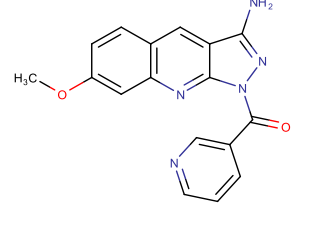
MW05-E13		<chem>COC1=CC2=C(C=C1)C=C1C(N)=NN(C(=O)C3=C(OC)C(OC)=CC=C3)C1=N2</chem>	Z4619442257	95
MW05-E14		<chem>COC1=CC2=C(C=C1)C=C1C(N)=NN(C(=O)CN3CCOCC3)C1=N2</chem>	Z3221672719	95
MW05-E15		<chem>COC1=CC2=C(C=C1)C=C1C(N)=NN(C(=O)C3=CN=CC=C3)C1=N2</chem>	Z3221672536	95

Table 9-3: Kinase panel of active and inactive derivatives of MW01 and MW05.

Percent inhibitions by two active and two inactive derivatives of MW01 and MW05 of selected kinases.

Lead compound	Percent Inhibition							
	MW01				MW05			
	active	active	inactive	inactive	active	active	inactive	inactive
Kinase	MW01-E18	MW01-E10	MW01-E14	MW01-E6	MW05-E9	MW05-E3	MW05-E10	MW05-E2
AKT1 (PKB alpha)	12	18	9	6	8	29	9	9
AKT2 (PKB beta)	3	18	14	4	5	20	7	8
AKT3 (PKB gamma)	19	24	23	12	14	33	12	11
ALK	35	75	15	19	20	19	9	24
BLK	23	42	9	23	5	30	17	10
BTK	30	69	29	30	7	37	12	7
CLK1	61	69	6	10	79	81	35	16
CLK2	70	70	20	18	87	86	28	74
CLK3	35	35	7	9	38	41	2	5
CLK4	98	99	67	58	84	99	92	75
CSF1R (FMS)	57	61	18	33	11	32	14	20
DNA-PK	94	62	43	9	64	67	8	16
DYRK1A	65	56	12	14	36	76	20	53
DYRK1B	68	81	23	20	46	58	14	84
EGFR (ErbB1)	14	15	9	11	5	12	6	33
FLT3	65	27	12	31	-4	22	9	17
FRAP1 (mTOR)	43	42	26	12	71	52	2	5
GSG2 (Haspin)	88	80	24	29	23	83	19	36
IKKB (IKK beta)	16	31	16	10	7	23	10	12
IRAK1	69	71	9	56	6	37	-19	2
IRAK4	2	-186	-15	-9	-11	-13	-6	-3
LRRK2	75	86	-4	64	-1	37	-6	8
MAP4K2 (GCK)	93	98	81	70	0	51	5	2
MINK1	85	92	12	57	19	16	13	29
PI4K2A (PI4K2 alpha)	30	13	35	22	-7	4	-3	-4
PI4K2B (PI4K2 beta)	24	22	21	11	-6	3	1	8
PI4KB (PI4K beta)	81	90	36	12	-14	24	1	9
PIK3C2A (PI3K-C2 alpha)	44	31	23	26	-6	17	6	10
PIK3C2G (PI3K-C2 gamma)	81	81	50	35	41	72	10	27

PIK3CA/PIK3R1	90	90	80	38	21	51	-9	26
PIK3CA/PIK3R3	94	90	59	10	16	47	-3	8
PIK3CB/PIK3R1	62	34	26	13	19	40	4	1
PIK3CB/PIK3R2	63	35	12	12	22	34	2	7
PIK3CD/PIK3R1	77	87	84	34	25	55	6	28
PIK3CG	99	93	49	-1	40	56	-7	2
PIP4K2A	-1	-2	53	-4	-6	2	-14	-6
PIP5K1A	28	5	11	20	-16	-2	-8	-9
PIP5K1B	-3	5	26	14		29	-8	-12
PIP5K1C	27	33	8	14	-5	39	-4	-2
PRKCN (PKD3)	52	74	-1	-8	14	31	5	7

10. Acknowledgments

Before I get to individual thanks, I would like express my gratitude for this life changing experience. During my PhD, I have grown so much as a scientist and a person, and I owe that to the many people who have shaped these last 6 years so far away from home.

First, I would like to thank my mentor Claus Scheidereit for his years of guidance on this interesting project. Despite the challenges we faced, you never gave up on me and the framework you developed enabled me to produce my own findings and realize myself as a scientist. The resulting final paper from our group is my proudest academic achievement and I owe that opportunity to you.

I would like to thank my university supervisor Oliver Daumke for being part of my committee and for your guidance, especially in navigating the thesis submission.

I would like to thank my SignGene co-mentor Ze'ev Ronai for his guidance during the early years of the project. I would also like to thank SignGene coordinators Sandra Krull and Hanna Singer.

I would like to thank Marc Nazaré and Peter Lindemann for their great contributions to our work and for their guidance on many critical aspects of the project. I still think medicinal chemistry is a dark and mysterious art, but you have de-mystified it ever so slightly for me.

I would like to thank Jens Peter von Kries and the FMP screening unit, especially for supporting my contract extension during the rebuttal period.

I would also like to thank Daniela Keyner, especially for your hard work in securing my final contract extension and for being there when I needed someone to talk to during those dark rebuttal days. You are absolutely an unsung hero of the MDC.

I would like to thank Bartolomeo Bosco for his help in the final years of the project. Your arrival in the lab helped change the trajectory of the project and together, we accomplished a lot. It was also very nice to have someone chat with about JRPGs, a first for AG Scheidereit.

I would like to thank all other former members of AG Scheidereit, especially Ahmet Tufan Bugra. Thank you for your years of friendship and I look forward to never texting you about NF- κ B antibodies again. I would also like to thank the famous "MW", Michael Willenbrock for his work on the identification of the compounds.

I would like to thank Michaela DiVirgilio and her group for supporting me in the final period of this work.

I would like to thank my love, best friend, and former lab mate Cristina Brischetto. As we began building our life outside the lab, we supported each other through our toughest times and that's something I will remember for the rest of my life. I couldn't have gotten to this page without you.

I would like to thank my parents, who have tirelessly supported me and provided me with the opportunities to become the scientist I am today. I could never have done this without you and this thesis is the result of a lifetime of your belief in me.

Finally, I would like to thank my friends for being there even when the author was occasionally a bit grumpy (not that often though, come on guys).

11. References

1. Sen, R., and Baltimore, D. (1986). Inducibility of kappa immunoglobulin enhancer-binding protein Nf-kappa B by a posttranslational mechanism. *Cell* 47, 921-928. 10.1016/0092-8674(86)90807-x.
2. Pahl, H.L. (1999). Activators and target genes of Rel/NF-kappaB transcription factors. *Oncogene* 18, 6853-6866. 10.1038/sj.onc.1203239.
3. Gilmore, T.D., and Wolenski, F.S. (2012). NF-kappaB: where did it come from and why? *Immunol Rev* 246, 14-35. 10.1111/j.1600-065X.2012.01096.x.
4. Hayden, M.S., and Ghosh, S. (2012). NF-kappaB, the first quarter-century: remarkable progress and outstanding questions. *Genes Dev* 26, 203-234. 10.1101/gad.183434.111.
5. Ghosh, G., Wang, V.Y., Huang, D.B., and Fusco, A. (2012). NF-kappaB regulation: lessons from structures. *Immunol Rev* 246, 36-58. 10.1111/j.1600-065X.2012.01097.x.
6. Schmitz, M.L., and Baeuerle, P.A. (1991). The p65 subunit is responsible for the strong transcription activating potential of NF-kappa B. *Embo j* 10, 3805-3817. 10.1002/j.1460-2075.1991.tb04950.x.
7. Palombella, V.J., Rando, O.J., Goldberg, A.L., and Maniatis, T. (1994). The ubiquitin-proteasome pathway is required for processing the NF-kappa B1 precursor protein and the activation of NF-kappa B. *Cell* 78, 773-785. 10.1016/s0092-8674(94)90482-0.
8. Senftleben, U., Cao, Y., Xiao, G., Greten, F.R., Krahn, G., Bonizzi, G., Chen, Y., Hu, Y., Fong, A., Sun, S.C., and Karin, M. (2001). Activation by IKKalpha of a second, evolutionary conserved, NF-kappa B signaling pathway. *Science* 293, 1495-1499. 10.1126/science.1062677.
9. Plaksin, D., Baeuerle, P.A., and Eisenbach, L. (1993). KBF1 (p50 NF-kappa B homodimer) acts as a repressor of H-2Kb gene expression in metastatic tumor cells. *J Exp Med* 177, 1651-1662. 10.1084/jem.177.6.1651.
10. Hayden, M.S., and Ghosh, S. (2008). Shared principles in NF-kappaB signaling. *Cell* 132, 344-362. 10.1016/j.cell.2008.01.020.
11. Christian, F., Smith, E.L., and Carmody, R.J. (2016). The Regulation of NF-kappaB Subunits by Phosphorylation. *Cells* 5. 10.3390/cells5010012.
12. Scheidereit, C. (2006). IkappaB kinase complexes: gateways to NF-kappaB activation and transcription. *Oncogene* 25, 6685-6705. 10.1038/sj.onc.1209934.
13. Rogers, S., Wells, R., and Rechsteiner, M. (1986). Amino acid sequences common to rapidly degraded proteins: the PEST hypothesis. *Science* 234, 364-368. 10.1126/science.2876518.

14. Hinz, M., Arslan, S.Ç., and Scheidereit, C. (2012). It takes two to tango: IκBs, the multifunctional partners of NF-κB. *Immunological Reviews* 246, 59-76. <https://doi.org/10.1111/j.1600-065X.2012.01102.x>.
15. Brockman, J.A., Scherer, D.C., McKinsey, T.A., Hall, S.M., Qi, X., Lee, W.Y., and Ballard, D.W. (1995). Coupling of a signal response domain in I kappa B alpha to multiple pathways for NF-kappa B activation. *Mol Cell Biol* 15, 2809-2818. 10.1128/MCB.15.5.2809.
16. Brown, K., Gerstberger, S., Carlson, L., Franzoso, G., and Siebenlist, U. (1995). Control of I kappa B-alpha proteolysis by site-specific, signal-induced phosphorylation. *Science* 267, 1485-1488. 10.1126/science.7878466.
17. Ghosh, S., and Baltimore, D. (1990). Activation in vitro of NF-kappa B by phosphorylation of its inhibitor I kappa B. *Nature* 344, 678-682. 10.1038/344678a0.
18. Naumann, M., and Scheidereit, C. (1994). Activation of NF-kappa B in vivo is regulated by multiple phosphorylations. *EMBO J* 13, 4597-4607. 10.1002/j.1460-2075.1994.tb06781.x.
19. Brown, K., Park, S., Kanno, T., Franzoso, G., and Siebenlist, U. (1993). Mutual regulation of the transcriptional activator NF-kappa B and its inhibitor, I kappa B-alpha. *Proc Natl Acad Sci U S A* 90, 2532-2536. 10.1073/pnas.90.6.2532.
20. Finco, T.S., Beg, A.A., and Baldwin, A.S., Jr. (1994). Inducible phosphorylation of I kappa B alpha is not sufficient for its dissociation from NF-kappa B and is inhibited by protease inhibitors. *Proc Natl Acad Sci U S A* 91, 11884-11888. 10.1073/pnas.91.25.11884.
21. Mellits, K.H., Hay, R.T., and Goodbourn, S. (1993). Proteolytic degradation of MAD3 (I kappa B alpha) and enhanced processing of the NF-kappa B precursor p105 are obligatory steps in the activation of NF-kappa B. *Nucleic Acids Res* 21, 5059-5066. 10.1093/nar/21.22.5059.
22. Miyamoto, S., Maki, M., Schmitt, M.J., Hatanaka, M., and Verma, I.M. (1994). Tumor necrosis factor alpha-induced phosphorylation of I kappa B alpha is a signal for its degradation but not dissociation from NF-kappa B. *Proc Natl Acad Sci U S A* 91, 12740-12744. 10.1073/pnas.91.26.12740.
23. Alkalay, I., Yaron, A., Hatzubai, A., Jung, S., Avraham, A., Gerlitz, O., Pashut-Lavon, I., and Ben-Neriah, Y. (1995). In vivo stimulation of I kappa B phosphorylation is not sufficient to activate NF-kappa B. *Mol Cell Biol* 15, 1294-1301. 10.1128/MCB.15.3.1294.
24. Chen, Z., Hagler, J., Palombella, V.J., Melandri, F., Scherer, D., Ballard, D., and Maniatis, T. (1995). Signal-induced site-specific phosphorylation targets I kappa B alpha to the ubiquitin-proteasome pathway. *Genes Dev* 9, 1586-1597. 10.1101/gad.9.13.1586.
25. Spencer, E., Jiang, J., and Chen, Z.J. (1999). Signal-induced ubiquitination of I kappa B alpha by the F-box protein Slimb/beta-TrCP. *Genes Dev* 13, 284-294. 10.1101/gad.13.3.284.

26. Yaron, A., Hatzubai, A., Davis, M., Lavon, I., Amit, S., Manning, A.M., Andersen, J.S., Mann, M., Mercurio, F., and Ben-Neriah, Y. (1998). Identification of the receptor component of the I κ B α -ubiquitin ligase. *Nature* 396, 590-594. 10.1038/25159.
27. Le Bail, O., Schmidt-Ullrich, R., and Israel, A. (1993). Promoter analysis of the gene encoding the I κ B α /MAD3 inhibitor of NF- κ B: positive regulation by members of the rel/NF- κ B family. *EMBO J* 12, 5043-5049. 10.1002/j.1460-2075.1993.tb06197.x.
28. Sun, S.C., Ganchi, P.A., Ballard, D.W., and Greene, W.C. (1993). NF- κ B controls expression of inhibitor I κ B α : evidence for an inducible autoregulatory pathway. *Science* 259, 1912-1915. 10.1126/science.8096091.
29. Huxford, T., Huang, D.B., Malek, S., and Ghosh, G. (1998). The crystal structure of the I κ B α /NF- κ B complex reveals mechanisms of NF- κ B inactivation. *Cell* 95, 759-770. 10.1016/s0092-8674(00)81699-2.
30. Potoyan, D.A., Zheng, W., Komives, E.A., and Wolynes, P.G. (2016). Molecular stripping in the NF- κ B/I κ B/DNA genetic regulatory network. *Proc Natl Acad Sci U S A* 113, 110-115. 10.1073/pnas.1520483112.
31. Hinz, M., and Scheidereit, C. (2014). The I κ B kinase complex in NF- κ B regulation and beyond. *EMBO Rep* 15, 46-61. 10.1002/embr.201337983.
32. Mercurio, F., Zhu, H., Murray, B.W., Shevchenko, A., Bennett, B.L., Li, J., Young, D.B., Barbosa, M., Mann, M., Manning, A., and Rao, A. (1997). IKK-1 and IKK-2: cytokine-activated I κ B kinases essential for NF- κ B activation. *Science* 278, 860-866. 10.1126/science.278.5339.860.
33. Regnier, C.H., Song, H.Y., Gao, X., Goeddel, D.V., Cao, Z., and Rothe, M. (1997). Identification and characterization of an I κ B kinase. *Cell* 90, 373-383. 10.1016/s0092-8674(00)80344-x.
34. Zandi, E., Chen, Y., and Karin, M. (1998). Direct phosphorylation of I κ B by IKK α and IKK β : discrimination between free and NF- κ B-bound substrate. *Science* 281, 1360-1363. 10.1126/science.281.5381.1360.
35. Clark, K., Nanda, S., and Cohen, P. (2013). Molecular control of the NEMO family of ubiquitin-binding proteins. *Nat Rev Mol Cell Biol* 14, 673-685. 10.1038/nrm3644.
36. Hadian, K., Griesbach, R.A., Dornauer, S., Wanger, T.M., Nagel, D., Metlitzky, M., Beisker, W., Schmidt-Supprian, M., and Krappmann, D. (2011). NF- κ B essential modulator (NEMO) interaction with linear and lys-63 ubiquitin chains contributes to NF- κ B activation. *J Biol Chem* 286, 26107-26117. 10.1074/jbc.M111.233163.
37. Laplantine, E., Fontan, E., Chiaravalli, J., Lopez, T., Lakisic, G., Veron, M., Agou, F., and Israel, A. (2009). NEMO specifically recognizes K63-linked poly-ubiquitin chains through a new bipartite ubiquitin-binding domain. *EMBO J* 28, 2885-2895. 10.1038/emboj.2009.241.

38. Sasaki, Y., Sano, S., Nakahara, M., Murata, S., Kometani, K., Aiba, Y., Sakamoto, S., Watanabe, Y., Tanaka, K., Kurosaki, T., and Iwai, K. (2013). Defective immune responses in mice lacking LUBAC-mediated linear ubiquitination in B cells. *EMBO J* *32*, 2463-2476. 10.1038/emboj.2013.184.
39. Iwai, K., and Tokunaga, F. (2009). Linear polyubiquitination: a new regulator of NF-kappaB activation. *EMBO Rep* *10*, 706-713. 10.1038/embor.2009.144.
40. Wu, Z.H., Shi, Y., Tibbetts, R.S., and Miyamoto, S. (2006). Molecular linkage between the kinase ATM and NF-kappaB signaling in response to genotoxic stimuli. *Science* *311*, 1141-1146. 10.1126/science.1121513.
41. Emmerich, C.H., Ordureau, A., Strickson, S., Arthur, J.S., Pedrioli, P.G., Komander, D., and Cohen, P. (2013). Activation of the canonical IKK complex by K63/M1-linked hybrid ubiquitin chains. *Proc Natl Acad Sci U S A* *110*, 15247-15252. 10.1073/pnas.1314715110.
42. Zhang, J., Clark, K., Lawrence, T., Peggie, M.W., and Cohen, P. (2014). An unexpected twist to the activation of IKKbeta: TAK1 primes IKKbeta for activation by autophosphorylation. *Biochem J* *461*, 531-537. 10.1042/BJ20140444.
43. Huang, T.T., Wuerzberger-Davis, S.M., Wu, Z.H., and Miyamoto, S. (2003). Sequential modification of NEMO/IKKgamma by SUMO-1 and ubiquitin mediates NF-kappaB activation by genotoxic stress. *Cell* *115*, 565-576. 10.1016/s0092-8674(03)00895-x.
44. Hinz, M., Stilmann, M., Arslan, S., Khanna, K.K., Dittmar, G., and Scheidereit, C. (2010). A cytoplasmic ATM-TRAF6-cIAP1 module links nuclear DNA damage signaling to ubiquitin-mediated NF-kappaB activation. *Mol Cell* *40*, 63-74. 10.1016/j.molcel.2010.09.008.
45. Adhikari, A., Xu, M., and Chen, Z.J. (2007). Ubiquitin-mediated activation of TAK1 and IKK. *Oncogene* *26*, 3214-3226. 10.1038/sj.onc.1210413.
46. Kulathu, Y., Akutsu, M., Bremm, A., Hofmann, K., and Komander, D. (2009). Two-sided ubiquitin binding explains specificity of the TAB2 NZF domain. *Nat Struct Mol Biol* *16*, 1328-1330. 10.1038/nsmb.1731.
47. Wang, C., Deng, L., Hong, M., Akkaraju, G.R., Inoue, J., and Chen, Z.J. (2001). TAK1 is a ubiquitin-dependent kinase of MKK and IKK. *Nature* *412*, 346-351. 10.1038/35085597.
48. Xia, Z.P., Sun, L., Chen, X., Pineda, G., Jiang, X., Adhikari, A., Zeng, W., and Chen, Z.J. (2009). Direct activation of protein kinases by unanchored polyubiquitin chains. *Nature* *461*, 114-119. 10.1038/nature08247.
49. Polley, S., Huang, D.B., Hauenstein, A.V., Fusco, A.J., Zhong, X., Vu, D., Schröfelbauer, B., Kim, Y., Hoffmann, A., Verma, I.M., et al. (2013). A structural basis for Ikb kinase 2 activation via oligomerization-dependent trans autophosphorylation. *PLoS Biol* *11*, e1001581. 10.1371/journal.pbio.1001581.

50. Sakurai, H., Chiba, H., Miyoshi, H., Sugita, T., and Toriumi, W. (1999). I κ B kinases phosphorylate NF- κ B p65 subunit on serine 536 in the transactivation domain. *J Biol Chem* 274, 30353-30356. 10.1074/jbc.274.43.30353.
51. Liu, F., Xia, Y., Parker, A.S., and Verma, I.M. (2012). IKK biology. *Immunol Rev* 246, 239-253. 10.1111/j.1600-065X.2012.01107.x.
52. Oeckinghaus, A., Hayden, M.S., and Ghosh, S. (2011). Crosstalk in NF- κ B signaling pathways. *Nat Immunol* 12, 695-708. 10.1038/ni.2065.
53. Iwasaki, H., Takeuchi, O., Teraguchi, S., Matsushita, K., Uehata, T., Kuniyoshi, K., Satoh, T., Saitoh, T., Matsushita, M., Standley, D.M., and Akira, S. (2011). The I κ B kinase complex regulates the stability of cytokine-encoding mRNA induced by TLR-IL-1R by controlling degradation of regnase-1. *Nat Immunol* 12, 1167-1175. 10.1038/ni.2137.
54. Mikuda, N., Kolesnichenko, M., Beaudette, P., Popp, O., Uyar, B., Sun, W., Tufan, A.B., Perder, B., Akalin, A., Chen, W., et al. (2018). The I κ B kinase complex is a regulator of mRNA stability. *The EMBO Journal* 37, e98658. <https://doi.org/10.15252/emboj.201798658>.
55. Lee, E.G., Boone, D.L., Chai, S., Libby, S.L., Chien, M., Lodolce, J.P., and Ma, A. (2000). Failure to regulate TNF-induced NF- κ B and cell death responses in A20-deficient mice. *Science* 289, 2350-2354. 10.1126/science.289.5488.2350.
56. Wertz, I.E., O'Rourke, K.M., Zhou, H., Eby, M., Aravind, L., Seshagiri, S., Wu, P., Wiesmann, C., Baker, R., Boone, D.L., et al. (2004). De-ubiquitination and ubiquitin ligase domains of A20 downregulate NF- κ B signalling. *Nature* 430, 694-699. 10.1038/nature02794.
57. Fiil, B.K., Damgaard, R.B., Wagner, S.A., Keusekotten, K., Fritsch, M., Bekker-Jensen, S., Mailand, N., Choudhary, C., Komander, D., and Gyrd-Hansen, M. (2013). OTULIN restricts Met1-linked ubiquitination to control innate immune signaling. *Mol Cell* 50, 818-830. 10.1016/j.molcel.2013.06.004.
58. Keusekotten, K., Elliott, P.R., Glockner, L., Fiil, B.K., Damgaard, R.B., Kulathu, Y., Wauer, T., Hospenthal, M.K., Gyrd-Hansen, M., Krappmann, D., et al. (2013). OTULIN antagonizes LUBAC signaling by specifically hydrolyzing Met1-linked polyubiquitin. *Cell* 153, 1312-1326. 10.1016/j.cell.2013.05.014.
59. Komander, D. (2009). The emerging complexity of protein ubiquitination. *Biochem Soc Trans* 37, 937-953. 10.1042/BST0370937.
60. Ruland, J. (2011). Return to homeostasis: downregulation of NF- κ B responses. *Nat Immunol* 12, 709-714. 10.1038/ni.2055.
61. Shiloh, Y., and Ziv, Y. (2013). The ATM protein kinase: regulating the cellular response to genotoxic stress, and more. *Nat Rev Mol Cell Biol* 14, 197-210.
62. Stilmann, M., Hinz, M., Arslan, S.C., Zimmer, A., Schreiber, V., and Scheidereit, C. (2009). A nuclear poly(ADP-ribose)-dependent signalosome confers DNA damage-

- induced IkappaB kinase activation. *Mol Cell* 36, 365-378.
10.1016/j.molcel.2009.09.032.
63. Lukas, J., Lukas, C., and Bartek, J. (2011). More than just a focus: The chromatin response to DNA damage and its role in genome integrity maintenance. *Nat Cell Biol* 13, 1161-1169. 10.1038/ncb2344.
 64. Wu, Z., Wang, C., Bai, M., Li, X., Mei, Q., Li, X., Wang, Y., Fu, X., Luo, G., and Han, W. (2015). An LRP16-containing preassembly complex contributes to NF-kappaB activation induced by DNA double-strand breaks. *Nucleic Acids Res* 43, 3167-3179. 10.1093/nar/gkv161.
 65. Hwang, B., McCool, K., Wan, J., Wuerzberger-Davis, S.M., Young, E.W.K., Choi, E.Y., Cingolani, G., Weaver, B.A., and Miyamoto, S. (2015). IPO3-mediated Nonclassical Nuclear Import of NF-kappaB Essential Modulator (NEMO) Drives DNA Damage-dependent NF-kappaB Activation. *J Biol Chem* 290, 17967-17984. 10.1074/jbc.M115.645960.
 66. Niu, J., Shi, Y., Iwai, K., and Wu, Z.H. (2011). LUBAC regulates NF-kappaB activation upon genotoxic stress by promoting linear ubiquitination of NEMO. *EMBO J* 30, 3741-3753. 10.1038/emboj.2011.264.
 67. Ducut Sigala, J.L., Bottero, V., Young, D.B., Shevchenko, A., Mercurio, F., and Verma, I.M. (2004). Activation of transcription factor NF-kappaB requires ELKS, an IkappaB kinase regulatory subunit. *Science* 304, 1963-1967. 10.1126/science.1098387.
 68. Jin, H.S., Lee, D.H., Kim, D.H., Chung, J.H., Lee, S.J., and Lee, T.H. (2009). cIAP1, cIAP2, and XIAP act cooperatively via nonredundant pathways to regulate genotoxic stress-induced nuclear factor-kappaB activation. *Cancer Res* 69, 1782-1791. 10.1158/0008-5472.CAN-08-2256.
 69. Wang, W., Huang, X., Xin, H.B., Fu, M., Xue, A., and Wu, Z.H. (2015). TRAF Family Member-associated NF-kappaB Activator (TANK) Inhibits Genotoxic Nuclear Factor kappaB Activation by Facilitating Deubiquitinase USP10-dependent Deubiquitination of TRAF6 Ligase. *J Biol Chem* 290, 13372-13385. 10.1074/jbc.M115.643767.
 70. Yang, Y., Xia, F., Hermance, N., Mabb, A., Simonson, S., Morrissey, S., Gandhi, P., Munson, M., Miyamoto, S., and Kelliher, M.A. (2011). A cytosolic ATM/NEMO/RIP1 complex recruits TAK1 to mediate the NF-kappaB and p38 mitogen-activated protein kinase (MAPK)/MAPK-activated protein 2 responses to DNA damage. *Mol Cell Biol* 31, 2774-2786. 10.1128/MCB.01139-10.
 71. Murakawa, Y., Hinz, M., Mothes, J., Schuetz, A., Uhl, M., Wyler, E., Yasuda, T., Mastrobuoni, G., Friedel, C.C., Dolken, L., et al. (2015). RC3H1 post-transcriptionally regulates A20 mRNA and modulates the activity of the IKK/NF-kappaB pathway. *Nat Commun* 6, 7367. 10.1038/ncomms8367.
 72. Jing, H., Kase, J., Dorr, J.R., Milanovic, M., Lenze, D., Grau, M., Beuster, G., Ji, S., Reimann, M., Lenz, P., et al. (2011). Opposing roles of NF-kappaB in anti-cancer

- treatment outcome unveiled by cross-species investigations. *Genes Dev* 25, 2137-2146. 10.1101/gad.17620611.
73. Shao, L., Zhou, H.J., Zhang, H., Qin, L., Hwa, J., Yun, Z., Ji, W., and Min, W. (2015). SENP1-mediated NEMO deSUMOylation in adipocytes limits inflammatory responses and type-1 diabetes progression. *Nat Commun* 6, 8917. 10.1038/ncomms9917.
 74. Niu, J., Shi, Y., Xue, J., Miao, R., Huang, S., Wang, T., Wu, J., Fu, M., and Wu, Z.H. (2013). USP10 inhibits genotoxic NF-kappaB activation by MCP1P1-facilitated deubiquitination of NEMO. *EMBO J* 32, 3206-3219. 10.1038/emboj.2013.247.
 75. Chien, Y., Scuoppo, C., Wang, X., Fang, X., Balgley, B., Bolden, J.E., Premssirut, P., Luo, W., Chicas, A., Lee, C.S., et al. (2011). Control of the senescence-associated secretory phenotype by NF-kappaB promotes senescence and enhances chemosensitivity. *Genes Dev* 25, 2125-2136. 10.1101/gad.17276711.
 76. Ohanna, M., Giuliano, S., Bonet, C., Imbert, V., Hofman, V., Zangari, J., Bille, K., Robert, C., Bressac-de Paillerets, B., Hofman, P., et al. (2011). Senescent cells develop a PARP-1 and nuclear factor-kappaB-associated secretome (PNAS). *Genes Dev* 25, 1245-1261. 10.1101/gad.625811.
 77. Rayet, B., and Gelinas, C. (1999). Aberrant rel/nfkb genes and activity in human cancer. *Oncogene* 18, 6938-6947. 10.1038/sj.onc.1203221.
 78. Feinman, R., Koury, J., Thames, M., Barlogie, B., Epstein, J., and Siegel, D.S. (1999). Role of NF-kappaB in the rescue of multiple myeloma cells from glucocorticoid-induced apoptosis by bcl-2. *Blood* 93, 3044-3052.
 79. Grosjean-Raillard, J., Tailler, M., Ades, L., Perfettini, J.L., Fabre, C., Braun, T., De Botton, S., Fenaux, P., and Kroemer, G. (2009). ATM mediates constitutive NF-kappaB activation in high-risk myelodysplastic syndrome and acute myeloid leukemia. *Oncogene* 28, 1099-1109. 10.1038/onc.2008.457.
 80. Giri, D.K., and Aggarwal, B.B. (1998). Constitutive activation of NF-kappaB causes resistance to apoptosis in human cutaneous T cell lymphoma HuT-78 cells. Autocrine role of tumor necrosis factor and reactive oxygen intermediates. *J Biol Chem* 273, 14008-14014. 10.1074/jbc.273.22.14008.
 81. Bargou, R.C., Leng, C., Krappmann, D., Emmerich, F., Mapara, M.Y., Bommert, K., Royer, H.D., Scheidereit, C., and Dorken, B. (1996). High-level nuclear NF-kappa B and Oct-2 is a common feature of cultured Hodgkin/Reed-Sternberg cells. *Blood* 87, 4340-4347.
 82. Krappmann, D., Emmerich, F., Kordes, U., Scharschmidt, E., Dorken, B., and Scheidereit, C. (1999). Molecular mechanisms of constitutive NF-kappaB/Rel activation in Hodgkin/Reed-Sternberg cells. *Oncogene* 18, 943-953. 10.1038/sj.onc.1202351.
 83. Batra, R.K., Guttridge, D.C., Brenner, D.A., Dubinett, S.M., Baldwin, A.S., and Boucher, R.C. (1999). IkappaBalpha gene transfer is cytotoxic to squamous-cell lung

- cancer cells and sensitizes them to tumor necrosis factor-alpha-mediated cell death. *Am J Respir Cell Mol Biol* 21, 238-245. 10.1165/ajrcmb.21.2.3470.
84. Nakshatri, H., Bhat-Nakshatri, P., Martin, D.A., Goulet, R.J., Jr., and Sledge, G.W., Jr. (1997). Constitutive activation of NF-kappaB during progression of breast cancer to hormone-independent growth. *Mol Cell Biol* 17, 3629-3639. 10.1128/MCB.17.7.3629.
 85. Shattuck-Brandt, R.L., and Richmond, A. (1997). Enhanced degradation of I-kappaB alpha contributes to endogenous activation of NF-kappaB in Hs294T melanoma cells. *Cancer Res* 57, 3032-3039.
 86. Sumitomo, M., Tachibana, M., Ozu, C., Asakura, H., Murai, M., Hayakawa, M., Nakamura, H., Takayanagi, A., and Shimizu, N. (1999). Induction of apoptosis of cytokine-producing bladder cancer cells by adenovirus-mediated IkappaBalpha overexpression. *Hum Gene Ther* 10, 37-47. 10.1089/10430349950019174.
 87. Wang, W., Abbruzzese, J.L., Evans, D.B., Larry, L., Cleary, K.R., and Chiao, P.J. (1999). The nuclear factor-kappa B RelA transcription factor is constitutively activated in human pancreatic adenocarcinoma cells. *Clin Cancer Res* 5, 119-127.
 88. Weichert, W., Boehm, M., Gekeler, V., Bahra, M., Langrehr, J., Neuhaus, P., Denkert, C., Imre, G., Weller, C., Hofmann, H.P., et al. (2007). High expression of RelA/p65 is associated with activation of nuclear factor- κ B-dependent signaling in pancreatic cancer and marks a patient population with poor prognosis. *British Journal of Cancer* 97, 523-530. 10.1038/sj.bjc.6603878.
 89. Hanahan, D., and Weinberg, R.A. (2011). Hallmarks of cancer: the next generation. *Cell* 144, 646-674. 10.1016/j.cell.2011.02.013.
 90. Baud, V., and Karin, M. (2009). Is NF-kappaB a good target for cancer therapy? Hopes and pitfalls. *Nat Rev Drug Discov* 8, 33-40. 10.1038/nrd2781.
 91. Liu, Z.G., Hsu, H., Goeddel, D.V., and Karin, M. (1996). Dissection of TNF receptor 1 effector functions: JNK activation is not linked to apoptosis while NF-kappaB activation prevents cell death. *Cell* 87, 565-576. 10.1016/s0092-8674(00)81375-6.
 92. Van Antwerp, D.J., Martin, S.J., Kafri, T., Green, D.R., and Verma, I.M. (1996). Suppression of TNF-alpha-induced apoptosis by NF-kappaB. *Science* 274, 787-789. 10.1126/science.274.5288.787.
 93. Wang, C.Y., Mayo, M.W., and Baldwin, A.S., Jr. (1996). TNF- and cancer therapy-induced apoptosis: potentiation by inhibition of NF-kappaB. *Science* 274, 784-787. 10.1126/science.274.5288.784.
 94. Lim, K.H., Yang, Y., and Staudt, L.M. (2012). Pathogenetic importance and therapeutic implications of NF-kappaB in lymphoid malignancies. *Immunol Rev* 246, 359-378. 10.1111/j.1600-065X.2012.01105.x.
 95. Luo, J.L., Kamata, H., and Karin, M. (2005). IKK/NF-kappaB signaling: balancing life and death--a new approach to cancer therapy. *J Clin Invest* 115, 2625-2632. 10.1172/JCI26322.

96. Wang, C.Y., Mayo, M.W., Korneluk, R.G., Goeddel, D.V., and Baldwin, A.S., Jr. (1998). NF-kappaB antiapoptosis: induction of TRAF1 and TRAF2 and c-IAP1 and c-IAP2 to suppress caspase-8 activation. *Science* 281, 1680-1683. 10.1126/science.281.5383.1680.
97. Jeremias, I., Kupatt, C., Baumann, B., Herr, I., Wirth, T., and Debatin, K.M. (1998). Inhibition of nuclear factor kappaB activation attenuates apoptosis resistance in lymphoid cells. *Blood* 91, 4624-4631.
98. Zhou, J., Ching, Y.Q., and Chng, W.J. (2015). Aberrant nuclear factor-kappa B activity in acute myeloid leukemia: from molecular pathogenesis to therapeutic target. *Oncotarget* 6, 5490-5500. 10.18632/oncotarget.3545.
99. Hideshima, T., Neri, P., Tassone, P., Yasui, H., Ishitsuka, K., Raje, N., Chauhan, D., Podar, K., Mitsiades, C., Dang, L., et al. (2006). MLN120B, a novel IkappaB kinase beta inhibitor, blocks multiple myeloma cell growth in vitro and in vivo. *Clin Cancer Res* 12, 5887-5894. 10.1158/1078-0432.CCR-05-2501.
100. Jourdan, M., Moreaux, J., Vos, J.D., Hose, D., Mahtouk, K., Abouladze, M., Robert, N., Baudard, M., Reme, T., Romanelli, A., et al. (2007). Targeting NF-kappaB pathway with an IKK2 inhibitor induces inhibition of multiple myeloma cell growth. *Br J Haematol* 138, 160-168. 10.1111/j.1365-2141.2007.06629.x.
101. DiDonato, J.A., Mercurio, F., and Karin, M. (2012). NF-kappaB and the link between inflammation and cancer. *Immunol Rev* 246, 379-400. 10.1111/j.1600-065X.2012.01099.x.
102. Verstrepen, L., and Beyaert, R. (2014). Receptor proximal kinases in NF-kappaB signaling as potential therapeutic targets in cancer and inflammation. *Biochem Pharmacol* 92, 519-529. 10.1016/j.bcp.2014.10.017.
103. Nogueira, L., Ruiz-Ontanon, P., Vazquez-Barquero, A., Moris, F., and Fernandez-Luna, J.L. (2011). The NFkappaB pathway: a therapeutic target in glioblastoma. *Oncotarget* 2, 646-653. 10.18632/oncotarget.322.
104. Sanofi (2013). 2013 Marks the End of the Patent Cliff Period.
105. Min, S.Y., Yan, M., Du, Y., Wu, T., Khobahy, E., Kwon, S.R., Taneja, V., Bashmakov, A., Nukala, S., Ye, Y., et al. (2013). Intra-articular nuclear factor-kappaB blockade ameliorates collagen-induced arthritis in mice by eliciting regulatory T cells and macrophages. *Clin Exp Immunol* 172, 217-227. 10.1111/cei.12054.
106. Tornatore, L., Sandomenico, A., Raimondo, D., Low, C., Rocci, A., Tralau-Stewart, C., Capece, D., D'Andrea, D., Bua, M., Boyle, E., et al. (2014). Cancer-Selective Targeting of the NF-kappaB Survival Pathway with GADD45beta/MKK7 Inhibitors. *Cancer Cell* 26, 938. 10.1016/j.ccell.2014.11.021.
107. Byrd, J.C., Furman, R.R., Coutre, S.E., Flinn, I.W., Burger, J.A., Blum, K.A., Grant, B., Sharman, J.P., Coleman, M., Wierda, W.G., et al. (2013). Targeting BTK with ibrutinib in relapsed chronic lymphocytic leukemia. *N Engl J Med* 369, 32-42. 10.1056/NEJMoa1215637.

108. de Claro, R.A., McGinn, K.M., Verdun, N., Lee, S.L., Chiu, H.J., Saber, H., Brower, M.E., Chang, C.J., Pfuma, E., Habtemariam, B., et al. (2015). FDA Approval: Ibrutinib for Patients with Previously Treated Mantle Cell Lymphoma and Previously Treated Chronic Lymphocytic Leukemia. *Clin Cancer Res* 21, 3586-3590. 10.1158/1078-0432.Ccr-14-2225.
109. Herrera, A.F., and Jacobsen, E.D. (2014). Ibrutinib for the treatment of mantle cell lymphoma. *Clin Cancer Res* 20, 5365-5371. 10.1158/1078-0432.CCR-14-0010.
110. Wang, M.L., Rule, S., Martin, P., Goy, A., Auer, R., Kahl, B.S., Jurczak, W., Advani, R.H., Romaguera, J.E., Williams, M.E., et al. (2013). Targeting BTK with ibrutinib in relapsed or refractory mantle-cell lymphoma. *N Engl J Med* 369, 507-516. 10.1056/NEJMoa1306220.
111. Wilson, W.H., Young, R.M., Schmitz, R., Yang, Y., Pittaluga, S., Wright, G., Lih, C.J., Williams, P.M., Shaffer, A.L., Gerecitano, J., et al. (2015). Targeting B cell receptor signaling with ibrutinib in diffuse large B cell lymphoma. *Nat Med* 21, 922-926. 10.1038/nm.3884.
112. Mucka, P., Lindemann, P., Bosco, B., Willenbrock, M., Radetzki, S., Neuenschwander, M., Brischetto, C., Peter von Kries, J., Nazaré, M., and Scheidereit, C. (2023). CLK2 and CLK4 are regulators of DNA damage-induced NF- κ B targeted by novel small molecule inhibitors. *Cell Chemical Biology*. <https://doi.org/10.1016/j.chembiol.2023.06.027>.
113. Jackson, S.P., and Bartek, J. (2009). The DNA-damage response in human biology and disease. *Nature* 461, 1071-1078. 10.1038/nature08467.
114. Groelly, F.J., Fawkes, M., Dagg, R.A., Blackford, A.N., and Tarsounas, M. (2023). Targeting DNA damage response pathways in cancer. *Nature Reviews Cancer* 23, 78-94. 10.1038/s41568-022-00535-5.
115. Gourley, C., Balmaña, J., Ledermann, J.A., Serra, V., Dent, R., Loibl, S., Pujade-Lauraine, E., and Boulton, S.J. (2019). Moving From Poly (ADP-Ribose) Polymerase Inhibition to Targeting DNA Repair and DNA Damage Response in Cancer Therapy. *Journal of Clinical Oncology* 37, 2257-2269. 10.1200/jco.18.02050.
116. Kim, G., Ison, G., McKee, A.E., Zhang, H., Tang, S., Gwise, T., Sridhara, R., Lee, E., Tzou, A., Philip, R., et al. (2015). FDA Approval Summary: Olaparib Monotherapy in Patients with Deleterious Germline BRCA-Mutated Advanced Ovarian Cancer Treated with Three or More Lines of Chemotherapy. *Clinical Cancer Research* 21, 4257-4261. 10.1158/1078-0432.Ccr-15-0887.
117. Mullard, A. (2014). European regulators approve first PARP inhibitor. *Nat Rev Drug Discov* 13, 877-877. 10.1038/nrd4508.
118. Lord, C.J., and Ashworth, A. (2017). PARP inhibitors: Synthetic lethality in the clinic. *Science* 355, 1152-1158. 10.1126/science.aam7344.
119. Bryant, H.E., Schultz, N., Thomas, H.D., Parker, K.M., Flower, D., Lopez, E., Kyle, S., Meuth, M., Curtin, N.J., and Helleday, T. (2005). Specific killing of BRCA2-

- deficient tumours with inhibitors of poly(ADP-ribose) polymerase. *Nature* 434, 913-917. 10.1038/nature03443.
120. Roy, R., Chun, J., and Powell, S.N. (2012). BRCA1 and BRCA2: different roles in a common pathway of genome protection. *Nature Reviews Cancer* 12, 68-78. 10.1038/nrc3181.
 121. Fugger, K., Hewitt, G., West, S.C., and Boulton, S.J. (2021). Tackling PARP inhibitor resistance. *Trends Cancer* 7, 1102-1118. 10.1016/j.trecan.2021.08.007.
 122. Antolin, A.A., Ameratunga, M., Banerji, U., Clarke, P.A., Workman, P., and Al-Lazikani, B. (2020). The kinase polypharmacology landscape of clinical PARP inhibitors. *Scientific Reports* 10. 10.1038/s41598-020-59074-4.
 123. Dias, M.P., Moser, S.C., Ganesan, S., and Jonkers, J. (2021). Understanding and overcoming resistance to PARP inhibitors in cancer therapy. *Nature Reviews Clinical Oncology* 18, 773-791. 10.1038/s41571-021-00532-x.
 124. Hunter, J.E., Willmore, E., Irving, J.A.E., Hostomsky, Z., Veuger, S.J., and Durkacz, B.W. (2012). NF- κ B mediates radio-sensitization by the PARP-1 inhibitor, AG-014699. *Oncogene* 31, 251-264. 10.1038/onc.2011.229.
 125. Cohen, P., Cross, D., and Jänne, P.A. (2021). Kinase drug discovery 20 years after imatinib: progress and future directions. *Nature Reviews Drug Discovery* 20, 551-569. 10.1038/s41573-021-00195-4.
 126. Collett, M.S., and Erikson, R.L. (1978). Protein kinase activity associated with the avian sarcoma virus src gene product. *Proceedings of the National Academy of Sciences* 75, 2021-2024. 10.1073/pnas.75.4.2021.
 127. Hidaka, H., Inagaki, M., Kawamoto, S., and Sasaki, Y. (1984). Isoquinolinesulfonamides, novel and potent inhibitors of cyclic nucleotide-dependent protein kinase and protein kinase C. *Biochemistry* 23, 5036-5041. 10.1021/bi00316a032.
 128. Gross, S., Rahal, R., Stransky, N., Lengauer, C., and Hoeflich, K.P. (2015). Targeting cancer with kinase inhibitors. *Journal of Clinical Investigation* 125, 1780-1789. 10.1172/jci76094.
 129. Paul, M.K., and Mukhopadhyay, A.K. (2004). Tyrosine kinase – Role and significance in Cancer. *International Journal of Medical Sciences*, 101-115. 10.7150/ijms.1.101.
 130. Goldman, J.M., and Melo, J.V. (2001). Targeting the BCR-ABL tyrosine kinase in chronic myeloid leukemia. *N Engl J Med* 344, 1084-1086. 10.1056/nejm200104053441409.
 131. Cohen, P. (2002). Protein kinases--the major drug targets of the twenty-first century? *Nat Rev Drug Discov* 1, 309-315. 10.1038/nrd773.
 132. Gujral, T.S., Peshkin, L., and Kirschner, M.W. (2014). Exploiting polypharmacology for drug target deconvolution. *Proceedings of the National Academy of Sciences* 111, 5048-5053. 10.1073/pnas.1403080111.

133. Kucharczak, J., Simmons, M.J., Fan, Y., and Gelinas, C. (2003). To be, or not to be: NF-kappaB is the answer-role of Rel/NF-kappaB in the regulation of apoptosis. *Oncogene* 22, 8961-8982. 10.1038/sj.onc.1207230
- 1207230 [pii].
134. Kim, D.-S., Camacho, C.V., and Kraus, W.L. (2021). Alternate therapeutic pathways for PARP inhibitors and potential mechanisms of resistance. *Experimental & Molecular Medicine* 53, 42-51. 10.1038/s12276-021-00557-3.
135. Ellis, H.P., Greenslade, M., Powell, B., Spiteri, I., Sottoriva, A., and Kurian, K.M. (2015). Current Challenges in Glioblastoma: Intratumour Heterogeneity, Residual Disease, and Models to Predict Disease Recurrence. *Frontiers in Oncology* 5.
136. Schmitt, M.J., Company, C., Dramaretska, Y., Barozzi, I., Göhrig, A., Kertalli, S., Großmann, M., Naumann, H., Sanchez-Bailon, M.P., Hulsman, D., et al. (2021). Phenotypic Mapping of Pathologic Cross-Talk between Glioblastoma and Innate Immune Cells by Synthetic Genetic Tracing. *Cancer Discov* 11, 754-777. 10.1158/2159-8290.Cd-20-0219.
137. Cahill, K.E., Morshed, R.A., and Yamini, B. (2015). Nuclear factor- κ B in glioblastoma: insights into regulators and targeted therapy. *Neuro-Oncology* 18, 329-339. 10.1093/neuonc/nov265.
138. Krishna, Balasubramaniyan, V., Vaillant, B., Ezhilarasan, R., Hummelink, K., Hollingsworth, F., Wani, K., Heathcock, L., Johanna, Lindsey, et al. (2013). Mesenchymal Differentiation Mediated by NF- κ B Promotes Radiation Resistance in Glioblastoma. *Cancer Cell* 24, 331-346. 10.1016/j.ccr.2013.08.001.
139. Avci, N.G., Ebrahimzadeh-Pustchi, S., Akay, Y.M., Esquenazi, Y., Tandon, N., Zhu, J.-J., and Akay, M. (2020). NF- κ B inhibitor with Temozolomide results in significant apoptosis in glioblastoma via the NF- κ B(p65) and actin cytoskeleton regulatory pathways. *Scientific Reports* 10. 10.1038/s41598-020-70392-5.
140. Wang, X., Jia, L., Jin, X., Liu, Q., Cao, W., Gao, X., Yang, M., and Sun, B. (2015). NF- κ B inhibitor reverses temozolomide resistance in human glioma TR/U251 cells. *Oncology Letters* 9, 2586-2590. 10.3892/ol.2015.3130.
141. Fiume, R., Stijf-Bultsma, Y., Shah, Z.H., Keune, W.J., Jones, D.R., Jude, J.G., and Divecha, N. (2015). PIP4K and the role of nuclear phosphoinositides in tumour suppression. *Biochim Biophys Acta* 1851, 898-910. 10.1016/j.bbali.2015.02.014.
142. Emerling, B.M., Hurov, J.B., Poulgiannis, G., Tsukazawa, K.S., Choo-Wing, R., Wulf, G.M., Bell, E.L., Shim, H.S., Lamia, K.A., Rameh, L.E., et al. (2013). Depletion of a putatively druggable class of phosphatidylinositol kinases inhibits growth of p53-null tumors. *Cell* 155, 844-857. 10.1016/j.cell.2013.09.057.
143. Jude, J.G., Spencer, G.J., Huang, X., Somerville, T.D.D., Jones, D.R., Divecha, N., and Somerville, T.C.P. (2015). A targeted knockdown screen of genes coding for phosphoinositide modulators identifies PIP4K2A as required for acute myeloid leukemia cell proliferation and survival. *Oncogene* 34, 1253-1262. 10.1038/onc.2014.77.

144. Hansen, S.D., Lee, A.A., Duewell, B.R., and Groves, J.T. (2022). Membrane-mediated dimerization potentiates PIP5K lipid kinase activity. *eLife* *11*, e73747. 10.7554/eLife.73747.
145. Clarke, J.H., and Irvine, R.F. (2013). Evolutionarily conserved structural changes in phosphatidylinositol 5-phosphate 4-kinase (PI5P4K) isoforms are responsible for differences in enzyme activity and localization. *Biochem J* *454*, 49-57. 10.1042/bj20130488.
146. Wang, D.G., Paddock, M.N., Lundquist, M.R., Sun, J.Y., Mashadova, O., Amadiume, S., Bumpus, T.W., Hodakoski, C., Hopkins, B.D., Fine, M., et al. (2019). PIP4Ks Suppress Insulin Signaling through a Catalytic-Independent Mechanism. *Cell Reports* *27*, 1991-2001.e1995. 10.1016/j.celrep.2019.04.070.
147. Uhlén, M., Fagerberg, L., Hallström, B.M., Lindskog, C., Oksvold, P., Mardinoglu, A., Sivertsson, Å., Kampf, C., Sjöstedt, E., Asplund, A., et al. (2015). Proteomics. Tissue-based map of the human proteome. *Science* *347*, 1260419. 10.1126/science.1260419.
148. Alessi, D.R., Andjelkovic, M., Caudwell, B., Cron, P., Morrice, N., Cohen, P., and Hemmings, B.A. (1996). Mechanism of activation of protein kinase B by insulin and IGF-1. *The EMBO Journal* *15*, 6541-6551. 10.1002/j.1460-2075.1996.tb01045.x.
149. Fruman, D.A., Chiu, H., Hopkins, B.D., Bagrodia, S., Cantley, L.C., and Abraham, R.T. (2017). The PI3K Pathway in Human Disease. *Cell* *170*, 605-635. 10.1016/j.cell.2017.07.029.
150. Lien, E.C., Dibble, C.C., and Toker, A. (2017). PI3K signaling in cancer: beyond AKT. *Current Opinion in Cell Biology* *45*, 62-71. 10.1016/j.ceb.2017.02.007.
151. Gustin, J.A., Ozes, O.N., Akca, H., Pincheira, R., Mayo, L.D., Li, Q., Guzman, J.R., Korgaonkar, C.K., and Donner, D.B. (2004). Cell Type-specific Expression of the IκB Kinases Determines the Significance of Phosphatidylinositol 3-Kinase/Akt Signaling to NF-κB Activation. *Journal of Biological Chemistry* *279*, 1615-1620. 10.1074/jbc.M306976200.
152. Hoesel, B., and Schmid, J.A. (2013). The complexity of NF-κB signaling in inflammation and cancer. *Molecular Cancer* *12*, 86. 10.1186/1476-4598-12-86.
153. Guha, M., and Mackman, N. (2002). The phosphatidylinositol 3-kinase-Akt pathway limits lipopolysaccharide activation of signaling pathways and expression of inflammatory mediators in human monocytic cells. *J Biol Chem* *277*, 32124-32132. 10.1074/jbc.M203298200.
154. Park, Y.C., Lee, C.H., Kang, H.S., Chung, H.T., and Kim, H.D. (1997). Wortmannin, a specific inhibitor of phosphatidylinositol-3-kinase, enhances LPS-induced NO production from murine peritoneal macrophages. *Biochem Biophys Res Commun* *240*, 692-696. 10.1006/bbrc.1997.7722.
155. Rousseau, A., McEwen, A.G., Poussin-Courmontagne, P., Rognan, D., Nominé, Y., Rio, M.-C., Tomasetto, C., and Alpy, F. (2013). TRAF4 Is a Novel Phosphoinositide-

- Binding Protein Modulating Tight Junctions and Favoring Cell Migration. *PLoS Biology* *11*, e1001726. 10.1371/journal.pbio.1001726.
156. Qian, Y., Commane, M., Ninomiya-Tsuji, J., Matsumoto, K., and Li, X. (2001). IRAK-mediated Translocation of TRAF6 and TAB2 in the Interleukin-1-induced Activation of NF κ B. *Journal of Biological Chemistry* *276*, 41661-41667. 10.1074/jbc.m102262200.
 157. Tufan, A.B., Lazarow, K., Kolesnichenko, M., Sporbert, A., von Kries, J.P., and Scheidereit, C. (2022). TSG101 associates with PARP1 and is essential for PARylation and DNA damage-induced NF- κ B activation. *Embo j* *41*, e110372. 10.15252/embj.2021110372.
 158. Escobedo, A., Gomes, T., Aragón, E., Martín-Malpartida, P., Ruiz, L., and Maria (2014). Structural Basis of the Activation and Degradation Mechanisms of the E3 Ubiquitin Ligase Nedd4L. *Structure* *22*, 1446-1457. 10.1016/j.str.2014.08.016.
 159. Raynaud, F.I., Eccles, S., Clarke, P.A., Hayes, A., Nutley, B., Alix, S., Henley, A., Di-Stefano, F., Ahmad, Z., Guillard, S., et al. (2007). Pharmacologic characterization of a potent inhibitor of class I phosphatidylinositide 3-kinases. *Cancer Res* *67*, 5840-5850. 10.1158/0008-5472.CAN-06-4615.
 160. Leahy, J.J., Golding, B.T., Griffin, R.J., Hardcastle, I.R., Richardson, C., Rigoreau, L., and Smith, G.C. (2004). Identification of a highly potent and selective DNA-dependent protein kinase (DNA-PK) inhibitor (NU7441) by screening of chromenone libraries. *Bioorg Med Chem Lett* *14*, 6083-6087. 10.1016/j.bmcl.2004.09.060.
 161. Nemec, V., Maier, L., Berger, B.-T., Chaikuad, A., Drapela, S., Soucek, K., Knapp, S., and Paruch, K. (2021). Highly selective inhibitors of protein kinases CLK and HIPK with the furo[3,2-b]pyridine core. *European Journal of Medicinal Chemistry* *215*, 113299. 10.1016/j.ejmech.2021.113299.
 162. Gilmore, T.D., and Herscovitch, M. (2006). Inhibitors of NF- κ B signaling: 785 and counting. *Oncogene* *25*, 6887-6899. 10.1038/sj.onc.1209982.
 163. Davis, M.I., Hunt, J.P., Herrgard, S., Ciceri, P., Wodicka, L.M., Pallares, G., Hocker, M., Treiber, D.K., and Zarrinkar, P.P. (2011). Comprehensive analysis of kinase inhibitor selectivity. *Nat Biotechnol* *29*, 1046-1051. 10.1038/nbt.1990.
 164. Bai, D., Ueno, L., and Vogt, P.K. (2009). Akt-mediated regulation of NF κ B and the essentialness of NF κ B for the oncogenicity of PI3K and Akt. *International Journal of Cancer* *125*, 2863-2870. 10.1002/ijc.24748.
 165. Ahmad, A., Biersack, B., Li, Y., Kong, D., Bao, B., Schobert, R., Padhye, S.B., and Sarkar, F.H. (2013). Targeted regulation of PI3K/Akt/mTOR/NF- κ B signaling by indole compounds and their derivatives: mechanistic details and biological implications for cancer therapy. *Anticancer Agents Med Chem* *13*, 1002-1013. 10.2174/18715206113139990078.
 166. Yoshida, T., Kim, J.H., Carver, K., Su, Y., Weremowicz, S., Mulvey, L., Yamamoto, S., Brennan, C., Mei, S., Long, H., et al. (2015). CLK2 Is an Oncogenic Kinase and

- Splicing Regulator in Breast Cancer. *Cancer Res* 75, 1516-1526. 10.1158/0008-5472.CAN-14-2443.
167. Iwai, K., Yaguchi, M., Nishimura, K., Yamamoto, Y., Tamura, T., Nakata, D., Dairiki, R., Kawakita, Y., Mizojiri, R., Ito, Y., et al. (2018). Anti-tumor efficacy of a novel CLK inhibitor via targeting RNA splicing and MYC-dependent vulnerability. *EMBO Mol Med* 10. 10.15252/emmm.201708289.
 168. Salvador, F., and Gomis, R.R. (2018). CLK2 blockade modulates alternative splicing compromising MYC-driven breast tumors. *EMBO Mol Med* 10. 10.15252/emmm.201809213.
 169. Ninomiya, K., Kataoka, N., and Hagiwara, M. (2011). Stress-responsive maturation of Clk1/4 pre-mRNAs promotes phosphorylation of SR splicing factor. *J Cell Biol* 195, 27-40. 10.1083/jcb.201107093.
 170. Martín Moyano, P., Němec, V., and Paruch, K. (2020). Cdc-Like Kinases (CLKs): Biology, Chemical Probes, and Therapeutic Potential. *Int J Mol Sci* 21. 10.3390/ijms21207549.
 171. Bruyere, D., Roncarati, P., Lebeau, A., Lerho, T., Poulain, F., Hendrick, E., Pilard, C., Reynders, C., Ancion, M., Luyckx, M., et al. (2023). Human papillomavirus E6/E7 oncoproteins promote radiotherapy-mediated tumor suppression by globally hijacking host DNA damage repair. *Theranostics* 13, 1130-1149. 10.7150/thno.78091.
 172. Duncan, P.I., Howell, B.W., Marius, R.M., Drmanic, S., Douville, E.M., and Bell, J.C. (1995). Alternative splicing of STY, a nuclear dual specificity kinase. *J Biol Chem* 270, 21524-21531. 10.1074/jbc.270.37.21524.
 173. Lin, J., Lin, G., Chen, B., Yuan, J., and Zhuang, Y. (2022). CLK2 Expression Is Associated with the Progression of Colorectal Cancer and Is a Prognostic Biomarker. *Biomed Res Int* 2022, 7250127. 10.1155/2022/7250127.
 174. Liu, B., Kong, X., Wang, R., and Xin, C. (2021). CLK2 promotes occurrence and development of non-small cell lung cancer. *J buon* 26, 58-64.
 175. Park, S.Y., Piao, Y., Thomas, C., Fuller, G.N., and de Groot, J.F. (2016). Cdc2-like kinase 2 is a key regulator of the cell cycle via FOXO3a/p27 in glioblastoma. *Oncotarget* 7, 26793-26805. 10.18632/oncotarget.8471.
 176. Riggs, J.R., Nagy, M., Elsner, J., Erdman, P., Cashion, D., Robinson, D., Harris, R., Huang, D., Tehrani, L., Deyanat-Yazdi, G., et al. (2017). The Discovery of a Dual TTK Protein Kinase/CDC2-Like Kinase (CLK2) Inhibitor for the Treatment of Triple Negative Breast Cancer Initiated from a Phenotypic Screen. *J Med Chem* 60, 8989-9002. 10.1021/acs.jmedchem.7b01223.
 177. Shimizu, T., Yonemori, K., Koyama, T., Katsuya, Y., Sato, J., Fukuhara, N., Yokoyama, H., Iida, H., Ando, K., Fukuhara, S., et al. (2022). A first-in-human phase I study of CTX-712 in patients with advanced, relapsed or refractory malignant tumors. *Journal of Clinical Oncology* 40, 3080-3080. 10.1200/JCO.2022.40.16_suppl.3080.

178. Tam, B.Y., Chiu, K., Chung, H., Bossard, C., Nguyen, J.D., Creger, E., Eastman, B.W., Mak, C.C., Ibanez, M., Ghias, A., et al. (2020). The CLK inhibitor SM08502 induces anti-tumor activity and reduces Wnt pathway gene expression in gastrointestinal cancer models. *Cancer Letters* 473, 186-197. <https://doi.org/10.1016/j.canlet.2019.09.009>.
179. Kang, E., Kim, K., Jeon, S.Y., Jung, J.G., Kim, H.K., Lee, H.B., and Han, W. (2022). Targeting CLK4 inhibits the metastasis and progression of breast cancer by inactivating TGF- β pathway. *Cancer Gene Ther* 29, 1168-1180. 10.1038/s41417-021-00419-0.
180. Kim, H., Choi, K., Kang, H., Lee, S.Y., Chi, S.W., Lee, M.S., Song, J., Im, D., Choi, Y., and Cho, S. (2014). Identification of a novel function of CX-4945 as a splicing regulator. *PLoS One* 9, e94978. 10.1371/journal.pone.0094978.
181. Walter, A., Chaikuad, A., Helmer, R., Loaëc, N., Preu, L., Ott, I., Knapp, S., Meijer, L., and Kunick, C. (2018). Molecular structures of cdc2-like kinases in complex with a new inhibitor chemotype. *PLoS One* 13, e0196761. 10.1371/journal.pone.0196761.
182. Němec, V., Hylsová, M., Maier, L., Flegel, J., Sievers, S., Ziegler, S., Schröder, M., Berger, B.T., Chaikuad, A., Valčíková, B., et al. (2019). Furo[3,2-b]pyridine: A Privileged Scaffold for Highly Selective Kinase Inhibitors and Effective Modulators of the Hedgehog Pathway. *Angew Chem Int Ed Engl* 58, 1062-1066. 10.1002/anie.201810312.
183. Zhu, D., Xu, S., Deyanat-Yazdi, G., Peng, S.X., Barnes, L.A., Narla, R.K., Tran, T., Mikolon, D., Ning, Y., Shi, T., et al. (2018). Synthetic Lethal Strategy Identifies a Potent and Selective TTK and CLK1/2 Inhibitor for Treatment of Triple-Negative Breast Cancer with a Compromised G1-S Checkpoint. *Molecular Cancer Therapeutics* 17, 1727-1738. 10.1158/1535-7163.Mct-17-1084.
184. Coombs, T.C., Tanega, C., Shen, M., Wang, J.L., Auld, D.S., Gerritz, S.W., Schoenen, F.J., Thomas, C.J., and Aubé, J. (2013). Small-molecule pyrimidine inhibitors of the cdc2-like (Clk) and dual specificity tyrosine phosphorylation-regulated (Dyrk) kinases: development of chemical probe ML315. *Bioorg Med Chem Lett* 23, 3654-3661. 10.1016/j.bmcl.2013.02.096.
185. Al-Tawil, M.F., Daoud, S., Hatmal, M.m.M., and Taha, M.O. (2022). Discovery of new Cdc2-like kinase 4 (CLK4) inhibitors via pharmacophore exploration combined with flexible docking-based ligand/receptor contact fingerprints and machine learning. *RSC Advances* 12, 10686-10700. 10.1039/D2RA00136E.
186. Rosenthal, A.S., Tanega, C., Shen, M., Mott, B.T., Bougie, J.M., Nguyen, D.T., Misteli, T., Auld, D.S., Maloney, D.J., and Thomas, C.J. (2011). Potent and selective small molecule inhibitors of specific isoforms of Cdc2-like kinases (Clk) and dual specificity tyrosine-phosphorylation-regulated kinases (Dyrk). *Bioorg Med Chem Lett* 21, 3152-3158. 10.1016/j.bmcl.2011.02.114.
187. C. Scheidereit, P.Mucka., M. Nazare, P. Lindemann, J. P. von Kries, M. Willenbrock, B. Bosco, (2023) Selective inhibitors of Genotoxic Stress Induced IKK-NF- κ B Pathways for Cancer Therapy. Germany patent application EP 23175081.1.

188. Mishra, R., Patel, H., Alanazi, S., Kilroy, M.K., and Garrett, J.T. (2021). PI3K Inhibitors in Cancer: Clinical Implications and Adverse Effects. *Int J Mol Sci* 22. 10.3390/ijms22073464.
189. Yang, J., Nie, J., Ma, X., Wei, Y., Peng, Y., and Wei, X. (2019). Targeting PI3K in cancer: mechanisms and advances in clinical trials. *Molecular Cancer* 18, 26. 10.1186/s12943-019-0954-x.